New Technology for Remote Testing of Response Time of Installed Thermocouples

Volume I — Background and General Details

H. M. Hashemian
Analysis and Measurement Services Corp.
AMS 9111 Cross Park Dr., N. W.
Knoxville, TN 37923

January 1992

Final Report for Period September 1987 — December 1990

ARNOLD ENGINEERING DEVELOPMENT CENTER
ARNOLD AIR FORCE BASE, TENNESSEE
AIR FORCE SYSTEMS COMMAND
UNITED STATES AIR FORCE

NOTICES

When U. S. Government drawings, specifications, or other data are used for any purpose other than a definitely related Government procurement operation, the Government thereby incurs no responsibility nor any obligation whatsoever, and the fact that the Government may have formulated, furnished, or in any way supplied the said drawings, specifications, or other data, is not to be regarded by implication or otherwise, or in any manner licensing the holder or any other person or corporation, or conveying any rights or permission to manufacture, use, or sell any patented invention that may in any way be related thereto.

Qualified users may obtain copies of this report from the Defense Technical Information Center.

References to named commercial products in this report are not to be considered in any sense as an endorsement of the product by the United States Air Force or the Government.

This report has been reviewed by the Office of Public Affairs (PA) and is releasable to the National Technical Information Service (NTIS). At NTIS, it will be available to the general public, including foreign nations.

Reproducibles used in the publication of this report were supplied by the authors. AEDC has neither edited nor altered this manuscript.

APPROVAL STATEMENT

This report has been reviewed and approved.

SETH SHEPHERD, Capt, USAF
Facility Technology Division
Directorate of Technology
Deputy for Operations

Approved for publication:

FOR THE COMMANDER

KEITH L. KUSHMAN
Director of Technology
Deputy for Operations

REPORT DOCUMENTATION PAGE

Public reporting burden for this collection of information is estimated to average 1 hour per response, including the time for reviewing instructions, searching existing data sources, gathering and maintaining the data needed, and completing and reviewing the collection of information. Send comments regarding this burden estimate or any other aspect of this collection of information, including suggestions for reducing this burden, to Washington Headquarters Services, Directorate for Information Operations and Reports, 1215 Jefferson Davis Highway, Suite 1204, Arlington, VA 22202-4302, and to the Office of Management and Budget, Paperwork Reduction Project (0704-0188), Washington, DC 20503.

1. AGENCY USE ONLY (Leave blank)	2. REPORT DATE January 1992	3. REPORT TYPE AND DATES COVERED Final, September 1987 - December 1990

4. TITLE AND SUBTITLE New Technology for Remote Testing of Response Time of Installed Thermocouples, Vol. I, Background and General Details	5. FUNDING NUMBERS F40600-87-C0003
6. AUTHOR(S) Hashemian, H. M. Analysis and Measurement Services Corp.	

7. PERFORMING ORGANIZATION NAME(S) AND ADDRESS(ES) Analysis and Measurement Services Corp. AMS 9111 Cross Park Drive, N.W. Knoxville, TN 37923-4599	8. PERFORMING ORGANIZATION REPORT NUMBER AEDC-TR-91-26, Vol. I

9. SPONSORING/MONITORING AGENCY NAMES(S) AND ADDRESS(ES) Arnold Engineering Development Center/DOT Air Force Systems Command Arnold Air Force Base, TN 37389-5000	10. SPONSORING/MONITORING AGENCY REPORT NUMBER

11. SUPPLEMENTARY NOTES

Available in Defense Technical Information Center (DTIC).

12a. DISTRIBUTION/AVAILABILITY STATEMENT Approved for public release; distribution is unlimited.	12b. DISTRIBUTION CODE

13. ABSTRACT (Maximum 200 words)

A comprehensive research and development project was completed to provide new technology for remote testing of response time of thermocouples as installed in operating processes.

A significant portion of this development depended on the Loop Current Step Response (LCSR) method. This method is based on heating the thermocouple internally by applying an electric current to its extension leads. The current produces Joule heating in the thermocouple and causes the thermocouple junction to settle several degrees above the ambient temperature. The current is then cut off and the thermocouple output is recorded as it cools to the ambient temperature. It has been established by experimental research and theoretical development carried out in this project that this cooling transient can be analyzed to provide the response time of the thermocouple under the conditions tested.

With little additional effort, the equipment that was developed in this project can be adapted to provide a capability for in-situ assessment of static health, reliability, and accuracy of installed thermocouples.

14. SUBJECT TERMS thermocouple, time constant, response time, aerospace, Loop Current Step Response Method, smart sensor, in-situ testing, accuracy	15. NUMBER OF PAGES 235
	16. PRICE CODE

17. SECURITY CLASSIFICATION OF REPORT UNCLASSIFIED	18. SECURITY CLASSIFICATION OF THIS PAGE UNCLASSIFIED	19. SECURITY CLASSIFICATION OF ABSTRACT UNCLASSIFIED	20. LIMITATION OF ABSTRACT SAME AS REPORT

PREFACE

This is Volume I of a three volume report prepared by Analysis and Measurement Services Corporation (AMS) for Arnold Engineering Development Center, Air Force Systems Command, Arnold Air Force Station, Tennessee. The report has been written as an account of work completed over a three year period under contract number F40600-87-C0003. The Air Force project manager was Mr. Robert W. Smith, AEDC/DOT. The report has been written by H. M. Hashemian of Analysis and Measurement Services Corporation.

This volume contains the background of the project, the theoretical aspects of the research and development carried out, and a summary of the key research results along with a description of the test equipment developed. Volume II contains the supporting research data, details on how the research was carried out, and a description of the equipment and procedures that were used in performing the work.

Volume III contains a detailed description of the test equipment that was developed in this project. It includes an operations and maintenance manual for the equipment, software flow charts and listings, parts list, drawings, photographs, and other details.

ABSTRACT

A comprehensive research and development project was successfully carried out to provide new technology for in-situ response time testing of thermocouples as installed in operating processes. The details are presented in this report.

This development was based on the Loop Current Step Response (LCSR) method. This method permits remote testing of installed thermocouples under process operating conditions. This capability is useful in all applications involving transient temperature measurements with thermocouples. Presently, transient temperature measurements are often restricted to small thermocouples that can be assumed to have a negligible response time. One advantage of the LCSR test is that It eliminates such restrictions by providing a means to measure and correct for the delay of the thermocouple. Another advantage is that it provides a tool for checking the installation integrity and to account for aging effects on response time of thermocouples that are used in hostile environments.

The response time of a thermocouple is normally measured from its transient output when the temperature of the environment is changed. In the LCSR test, the same response time is determined by analysis of a transient that results from a change In temperature inside the thermocouple. The change in temperature inside the thermocouple is induced by applying an electric current to the thermocouple's extension leads.

The validity and the accuracy of the LCSR test for measurement of response time of thermocouples was established in this project. The results of the validation work were used as a guide in the design of optimum test equipment that was constructed in this project to implement the LCSR test in aerospace and other applications.

TABLE OF CONTENTS

TABLE OF CONTENTS
(continued)

LIST OF FIGURES

LIST OF FIGURES
(continued)

LIST OF FIGURES
(continued)

LIST OF TABLES

1. INTRODUCTION

This report presents the details of a research and development project conducted by Analysis and Measurement Services Corporation (AMS) for the United States Air Force, Arnold Engineering Development Center (AEDC).

The purpose of the work was to provide a capability for in-situ response time testing of thermocouples as installed in operating processes. The specific need of AEDC was remote testing of response time of thermocouples in turbine engine test facilities. As such, much of this development was concentrated on validation tests in flowing gases. Furthermore, the project concentrated on thermocouple types of interest to AEDC (types K, J, E, and to a lesser extent, type T). Both sheathed and bare wire thermocouples were tested.

The research and development carried out here was based on the Loop Current Step Response (LCSR) test. The LCSR test involves heating the thermocouple internally with an electric current applied to the thermocouple extension leads. The amount and duration of the applied current is controlled in a manner to raise the temperature of the thermocouple a few degrees above the ambient temperature. The current is then cut off and the thermocouple output is recorded as it cools to the ambient temperature. The cooling transient is then analyzed with a computer using a special algorithm that gives the response time of the thermocouple under the conditions tested.

Note that the response time of a thermocouple is normally obtained from a step change in the temperature outside the thermocouple as opposed to a step change in temperature inside the thermocouple as occurs in a LCSR test. The special algorithm mentioned earlier is designed to convert the internal heating data to give the response that would have resulted if the

thermocouple experienced a step change in the surrounding temperature. A significant advantage of the LCSR test is that it provides a method for response time testing of thermocouples without having to remove them from their normal installation.

The LCSR technology was implemented on an instrument developed in this project to perform the test and analyze the data. This instrument consists of two separate modules assembled in the same package. One module, called ETC-2, is used to perform the LCSR test, and the other called ESA-1, is used to analyze the data. The ETC-2 consists of a programmable AC power supply and a set of instrumentation amplifiers and filters. A feature of the ETC-2 is the ability to limit the amount of electric current used in performing a LCSR test to a safe level. The ESA-1 consists of a microprocessor with an analog-to-digital converter to sample and analyze the LCSR data. An important feature of the ESA-1 is that it has a "touch-screen" on the front panel through which the operation of both the ESA-1 and ETC-2 is controlled. The LCSR raw data and the results are displayed on the front panel as the test is performed. Provisions are made in this system to permit remote communication through a built-in modem used with a regular telephone line. This feature allows the user to link the system to AMS for any training, troubleshooting, or assistance in performing the tests or interpretation of the results.

The work reported herein represents a 30-month Phase II project that has resulted in the development of both technology and equipment for dynamic testing of thermocouples in liquid and gaseous process media. The experimental research and equipment development portion of the project was carried out during the 1987 to 1990 time frame, and the final report of the project was written in three volumes in 1991. This was preceded by a Phase I project carried out in the 1985 to 1986 period with the final Phase I report published in December 1986 as AEDC-TR-86-46 report entitled, "Determination of Installed Thermocouple Response".

2. HISTORICAL PERSPECTIVE

The LCSR test was introduced about 15 years ago by Warshawsky[1], then working for the Lewis Research Center of the National Aeronautical and Space Administration (NASA). Although Warshawsky's initiative did not lead to much development at NASA, it soon gained popularity in the nuclear industry[2]. More specifically, the Oak Ridge National Laboratory (ORNL) began working on the LCSR method in the mid 1970's. The purpose of the ORNL work was to develop in-situ response time testing capability for thermocouples for the Liquid Metal Fast Breeder Reactor (LMFBR). The LMFBR was to be built on the Clinch River near Oak Ridge, Tennessee. The LMFBR project was later canceled by the United States Congress and the work of ORNL on the LCSR method came to a halt. However, through a research project funded by the Electric Power Research Institute, the LCSR method was later developed for response time testing of resistance temperature detectors (RTDs) in nuclear power plants[3]. The method has been approved by the U.S. Nuclear Regulatory Commission[4], and is now routinely used for in-situ response time testing of safety system RTDs in nuclear power plants.

Although the LCSR method had been fully developed for RTDs when this project began for AEDC, a number of major areas had to be addressed to adapt the LCSR method for thermocouples. Thermocouples are fundamentally different than RTDs, thus requiring a different strategy for implementation of the LCSR test. Furthermore, an integrated system for performing the LCSR test and analysis had to be developed for AEDC.

3. DEFINING THERMOCOUPLE PERFORMANCE

The performance of a thermocouple is judged by its accuracy and response time. Accuracy is a measure of how well the thermocouple indicates a static temperature, and response time characterizes how quickly it detects a temperature change. Sensor manufacturers usually specify the generic accuracy and response time of the sensors in a reference condition. While useful for comparative evaluation and selection of thermocouples, this information has very little bearing on the actual performance achieved in an operating process. The in-service performance of thermocouples depends not only on their as-built characteristics, but also on their installation details, aging characteristics, and the process conditions.

This report is concerned with the dynamic characteristics, i.e., the response time of thermocouples. Nevertheless, a review of the steady state performance, i.e., the calibration of thermocouples is also presented to provide a complete picture.

The response time of a temperature sensor is characterized by its time constant (τ). The time constant is defined as the time required for the sensor output to reach 63.2 percent of its final value following a step change in the process temperature. Although this definition is unambiguous only for a first order system, it is conventionally used for determining the response time of thermocouples, resistance thermometers, and most other temperature sensors.

As will be seen later, for first order dynamic systems, the time constant as defined above is equal to the time lag in the sensor response to a ramp temperature change. The responses of a typical first order dynamic system to a step and a ramp input are illustrated in Figure 3.1.

AMS—DWG PXT101A
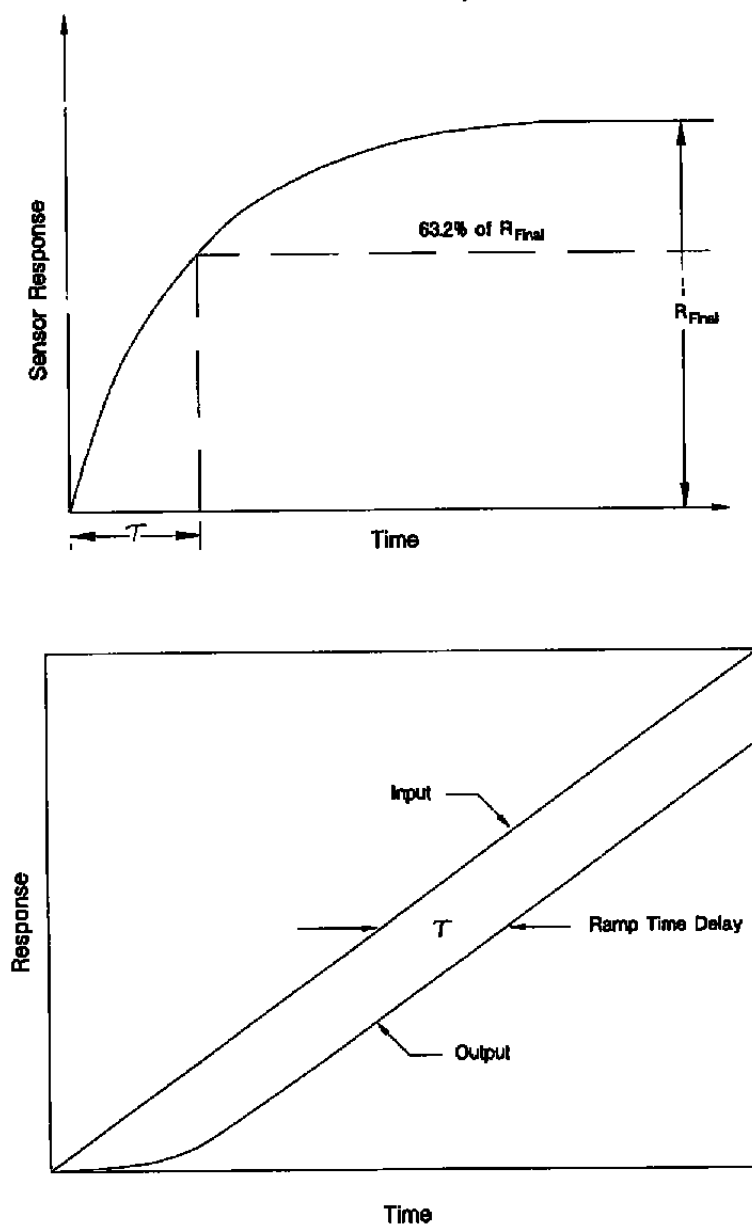
Figure 3.1. Typical Step and Ramp Responses of a First Order System.

An analysis of the ramp response is shown in Figure 3.2 to help demonstrate the importance of the response time on measurement results. It is clear from the illustration in Figure 3.2 that the error in an instantaneous temperature reading is proportional to the sensor response time. Therefore, the response time must be measured and taken into account if accurate transient temperature measurements are required.

The response time of thermocouples depends on the properties of the medium being measured and the thermocouple's internal composition and installation details. The velocity, temperature, and pressure of the medium can affect response time by controlling the heat transfer rate between the process and the sensing element. In low conductivity environments, such as gases and low-velocity liquids, the time constant depends primarily on the process conditions. On the other hand, in high conductivity environments, the time constant is relatively insensitive to process conditions and is controlled by the thermocouple's internal heat transfer characteristics. A detailed discussion on the effects of process conditions such as flow rate and temperature on response time is carried out later in this report. The terms flow rate and velocity are used in this report interchangeably to refer to the speed of fluids in a laboratory or process environment.

Process   Thermocouple

T = Response Time

e = Steady State Error

Temperature

Time

Response Time
Tolerence

Tolerence of e

Temperature

Time
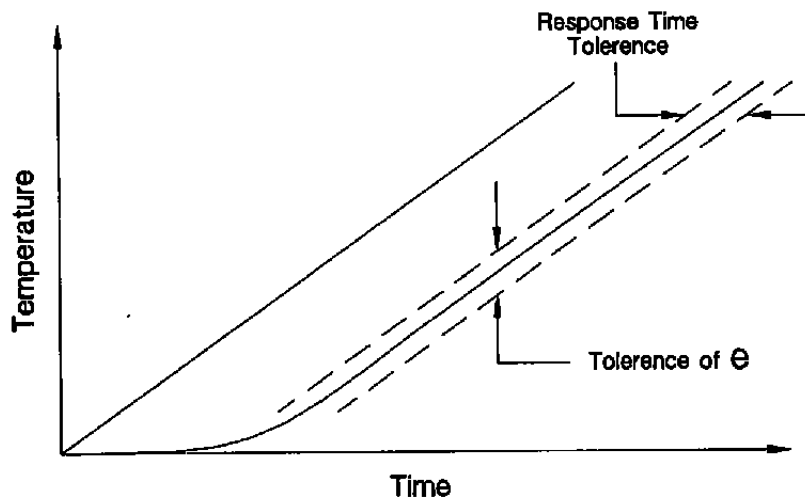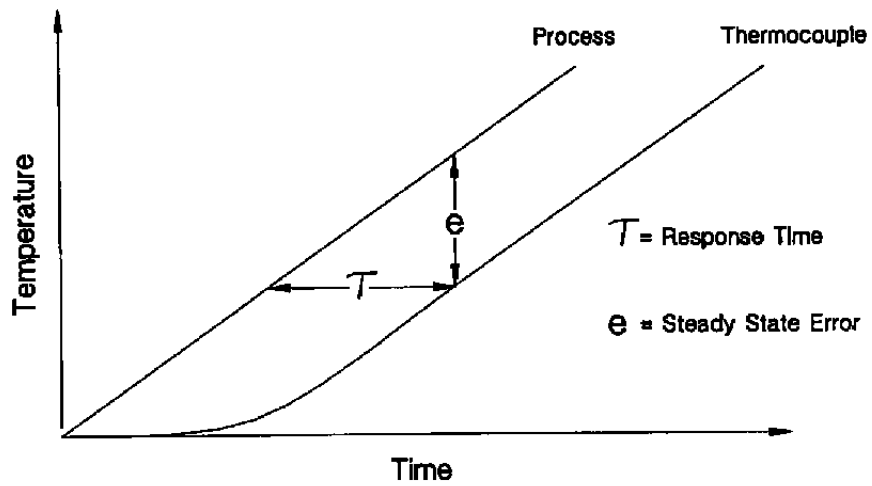
Figure 3.2. Analysis of a Ramp Response.

17

4. COMPARISON OF THERMOCOUPLES WITH RTDs

The choice between thermocouples and Resistance Temperature Detectors (RTDs) depends on the application. If either sensor can be used, thermocouples are better for a faster response and RTDs are better for a higher accuracy. For temperatures of 500°C or less, RTDs are generally more stable, reliable, and can be calibrated before and after installation to establish the accuracy of the measured temperature. Furthermore, the output versus temperature relationship of RTDs is more linear than thermocouples. A disadvantage of RTDs is the self heating error which limits their usefulness in media with poor heat transfer properties such as gases and liquids at low velocities. In fact, because of the self heating problem, most aerospace applications, especially those involving gas temperature measurements, use thermocouples. The self heating error in RTDs arises from Joule heating due to an electric current that must be applied to the sensing element of the RTD to measure its resistance.

Thermocouples provide point measurement, which is useful in some applications and detrimental in others. For example, significant errors may result from point measurement characteristics of thermocouples when large temperature gradients exist in the process stream. In these situations, several thermocouples should be used and the results averaged. Another option is to use an RTD with a long sensing element.

The main disadvantage of thermocouples, besides a need for a reference junction, is that they are not readily calibrated to establish their accuracy beyond the manufacturer's data. This limits their usefulness in applications where accuracy is critical. However, for temperature estimates where accuracy within a few degrees is acceptable, thermocouples are more suitable

than RTDs because of their installation flexibility, higher temperature range, and faster response time.

The temperature limit of RTDs and thermocouples depends on the type and size of the sensing element and the construction material of the sensor. Typically, platinum RTDs, which are the most popular type, are used predominately at temperatures up to 500°C. Thermocouples are typically used at temperatures of up to 1000°C, except for Tungsten-Rhenium thermocouples which are rated for up to about 3000°C.

The temperature ranges mentioned above are typical for industrial sensors as opposed to standard sensors such as Standard Platinum Resistance Thermometers (SPRTs) and type S thermocouples. Figure 4.1 shows some of the most commonly used temperature sensors and the most typical temperature ranges in which they are used. Some of the temperature ranges shown in Figure 4.1 do not represent the temperature extremes in which these sensors can be used. However, the use of the sensors outside of the ranges shown may jeopardize their useful life and calibration stability.

The choice between RTDs and thermocouples is often clear in processes where severe mechanical vibrations or high electrical noise levels are present. Where vibration is involved, thermocouples are preferred because experience has shown that RTDs have larger failure rates due to detachment of the sensing element from the extension wires inside the RTD. Where noise is involved, RTDs are preferred because they are less susceptible to electrical interferences, and their output can be controlled by the excitation current to increase the signal-to-noise ratio.

AMS-DWG THC049C
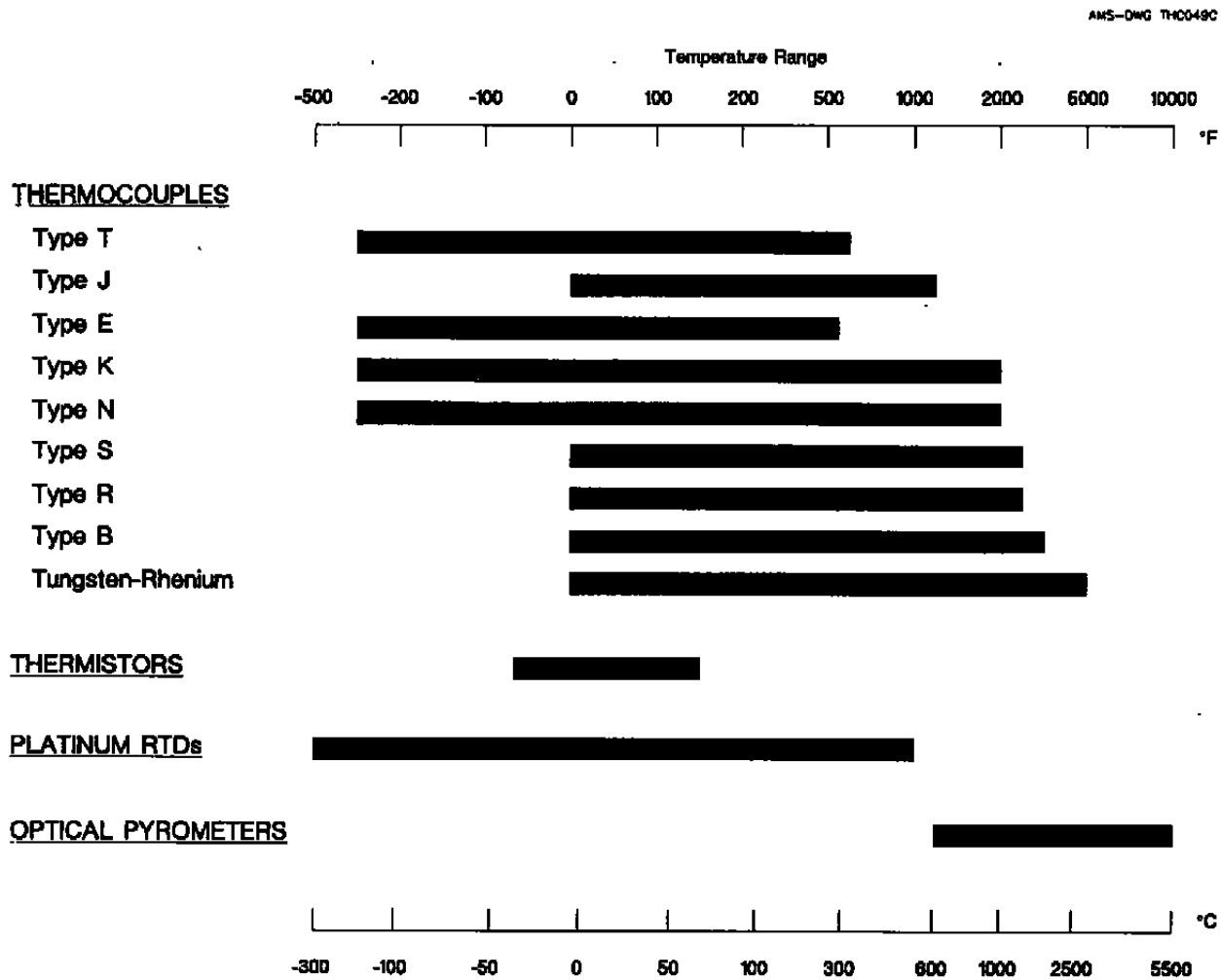
Figure 4.1. Typical Temperature Sensors and Their Useful Temperature Ranges.

Cost is often cited as an advantage of thermocouples over RTDs. It is true that the cost of a thermocouple assembly alone is usually less than a comparable RTD. But when the cost of thermocouple extension wires, connectors, reference junction, and indicating equipment are added, the cost of RTDs and thermocouples would be essentially comparable.

Thermocouples and RTDs currently provide about 70 percent of the industrial temperature measurement needs of the United States. Thermocouples are used in about 40 percent of applications, and RTDs in about 30 percent. The remaining 30 percent of industrial temperature measurements are made with a variety of temperature sensors including thermistors and optical pyrometers that were shown in Figure 4.1. Thermistors, however, are not very widely used in industrial processes due to their limited temperature range. They are more widely used in laboratory measurements and medical applications where sensitivity is important for detecting small changes from room temperature to about 60°C. Figure 4.2 compares the temperature range and linearity characteristics of thermocouples, RTDs, and thermistors. It is apparent that thermocouples provide the highest temperature, RTDs provide the best linearity, and thermistors provide the best sensitivity.

AMS—DWG GRF010C
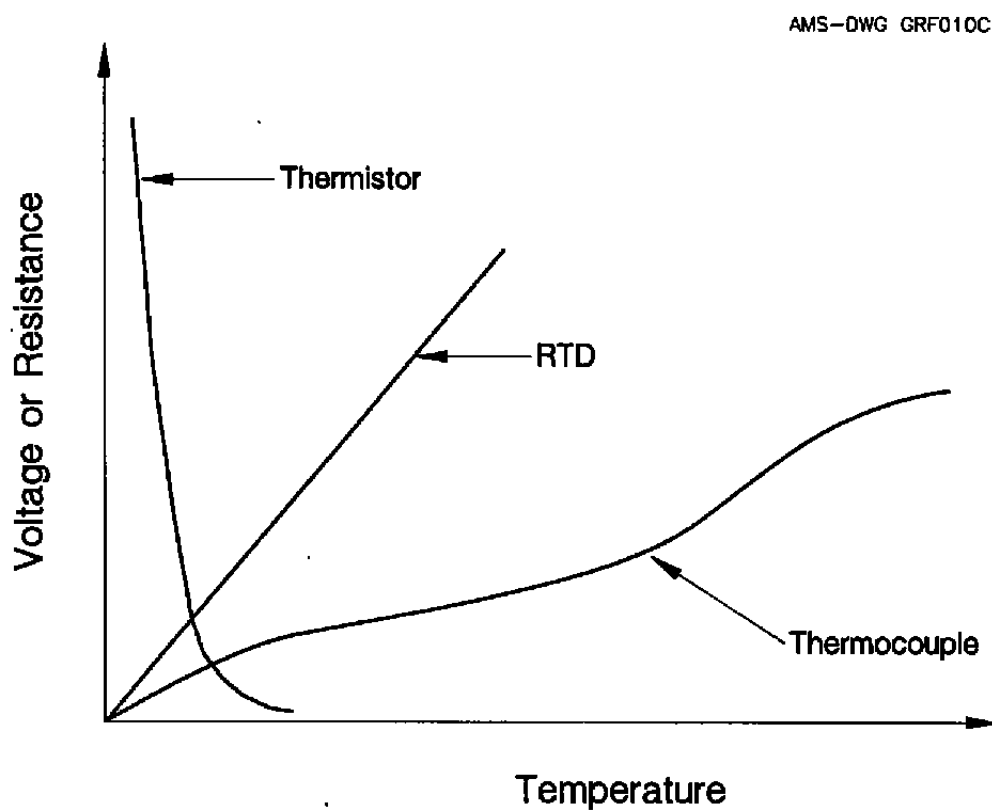
Figure 4.2. Dominant Characteristics of Typical
Temperature Sensors.

5. PHYSICAL CHARACTERISTICS OF THERMOCOUPLES

Thermocouples are among the most simple temperature sensors for industrial applications. Basically, a thermocouple is made of two different metals (wires) joined together at one end and kept open at the other end (Figure 5.1). The point where the two wires are joined is referred to as the measuring junction, hot junction, or simply the junction. The point at which the thermocouple wires are attached to the extension wires leading to a temperature indicator is referred to as reference junction or cold junction. If the measuring junction and the reference junction are at two different temperatures, a voltage called Electromotive Force or EMF is produced. The magnitude of the EMF normally depends on the properties of the two thermocouple wires and the temperature difference between the measuring junction and the reference junction. For laboratory work and in performing calibration on thermocouples, the reference junction is usually kept in an ice bath (at 0°C). However, in industrial applications, a circuit referred to as cold junction compensation circuit is usually used to automatically account for the temperature of the reference junction.

Thermocouple materials are supplied as bare wires or flexible insulated pairs of wires. For use at high temperatures or hostile environments, thermocouples are often protected in a metallic tube called a sheath. The sheath is packed with dry insulation material to secure the thermocouple wires and provide for electrical isolation (Figure 5.2). The assembly is then hermetically sealed to keep the insulation material from any exposure to humid air. The insulation material in most thermocouples is often highly hygroscopic and can easily lose its insulation capability with moisture ingress through the thermocouple seal. One of the consequences of moisture ingress is a noisy thermocouple signal.
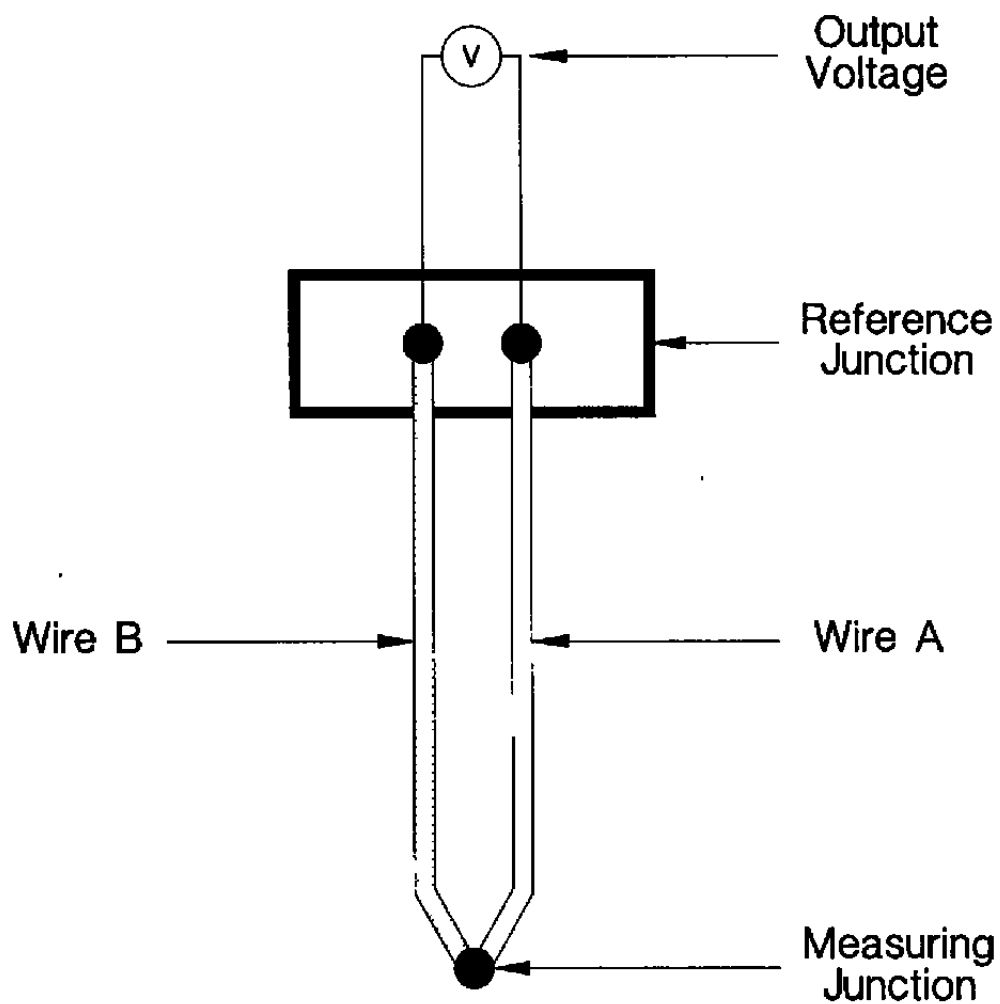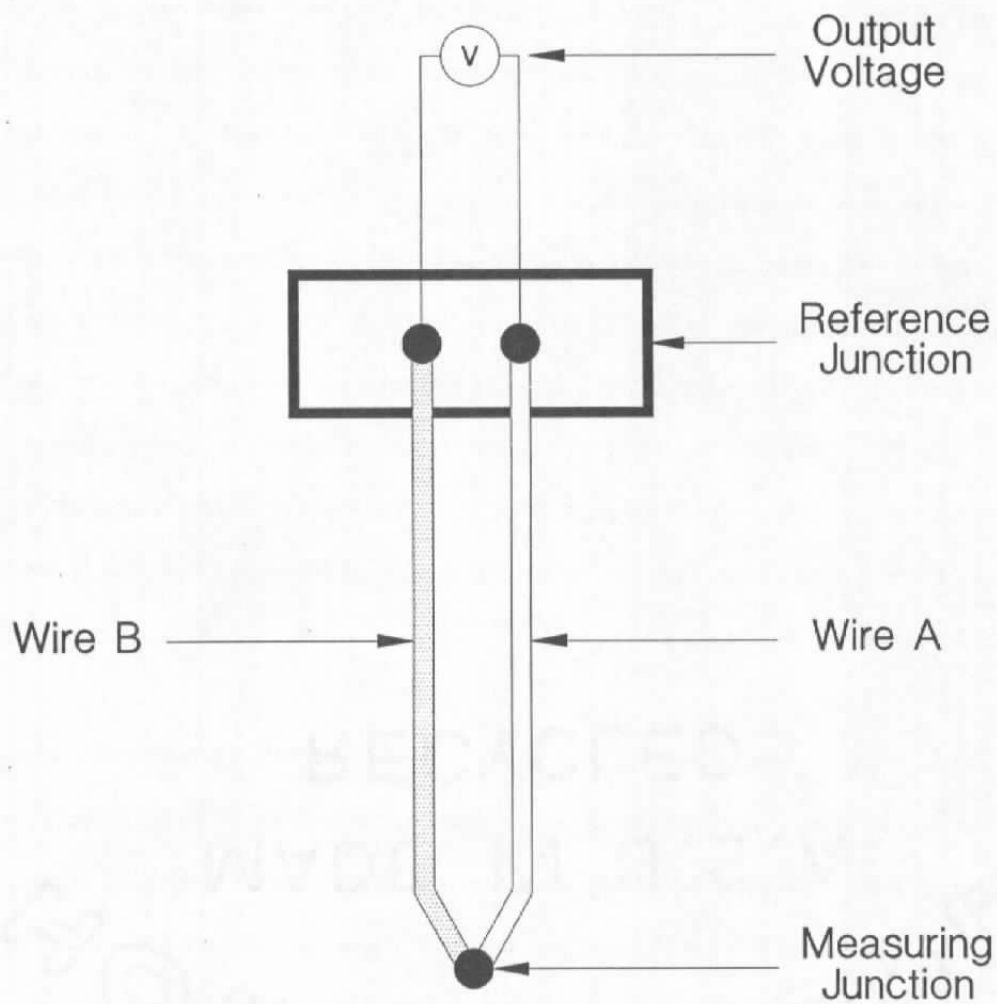
Figure 5.1. Components of a Basic Thermocouple Circuit.

AMS—DWG THC036B

Output
Voltage

Reference
Junction

Wire B

Wire A

Measuring
Junction

Figure 5.1. Components of a Basic Thermocouple Circuit.

Extension
Wires

Seal

Insulation
Material

Sheath

Wire A

Wire B

Measuring
Junction
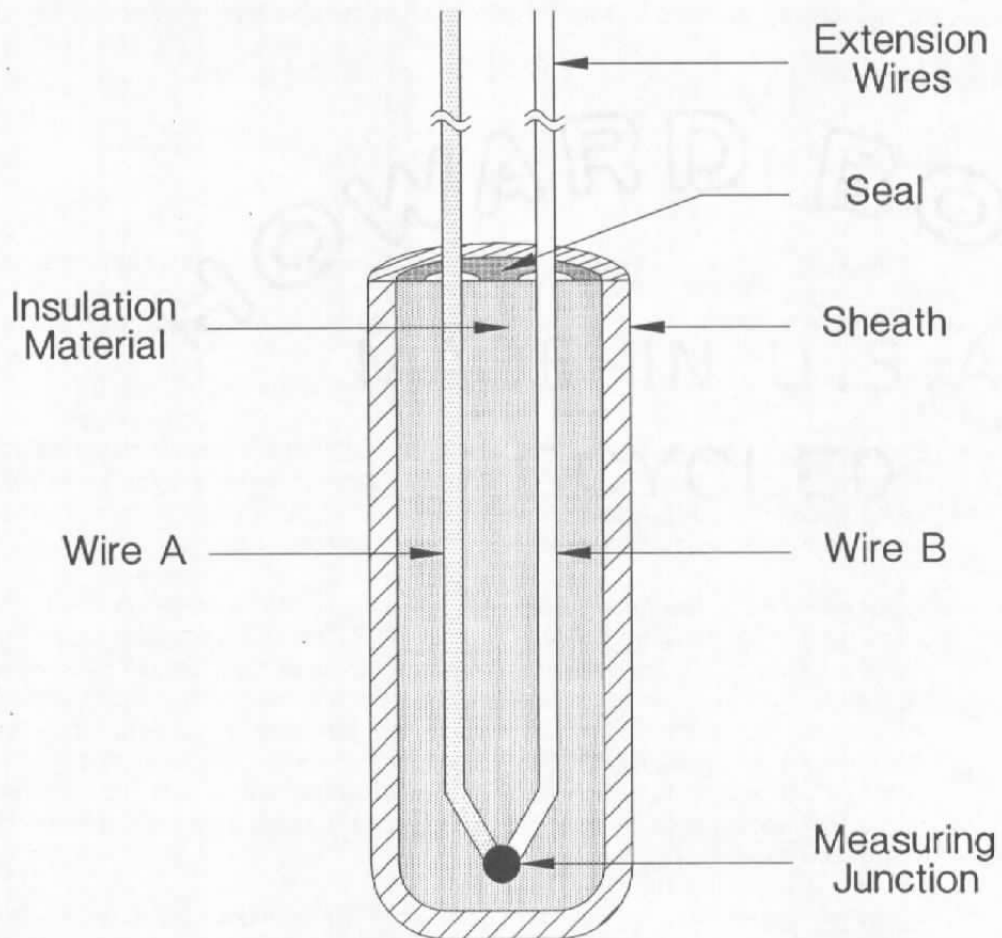
Figure 5.2. A Typical Thermocouple Sensor.

For additional protection beyond what is provided by the sheath, especially when the thermocouple is used in high velocity flow fields or reactive environments, an additional metallic jacket called a thermowell is sometimes used (Figure 5.3). In addition to protecting the sensor, a thermowell provides for easy replacement of the thermocouple and is sometimes used in industrial processes only for this purpose, especially when the transient response of the sensor is not important.

5.1   Junction Styles

The measuring junction of a thermocouple may be formed by any one of several methods. The most common methods for sheathed thermocouple junctions are (Figure 5.4):

- **Exposed Junction**. In this method, the measuring junction comes in direct contact with the medium being measured. The junction is formed by a twist-and-weld procedure or it is butt-welded. There are other ways to form the junction, but the two we mentioned are among the most common methods.

  Exposed junction thermocouples are usually used for measurement of gas temperatures and temperature of solid materials. The advantage of this construction is a fast response and the disadvantage is that the wires are not secured or protected from the environment, and are therefore subject to mechanical and chemical damage. If the exposed junction thermocouple is to be used in a liquid or moisture environment, its measuring junction should be covered with an insulating paint or epoxy. Furthermore, in these environments, it is important to seal the measuring tip of the thermocouple in a manner that would help avoid moisture ingress into the thermocouple.

- **Insulated Junction**. An insulated junction thermocouple is usually made of a sheathed thermocouple stock cut to a desired length. The junction is made by removing some of the insulation from the tip of the assembly and forming the junction with a similar procedure as in exposed junction. After the junction is formed, it is recessed into the assembly and tightly packed with insulation material. The tip is then welded closed with the same metal as the sheath material.

  The advantage of insulated junction thermocouples is that their circuit is isolated from the ground, and their insulation resistance can be readily measured to diagnose insulation defects if they occur. Their disadvantage is a larger response time

AMS—DWG THC082B

Terminal Block

Thermocouple

Thermowell

Connection Head
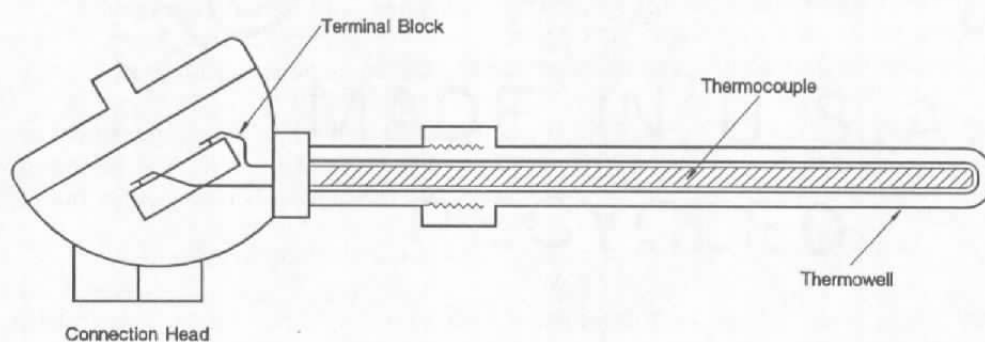
Figure 5.3. A Typical Thermocouple in Thermowell Installation.

AMS—DWG THC048E

Seal

Exposed Junction

End Cap

Insulated Junction

End Cap
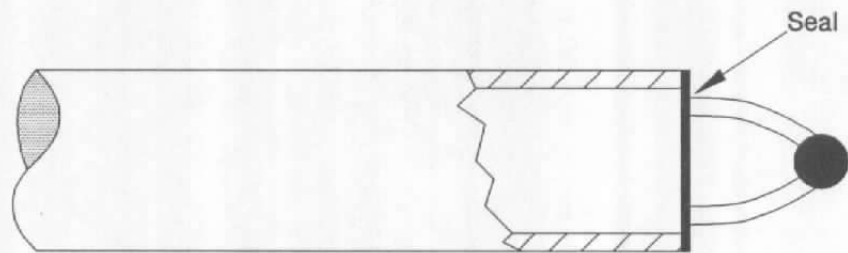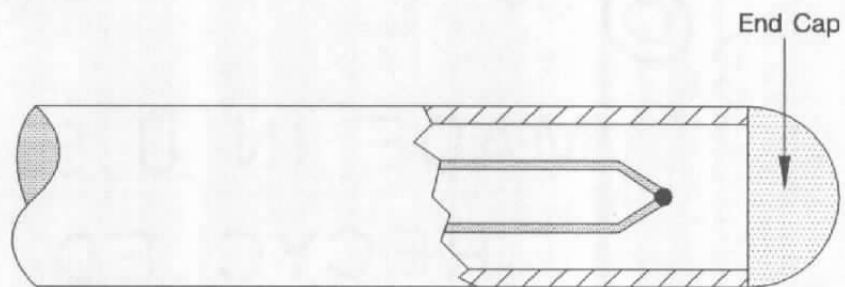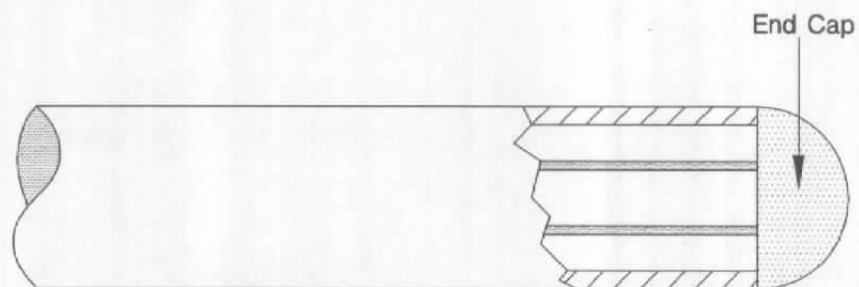
Grounded Junction

Figure 5.4. Typical Configurations of Measuring Junction
of Sheathed Thermocouples.

than exposed junction thermocouples and difficulty in fabricating them in small diameters. Insulated junction thermocouples are also called ungrounded junction thermocouples.

- **Grounded Junction.** These thermocouples are sheathed, but their junction style is much different than the two discussed above. The thermocouple is made using the same procedure as insulated junction thermocouples. Namely, sheathed thermocouple stock is cut to length and the tip is then welded closed forming the junction with the sheath closure weld. The advantage of this thermocouple is a fast response and ease of construction. The disadvantage is susceptibility to electrical ground loops and noise pickup and a possibility that the thermoelements may alloy with the sheath. Grounded junction thermocouples are also known to be more susceptible to open circuit failure with thermal cycling. Another disadvantage of grounded junction thermocouples is that their response times are not readily testable by the Loop Current Step Response (LCSR) method.

  Grounded junction thermocouples are sometimes found to have a slower response time than expected, and are occasionally found to be slower than insulated junction thermocouples of the same size and type. This happens when the hot junction is inadvertently formed somewhere other than the inside wall of the sheath. When grounded junction thermocouples are manufactured, the sheath and the thermocouple wires are melted together and allowed to solidify and form a junction at the tip of the assembly. If instead of forming on the inside wall at the tip of the sheath, the junction is formed inside the thermocouple wire and away from the sheath, then the thermocouple can have a slow response time. In fact, some grounded junction thermocouples are made by bending and welding the wires to the inside wall of the sheath rather than the tip to ensure a fast response time (Figure 5.5).

The junction styles discussed above apply mostly to sheathed thermocouples. For unsheathed thermocouples (also called bare wire thermocouples), the hot junction is formed much like an exposed junction thermocouple. More specifically, the junction may be in the form of a bead or it may be butt welded, lap welded, twisted and silver soldered, etc.

5.2   Standardized Thermocouples

There are approximately 300 types of thermocouples that have been researched or used among which only eight have gained popularity and are in common industrial use. These thermocouples are listed in Table 5.1 in two groups as base metal and noble metal depending on whether or not a noble or precious metal such as platinum is included in the thermocouple

AMS—DWG THC048D
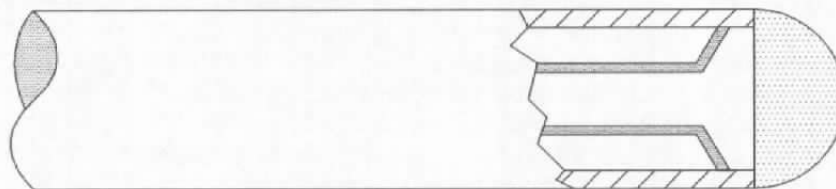
Figure 5.5. Junction Style of a Grounded Junction Thermocouple
Designed for Fast Response.

TABLE 5.1

Standardized Thermocouples

Type	Name	Material	
		Positive Leg	Negative Leg

Base Metal

Type	Name	Positive Leg	Negative Leg
E	Chromel/Constantan	Ni - 10% CR	Constantan
J	Iron/Constantan	Fe	Constantan
K	Chromel/Alumel	Ni - 10% CR	Ni - 5% (Al, Si)
N	Nicrosil/Nisil	Ni - 14% CR - 1.5% Si	Ni - 4.5% Si - 0.1% Mg
T	Copper/Constantan	Cu	Constantan

Noble Metal

Type	Name	Positive Leg	Negative Leg
B	Platinum-Rhodium/Rhodium-Platinum	Pt - 30% Rh	Pt - 6% Rh
R	Platinum-Rhodium/Platinum	Pt - 13% Rh	Pt
S	Platinum-Rhodium/Platinum	Pt - 10% Rh	Pt

Pt = platinum   *Cu = copper*
Rh = rhodium   *Constantan = A copper-nickel alloy*
Ni = nickel   *Si = Silicon*
CR = Chromium   *Mg = magnesium*

material. Two of the eight thermocouples, type K and N, are identical in most characteristics. In fact, type N is a new thermocouple that has been developed to overcome some of the drawbacks of the type K thermocouple such as the atomic ordering, the drift, and the oxidation problems.

Prior to the early 1960's, thermocouples were known by their proprietary names assigned by the manufacturers. The letter designation presently used was introduced by the Instrument Society of America (ISA) and later adopted (in 1964) as an American Standard. The letter designations are recognized in the ANSI-MC 96.1 Standard issued by the American National Standard Institute (ANSI) and the ASTM 230 Standard issued by the American Society for Testing and Materials (ASTM). These standards specify that if a thermocouple meets the nominal tolerances for their letter designations, then the tables given in the Monograph 125 published by the National Bureau of Standards (NBS), may be used to relate their EMF to temperature. (NBS is now known as the National Institute of Standards and Technology or NIST.)

5.3   Thermocouple Extension Wires

Thermocouple extension wires are used when it is necessary to locate the reference junction away from the thermocouple. In order to avoid any inhomogeneity in the thermocouple circuit before reaching the reference junction, the extension wires for base metal thermocouples are usually made of the same material as the thermocouple wires. However, noble metal thermocouples often use compensating extension wires fabricated from material different in composition from the thermocouple but with similar thermoelectric properties within a limited temperature range.

Thermocouple assemblies for regular industrial use are often made with the extension wires and thermocouple joined together through a connector. In other designs, the thermocouple wires themselves are made long enough to also serve as extension wires. In this design, the extension wires penetrate out of the thermocouple assembly through a transition piece with no discontinuity in thermocouple wires. The two different designs are referred to as Quick-Disconnect and Transition Type (Figure 5.6). In the Quick-Disconnect design, the metal contacts inside the connector are made of the same material as the thermocouple and the extension wires.

.

Thermocouples and their extension wires are usually color coded to aid in identification and to avoid inadvertent cross wiring. Table 5.2 shows the color codes for the eight most common thermocouples.

5.4   Reference Junction Compensation

The EMF output of a thermocouple can be converted to temperature of the measuring junction only if the reference junction temperature is known and its changes are compensated for in the measuring circuitry. A simple remedy is to keep the reference junction at a known and constant temperature medium such as an ice bath (Figure 5.7), or an oven.

In measurement and control instrumentation, maintaining a constant reference junction temperature is frequently inconvenient. Consequently, some measuring instruments use a reference junction compensating resistor (R_r) to automatically compensate for the changes in reference junction temperature (Figure 5.8). The reference junction resistor is at reference junction temperature and is usually sized so that the EMF from the voltage divider is zero at a

AMS–DWG THC053A

Thermocouple Connector   Sheathed Thermocouple

Transition Piece   Sheatned Thermocouple

Insulated Thermocouple
Extension Wire
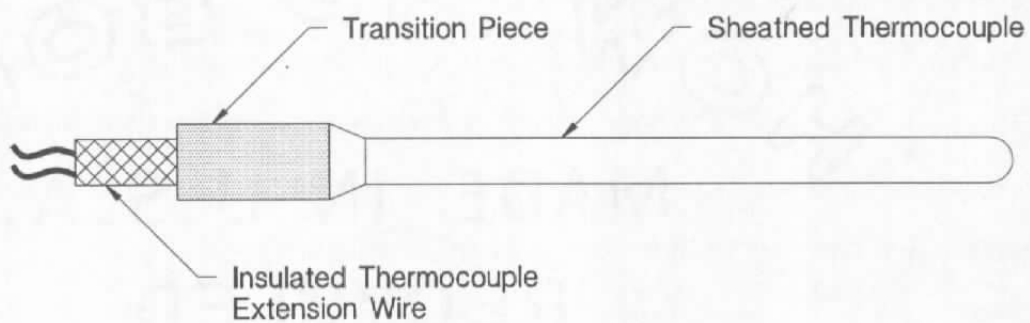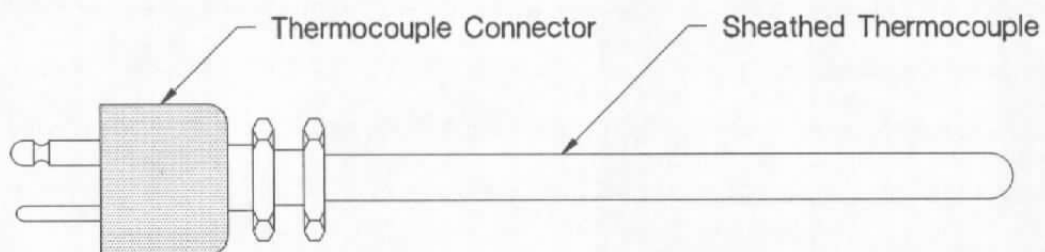
Figure 5.6. Quick-Disconnect and Transition-Type Designs of
Thermocouple Extension.

TABLE 5.2

Color Codes of Standardized
Thermocouples and Extension Wires

		Color of Insulation		
Type	Name	Positive Leg	Negative Leg	Overall

Base Metal

E	Chromel/Constantan	Purple	Red	Purple
J	Iron/Constantan	White	Red	Black
K	Chromel/Alumel	Yellow	Red	Yellow
N	Nicrosil/Nisil	Orange	Red	Brown
T	Copper/Constantan	Blue	Red	Blue

Noble Metal

B	Platinum-Rhodium/Rhodium-Platinum	Gray	Red	Gray
R	Platinum-Rhodium/Platinum	Black	Red	Green
S	Platinum-Rhodium/Platinum	Black	Red	Green

AMS—DWG THC043A

+ Wire

Measuring
Junction

Voltage
Measuring
Instrument

- Wire

Copper
Leads

Ice
Bath

Reference Junction
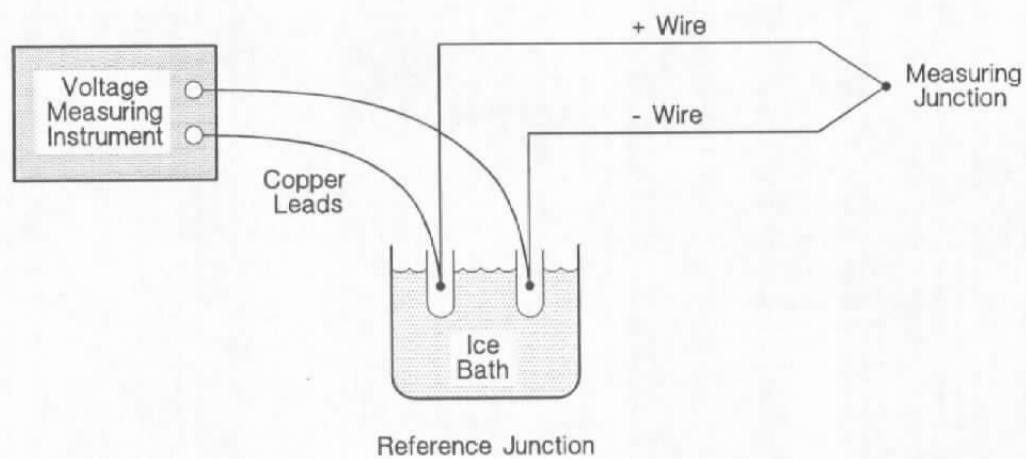
Figure 5.7. Equipment Setup for Temperature Measurement
With a Thermocouple.

AMS—DWG THC042A
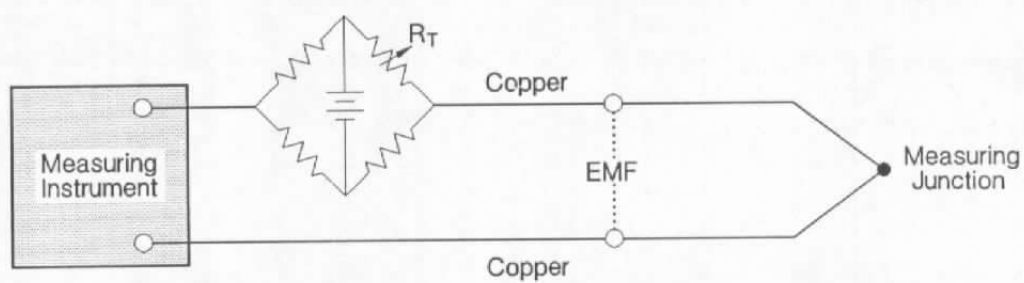
Figure 5.8. Reference Junction Compensation Circuitry.

reference ambient temperature. If the reference junction temperature increases, thermocouple EMF decreases, however, the reference junction resistor increases in resistance, adding an EMF in series with the thermocouple that is equal to the decrease in the thermocouple EMF. The measuring instrument consequently sees an EMF that is related only to the temperature of the measuring junction, regardless of a changing ambient temperature.

In digital instruments, compensation for changes in reference junction temperature is implemented differently. The incremental EMF caused by changes in reference junction temperature is directly added to or subtracted from the thermocouple EMF. A small constant current is supplied to the compensating resistor and the variations of the corresponding voltage is digitized and combined with the thermocouple EMF[5] to account for temperature changes at the reference junction.

6. THERMOCOUPLE CALIBRATION

Industrial thermocouples are not normally calibrated. Rather, they are used with standard reference tables or polynomial expressions given in the NBS Monograph 125 or the ASTM Standard 230. Each thermocouple type has its own reference table or polynomial expression. The manufacturers of thermocouple wires and thermocouple sensors usually calibrate representative samples of the wire after it is made, and apply the calibration to the rest of the wire or to the thermocouples that are made with the wire.

The standard reference tables are subject to the tolerances shown in Table 6.1. If these tolerances are not acceptable, then a representative sample of the thermocouple wire or the thermocouple sensor must be calibrated in a laboratory to provide a better accuracy.

6.1   Calibration Procedure

The calibration of thermocouples may be done by either of two methods: the comparison method and the fixed-point method. In the comparison method, the EMF of the thermocouple is measured at a number of temperatures and compared to a calibrated reference sensor such as a standard platinum resistance thermometer (SPRT), or a standard thermocouple. In the fixed-point method, the EMF is measured at several established reference conditions such as metal freezing baths whose temperatures are known from the laws of nature. The fixed points used for this purpose at the NIST are the freezing point of zinc (419.58°C), silver (961.43°C), and gold (1064.43°C). In addition, in fixed point calibration of thermocouples, NIST includes a measurement at 630.74°C. Almost all thermocouple calibrations performed by the NIST and others are done with the reference junction at ice point (0°C).

TABLE 6.1

Typical Temperature Ranges and Representative
Tolerances For Standardized Thermocouples

Type	Temperature Range (°C)	Tolerance (°C)	
		Standard Grade	Special Grade
Base Metal			
E	0 to 900	1.7 or 0.5%	1 or 0.4%
J	0 to 750	2.2 or 0.75%	1.1 or 0.4%
K	0 to 1250	2.2 or 0.75%	1.1 or 0.4%
N	0 to 1250	2.2 or 0.75%	1.1 or 0.4%
T	0 to 350	1.0 or 0.75%	0.5 or 0.4%
Noble Metal			
B	870 to 1700	0.5%	0.25%
R	0 to 1450	1.5 or 0.25%	0.6 or 0.1%
S	0 to 1450	1.5 or 0.25%	0.6 or 0.1%

Notes: 1. *Above tolerances apply to new thermocouple wires in the size range 0.25 to 3 mm in diameter.*

2. *Above tolerances do not apply below 0°C.*

3. *Above tolerances have a ± sign in all cases.*

The calibration data are tabulated as EMF versus temperature for the number of different temperatures in which the thermocouple is calibrated. Each pair of EMF versus temperature data is referred to as a calibration point. The number and the choice of the calibration points depends on the type of thermocouple being calibrated, the range of temperatures in which the thermocouple will be used, and the accuracy requirements. As little as four points are sometimes adequate, but there is an advantage in taking more calibration points especially if the thermocouple is to be used over a wide range. The static output of thermocouples is not linear and their EMF versus temperature cannot be modeled exactly for a wide temperature range. The best that is known to date is that the steady state behavior of commonly used thermocouples is reasonably represented by polynomial expressions of varying order except for type K. For type K, an exponential term should be added to the polynomial to provide for a complete characterization of EMF versus temperature. The general form of a polynomial expression for the EMF output of a thermocouple (E) versus temperature is written as:

$$E = a_0 + a_1 T + a_2 T^2 + a_3 T^3 + \ldots + a_n T^n \tag{6.1}$$

where a_0, a_1, a_2, $\ldots$ are constants called the coefficients of the polynomial, and n is the order of the polynomial. An optimum order depends on the thermocouple type and the temperature range for which the thermocouple is calibrated. Sometimes, more than one polynomial is used to cover the EMF versus temperature of a thermocouple over its entire operating range. For the eight most commonly used thermocouples and temperature ranges, the order n has values of as little as 2 or as large as 14 (Table 6.2).

In preparing the thermocouple for calibration, the measuring junction is usually welded to the measuring junction of a standard thermocouple. If welding is not possible, such as when

TABLE 6.2

Order of Polynomials for
Standardized Thermocouples

Type	Temperature Range (°C)	Order (n)
Base Metal		
E	-270 to 0	13
	0 to 1000	9
J	-210 to 760	7
	760 to 1200	5
K	-270 to 0	10
	0 to 1372	8
N	-270 to 0	8
	0 to 1300	9
T	-270 to 0	14
	0 to 400	8
Noble Metal		
B	0 to 1820	8
R	-50 to 630.74	7
	1064.43 to 1665	3
	1665 to 1767.6	3
S	-50 to 630.74	6
	630.74 to 1064.43	2
	1064.43 to 1665	3
	1665 to 1767.6	3

an SPRT is used, the junction of the thermocouple and the tip of the SPRT are attached together with a wire, or placed adjacent to one another.

Figure 6.1 shows a block diagram of the steps followed by the NIST in calibrating a thermocouple by the comparison method in a furnace. Bare wire thermocouples and sheathed thermocouples are calibrated the same way. Figure 6.1 shows the process for both the noble metal and base metal thermocouples. The differences between the calibration processes for the two groups of thermocouples are that the base metal thermocouples are not annealed, and the calibration data for base metal thermocouples is taken in order of increasing temperatures specified by the user. In contrast, the noble metal thermocouples are annealed before calibration, and the calibration process proceeds from high to low temperatures. Instead of annealing the base metal thermocouples, the NIST requires that new thermocouple wires that can safely be assumed as homogeneous be sent for calibration.

It should be noted that a homogeneity test is necessary before a thermocouple is calibrated whether it is a noble metal or a base metal thermocouple. A thermocouple that has any inhomogeneous section may have a different EMF versus temperature relationship when it is placed in service than it does during the calibration process, depending on the temperature gradient across the inhomogeneity. It is due to the potential for inhomogeneity that thermocouples which have been previously heated or installed in a process are not calibrated without a systematic inspection for inhomogeneity.

NIST also calibrates single leg thermocouple wires. These wires are sometimes referred to as thermoelements. A single wire is calibrated against the platinum thermoelectric reference

Comparison Calibration of
Thermocouples (T/Cs) at NIST

Noble Metal T/C
S,R,B

Base Metal T/C

Visual Examination at Receipt
(Record Dimensions and Conditions)

Visual Examination at Receipt
(Reject if Not New)

Electrical Anneal
1450°C for 45 Minutes

Mount T/C in Insulating Tube

Mount T/C in Insulating Tube

Weld the Test T/C to a
Calibrated Reference T/C

Weld the Test T/C to a
Calibrated Reference T/C

Furnace Anneal
1100°C for 30 Minutes

Homogenity Check
(Immersion Test in a Furnace
at 1100°C). Reanneal
or Reject if Not Homogeneous

Calibrate From 1100°C Down
to 100°C (Measure EMFs of
Test T/C and Reference
T/C Simultaniously)

Calibrate (Slowly Increasing
Temperature and Measure
EMFs of Test T/C and
Reference T/C Simultaniously)

Figure 6.1. NIST Procedure for Comparison
Calibration of Thermocouples.

standard identified and maintained by the NIST as Pt-67. Both the noble metal and the base metal wires are calibrated against Pt-67. The thermoelement is joined with Pt-67 to form a thermocouple and is calibrated using the process shown in Figure 6.1.

As mentioned earlier, the comparison calibration can be performed with a standard thermocouple (such as type S), or a standard platinum resistance thermometer (SPRT) as a reference. When an SPRT is used, the calibrations are performed in stirred liquid baths as opposed to a furnace (for temperatures above ice point), and the measuring junction of the test thermocouple is placed adjacent to the tip of the SPRT in the bath, but not attached or welded to it.

6.2   Processing of Calibration Data

Processing of calibration data generally begins by calculating the difference between the measured EMFs and the EMFs given in the standard reference tables for the thermocouple being calibrated (test thermocouple). The differences are calculated for all calibration points and mathematically fit to a low order polynomial. The coefficients of the low order polynomial are identified from the fit and summed with the corresponding coefficients in the polynomial given for the test thermocouple in Monograph 125 or ASTM Standard 230. This will provide a new polynomial representing the EMF versus temperature relationship of the test thermocouple after calibration. The procedure is shown in Figure 6.2 and is summarized below:

1.   Measure the calibration medium's temperature (T) with a reference sensor (a type S thermocouple or an SPRT).

2.   Measure the EMF of the test thermocouple (E_M) at temperature T.

45

AMS-DWG BLKO14A

```
┌─────────────────────────────┐
│      Data Processing for     │
│     Comparison Calibration   │
└─────────────────────────────┘
                │
┌─────────────────────────────┐
│    Measure Bath Temperature  │
│         with SPRT or         │
│     Reference Thermocouple   │
└─────────────────────────────┘
         │                │
┌──────────────────┐  ┌──────────────────────┐
│  Measure EMF of  │  │  Look up EMFs from   │
│     Test T/C     │  │ Monograph 125 for the│
│                  │  │   Type of Test T/C   │
│     EMF(T)       │  │      EMF(S)          │
└──────────────────┘  └──────────────────────┘
         │                │
┌─────────────────────────────┐
│   Calculate the Difference   │
│    Between the Two EMFs      │
│                              │
│   De = EMF(T) − EMF(S)       │
└─────────────────────────────┘
                │
┌─────────────────────────────┐
│   Fit De Data to a Polynomial│
│                              │
│        De = f(t)             │
└─────────────────────────────┘
                │
┌─────────────────────────────┐
│  Combine the Polynomial with │
│ Monograph 125 Polynomial for │
│  the Same Type Thermocouple  │
└─────────────────────────────┘
```

Figure 6.2. Procedure for Processing of
Thermocouple Calibration Data.

3. . Look up in the standard reference tables, the EMF of the test thermocouple at temperature T, or use the polynomial expression for the test thermocouple to obtain the EMF (Es):

$$E_s = a_0 + a_1 T + a_2 T^2 + a_3 T^3 + \ldots + a_n T^n \tag{6.2}$$

4. Calculate the difference between the measured and the reference table EMFs; $\Delta E = E_M - E_s$

5. Repeat from step 1 with a different temperature until the differences are identified at all calibration points.

6. Fit ΔE to a low order polynomial such as:

$$\Delta E = b_0 + b_1 T + b_2 T^2 + \ldots \tag{6.3}$$

Identify b_0, b_1, b_2, ... from the fit. Usually, a low order polynomial such as second or third order is used for the fit of the EMF differences. The decision on the order of the polynomial for fitting the difference may be made by implementing an error minimization algorithm to find the best fit.

7. Combine Equations 6.2 and 6.3 to obtain the new polynomial for the test thermocouple:

$$E_0 = (a_0 + b_0) + (a_1 + b_1) T + (a_2 + b_2) T^2 + a_3 T^3 + \ldots + a_n T^n \tag{6.4}$$

An alternative data processing procedure is to fit the raw calibration data for the test thermocouple to a polynomial directly and select an appropriate order for the polynomial that gives the best fit. This is a more straightforward procedure that can be implemented on a calculator or a small computer. The procedure outlined in the 7 steps above is the conventional approach that was developed to facilitate data reduction when computer data processing was not as simple as it is now.

It should be pointed out that the discussions that we have carried in this chapter do not reflect the new International Temperature Scale of 1990 (ITS 90). The new scale became effective on January 1, 1990. In light of the ITS 90, new guidelines may be applicable to the calibration of thermocouples.

7. PRINCIPLES OF THERMOELECTRIC THERMOMETRY

7.1   Thermoelectric Effects

Thermocouples are reversible heat engines that convert thermal energy to electricity according to three phenomenon known by the names of the scientists who discovered them. These phenomenon are referred to as Seebeck effect, Peltier effect, and Thomson effect. These effects are reviewed below:

Seebeck Effect. The Seebeck effect defines the relationship between EMF, also called the open circuit voltage (E), and the temperatures at the two junctions of a thermocouple (Figure 7.1).

$$E = s_{ab} (T_2 - T_1) \qquad (7.1)$$

where s_{ab} is referred to as the relative Seebeck coefficient for the two wires a & b, and T_1 & T_2 are the temperatures of the two thermocouple junctions. It is important to point out that the open circuit voltage, also known as Seebeck voltage, is not generated at the junction. Rather, it is a cumulative voltage developed along the thermocouple wires. As such, the equation relating the EMF to temperature is generally written as:

$$E = \int^l s \, \nabla T \cdot d \, x \qquad (7.2)$$

where s is the Seebeck coefficient for the thermocouple wires, ∇T is the temperature gradient at any position x along the thermocouple wires, and l is the length of the wire. If the thermocouple wires are homogeneous, s would be a function of only T and not x, and we can therefore write:

$$E = \int_{T_1}^{T_2} s \, d \, t \qquad (7.3)$$

Peltier Effect. The Peltier effect is the basis for thermoelectric heating and cooling. Peltier found that cooling and heating occurs in a thermocouple junction by passage of an electric current. This happens whether the current is originated in the circuit due to the Seebeck voltage or it is applied to the circuit by an external source. If the current flow is in the same direction as the Seebeck current, the junction is cooled and if it flows in the opposite direction, the junction is heated.

48

AMS—DWG THC046A
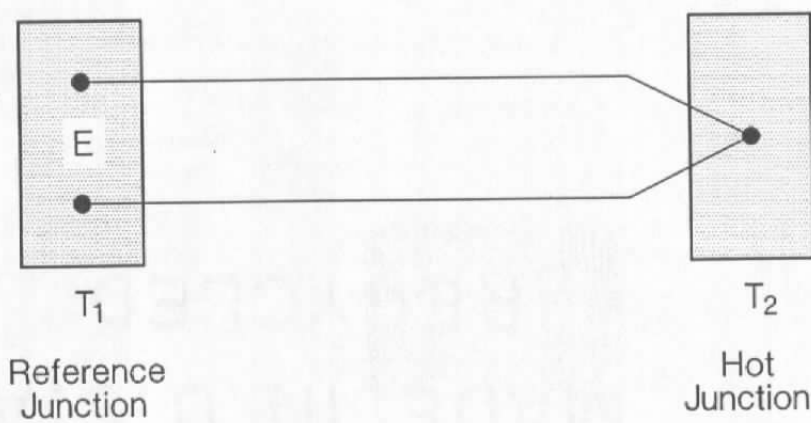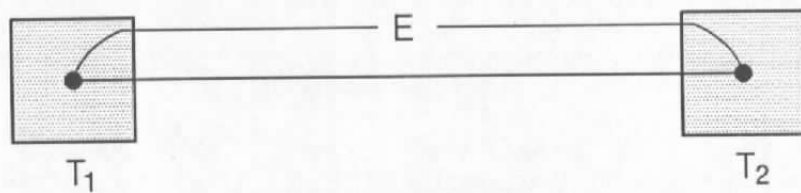
Figure 7.1. Typical Thermocouple Circuits.

49

The Peltier effect is not related to thermoelectric thermometry, but it has an implication in the response time testing of thermocouples using the Loop Current Step Response (LCSR) method described later in this report. If a DC current is used in performing the LCSR test, then the thermocouple may undergo cooling or heating, depending on the direction of the applied DC current. Initially, this effect was thought to be detrimental to the LCSR test if it cooled the junction, and subsequently it was thought to be helpful to the LCSR test if it heated the junction. However, laboratory tests performed in this project have shown that the Peltier effect is neither significantly harmful nor significantly helpful in testing the thermocouple types and sizes studied here. Nevertheless, in the LCSR developments which were carried out in this project, high frequency AC currents were employed to avoid the Peltier question altogether.

Thomson Effect. The Thomson effect occurs in a single conductor as demonstrated in Figure 7.2. If a conductor is heated at a point to a temperature T_1, two points p_1 and p_2, on either side will be at a lower temperature T_2. If a current flows in the wire as shown in Figure 7.2, electrons absorb energy at point p_2, as the current flows opposite to the temperature gradient, and release this energy at point p_1, as the current flows in the same direction as the temperature gradient. Because the gain and the loss are equal, there is no net effect along the wire. That is, the application of heat to a single homogeneous wire does not generate a net thermoelectric voltage according to Thomson (Thomson is also known as Lord Kelvin).

Although the behavior of a thermocouple can be described in terms of the simple relationships such as Equation 7.1, it is not simple to model a thermocouple to predict its output analytically from information about its structure or composition. The EMF versus temperature relationships of thermocouples are predominantly empirical, even though thermodynamic principles and free electron theory of metals can help provide a qualitative insight into their theory of operation.

7.2   The Laws of Thermoelectricity

The behavior of thermocouple circuits has been summarized in terms of statements referred to as the laws of thermoelectricity. There are about six laws, three of which are the most important and useful and are discussed below.

AWS-DWG THCB41A
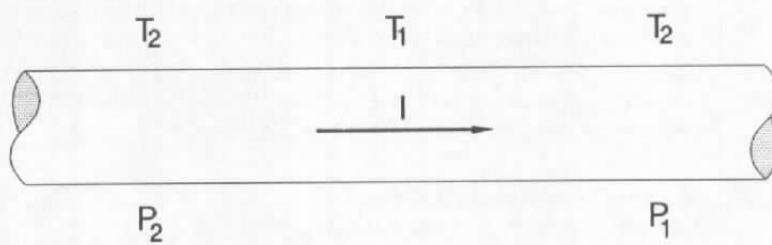
Figure 7.2. Illustration of Thomson Effect.

1. **Law of Homogeneous Metals**. The EMF output of a thermocouple made of two homogeneous metals is not affected by temperature other than the temperatures at the two junctions.

2. **Law of Intermediate Metals**. In a circuit of dissimilar metals, if a third homogeneous wire is added between points X and Y, as shown in Figure 7.3, no additional EMF will be generated if points X and Y are at the same temperature. Stated differently, the algebraic sum of the EMFs in a circuit of any number of dissimilar metals is zero if all the wires are at a uniform temperature, i.e,

$$EMF = \sum_{i=1}^{n} s_i \, (T_{i+1} - T_i) \qquad (7.4)$$

    A special case of the law of intermediate metals is described below:

    > If metal C is inserted between metals A and B, at one of the junctions, the temperature of C at any point away from AC and BC junctions is immaterial as long as the junction AC and BC are at the same temperature (Figure 7.4). This law indicates that the measuring junction can be formed by any number of ways such as a wire made of any material, soft solder, silver solder, brazing, or wrapping the metals together and/or welding as long as the thermoelements of the measuring junction are connected electrically.

3. **Law of Intermediate Temperatures**. The EMF generated by a thermocouple between temperatures T_A and T_C is the sum of the EMF generated (by the same thermocouple) between T_A and T_B and that generated between T_B and T_C if $T_A < T_B < T_C$. This is the basis for using the generic thermocouple calibration charts that are written with reference to 0°C.

7.3 Thermocouple Circuit Analysis

A few examples of typical thermocouple circuits are discussed below to illustrate how the three laws of thermoelectricity are used and to help in diagnosis of thermocouple circuit problems.

> **Example 1**. Recalling that the sum of individual Seebeck voltages in a thermocouple circuit equals to the thermocouple output EMF, we start with the simplest thermocouple circuit (Figure 7.5a):

AMS—DWG THC054A
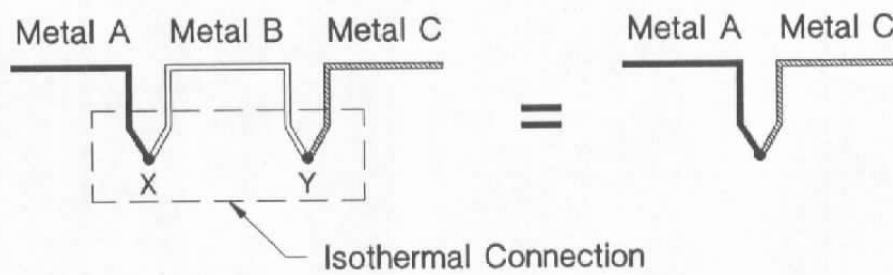
Figure 7.3. Law of Intermediate Metals.

AMS—DWG THC070C
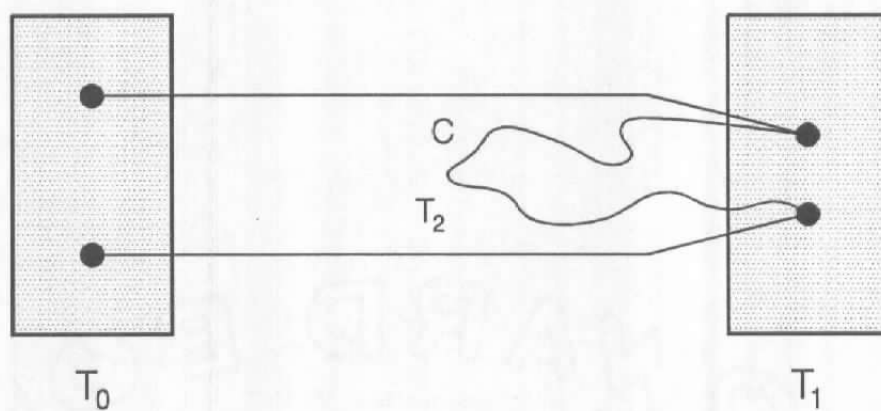
Figure 7.4. Special Case of Laws of Intermediate Metals.
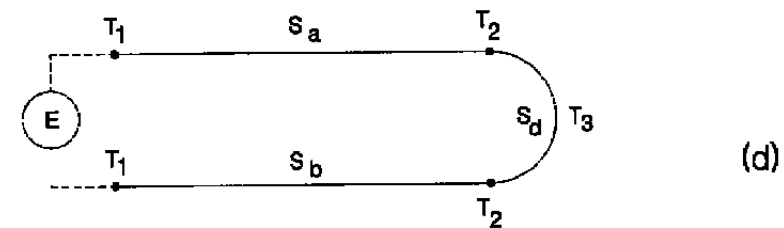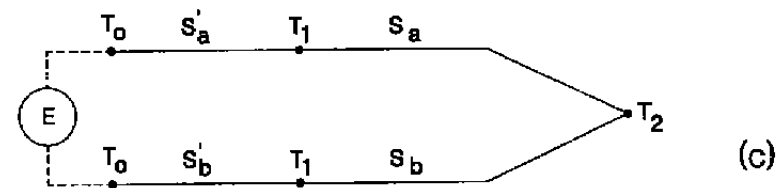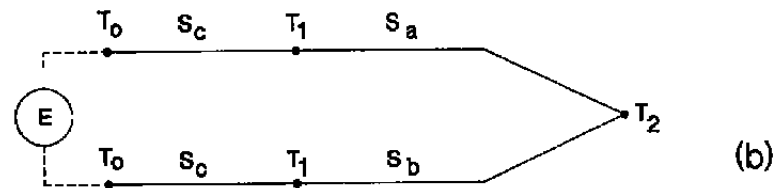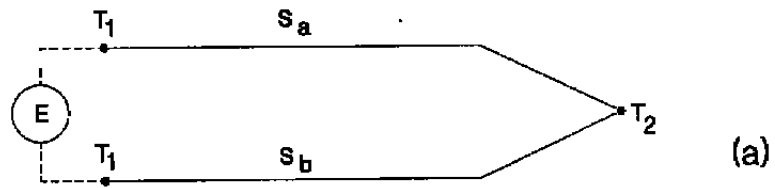
Figure 7.5. Thermocouple Circuit Analysis.

$$E = s_a \left(T_2 - T_1\right) + s_b \left(T_1 - T_2\right)$$

$$= s_a \left(T_2 - T_1\right) - s_b \left(T_2 - T_1\right) = \left(s_a - s_b\right)\left(T_2 - T_1\right) \tag{7.5}$$

where E is the open circuit voltage of the thermocouple, T_1 & T_2 are the temperatures of the two thermocouple junctions, and s_a & s_b are the absolute Seebeck coefficients for the two thermocouple wires. If the relative Seebeck coefficient is denoted as s_{ab}, we can write:

$$s_a - s_b = s_{ab}$$

$$E = s_{ab} \left(T_2 - T_1\right) \tag{7.6}$$

Example 2. We now show the effect of extension wires on the output of a thermocouple (Figure 7.5b). Assuming that the extension wires are made of copper with Seebeck coefficient s_c, we can write:

$$E = s_c \left(T_1 - T_0\right) + s_a \left(T_2 - T_1\right) + s_b \left(T_1 - T_2\right)$$

$$+ s_c \left(T_0 - T_1\right) = s_{ab} \left(T_2 - T_1\right) \tag{7.7}$$

That is, the addition of the extension wires does not alter the thermocouple output.

Example 3. Sometimes thermocouples are extended with thermocouple extension wires made of similar materials so that the reference junction can be placed remote from the thermocouple site. Assuming that the extension wires have Seebeck coefficients s_a' and s_b' (Figure 7.5c) we can write:

$$E = s_a' \left(T_1 - T_0\right) + s_a \left(T_2 - T_1\right) + s_b \left(T_1 - T_2\right)$$

$$+ s_b' \left(T_0 - T_1\right) = s_{ab} \left(T_2 - T_1\right) + s_{ab}' \left(T_1 - T_0\right) \tag{7.8}$$

$$E = s_{ab} \left(T_2 - T_0\right) \quad \text{if} \quad s_{ab}' = s_{ab}.$$

Note that the temperature T_1 (which occurs at the thermocouple connector site) does not have any effect in the output as long as $s_{ab}' = s_{ab}$. Note also that it is not required for the absolute Seebeck coefficients to be equal as long as the relative Seebeck coefficients are equal ($s_{ab}' = s_{ab}$).

Example 4. This example corresponds to the law of thermoelectricity which allows for the junction to be made of a third material such as soft solder, silver solder, etc. If the Seebeck coefficient of the third material is s_d, we can write (Figure 7.5d):

$$E = s_a \ (T_2 - T_1) + s_d \ (T_3 - T_2) + s_d \ (T_2 - T_3)$$

$$+ \ s_b \ (T_1 - T_2) = s_{ab} \ (T_2 - T_1)$$

(7.9)

A consequence of the above analysis is in cases where thermocouple wires are individually attached to a metallic object to measure its temperature. This analysis shows that the thermoelectric properties of the metallic object play no role in the temperature measurement.

8. FUNDAMENTALS OF SENSOR DYNAMICS

The dynamic response of a sensor or a system may be identified theoretically or experimentally. For a temperature sensor such as a thermocouple, the theoretical approach requires a thorough knowledge of properties of the sensor internal materials and their geometries as well as a knowledge of the properties of the medium surrounding the sensor. Since these properties are not known thoroughly, or may change under process operating or aging conditions, the analytical approach alone can only provide approximate results. A remedy is to combine the theory with experiments.

The theory is used to determine the expected behavior of the sensor in terms of an equation called the *"model"* which relates the input and the output of the system. The system is then given an experimental input signal and its output is measured and matched with the model. That is, the coefficients of the model are changed iteratively until the model matches the data within a predetermined convergence criterion. This process is carried out on a digital computer and is referred to as *"fitting"*. Once the fitting is successfully completed; the coefficients of the model are identified and used to determine the response time of the sensor. However, if the sensor can be represented with a first order model, a fitting is not necessary because the response time can be determined directly from the output of the sensor. The definition of a first order model and its dynamic response is described later in this chapter.

The model for a sensor or a system may be expressed in terms of a time domain or a frequency domain equation. The time domain model is usually a specific relationship giving the transient output of the system for a given input signal such as a step or a ramp signal. The

frequency domain model is often represented as a general relationship called the "*transfer function*" which includes the input. If the transfer function is known, the system response can be obtained for any input. As such, the transfer function is often used in analysis of system dynamics.

In steady state analysis, the transfer function is a constant called "*Gain*" which relates the DC output to the DC input (Figure 8.1). The Gain is also referred to as the zero order transfer function. In dynamic system analysis, the transfer function is defined in terms of the Laplace transforms of changes that occur in system output per changes in system input (Figure 8.2):

$$G(s) = \frac{\delta O(s)}{\delta I(s)} \tag{8.1}$$

$G(s)$ = transfer function
δO = changes in system output
δI = changes in system input
s = frequency domain parameter

The section that follows uses a simple example to illustrate how the transfer function of a thermal system is derived and how it is used to interpret experimental results.

8.1 Response of a Simple Thermal System

Consider a thermocouple whose sensing section is assumed to be made of a homogeneous material represented by the mass "m" and specific heat capacity "c" as shown in Figure 8.3. The response time of this system, when it is suddenly exposed to a medium with temperature T_f, may be derived theoretically using the energy balance equation describing the

$$G = \frac{Ka}{a}$$
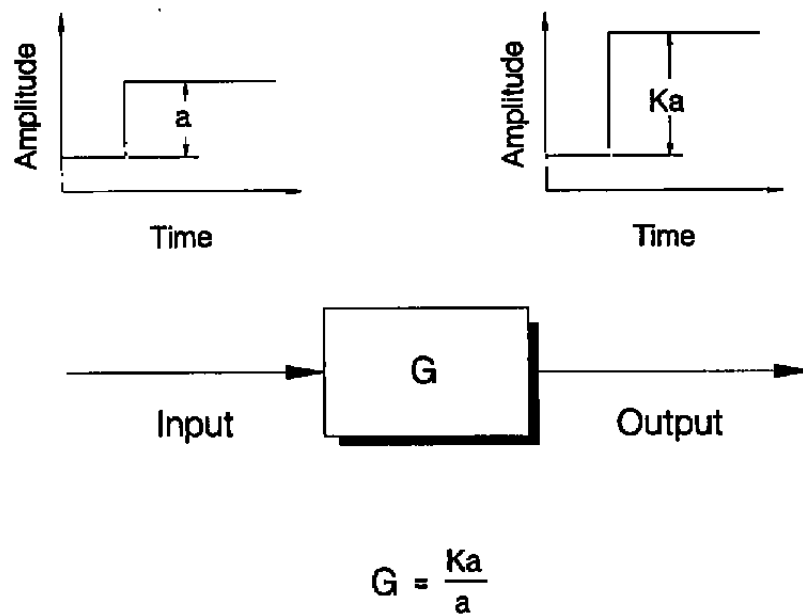
Figure 8.1. Illustration of Zero Order Transfer Function.

AMS—DWG PXT014Q

Transfer
Function

G

Input δI

Output δO

$$G = \frac{\delta O}{\delta I}$$
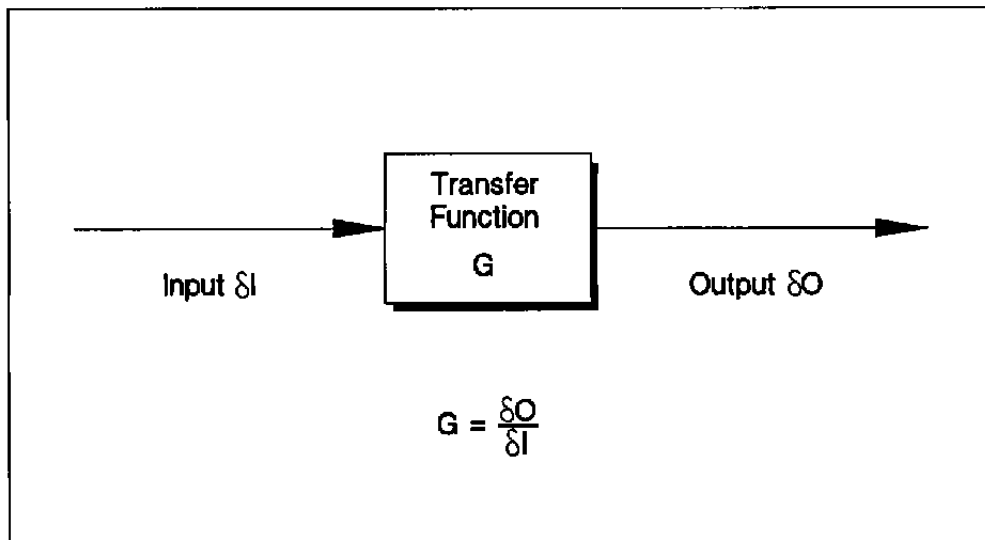
Figure 8.2. General Representation of Dynamic
Transfer Function.
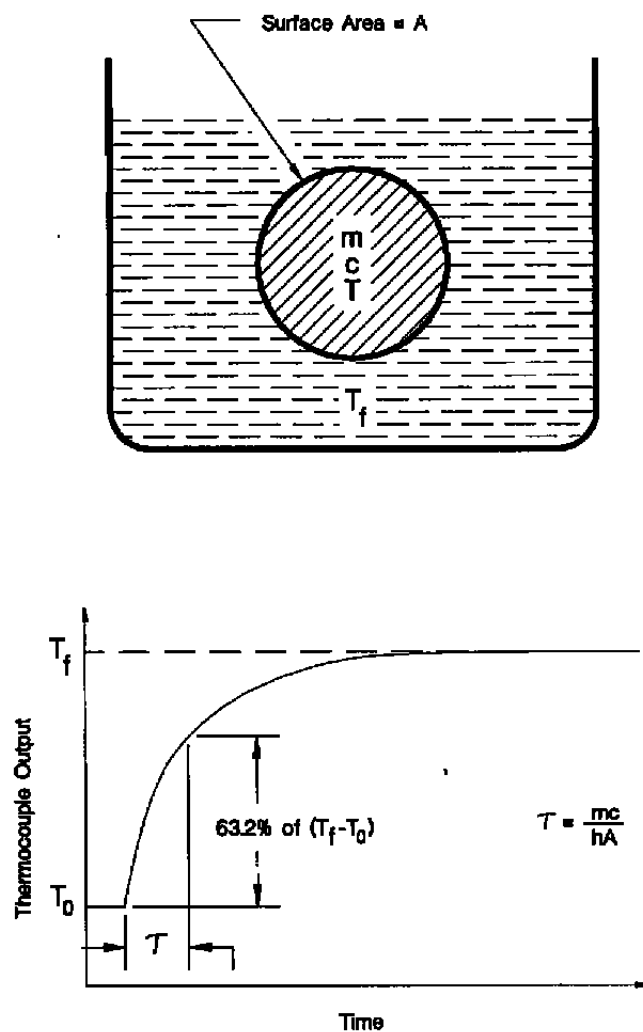
Figure 8.3. Step Response of a First Order Thermal System.

system. Assuming that the thermal conductivity of the thermocouple material is infinite, we can write:

$$mc \ \frac{dT}{dt} = hA \ (T_f - T)$$ (8.2)

Equation 8.2 is a first order differential equation representing the dynamics of the first order thermal model, and its parameters are:

h = heat transfer coefficient
A = affected surface area
T = response of the system as a function of time, t.

Equation 8.2 may be solved in time domain by integration, or in frequency domain by Laplace transformation of both sides of the equation. We will proceed with the latter approach. This will allow us to express the solution in terms of a transfer function of the following from which relates the Laplace transform of the output, $T(s)$, to the Laplace transform of the input, $T_f (s)$:

$$G(s) = \frac{T(s)}{T_f(s)}$$ (8.3)

The Laplace transformation of Equation 8.1 is:

$$sT(s) - T(0) = p[T_f(s) - T(s)]$$ (8.4)

where
$$p = \frac{hA}{mc}$$

s = Laplace transform variable

To simplify our derivation, let's assume that $T(0) = 0$, then:

$$G(s) = \frac{T(s)}{T_f(s)} = \frac{p}{s + p} \qquad (8.5)$$

where $G(s)$ is the transfer function of the first order system and p is referred to as the pole of the transfer function. The reciprocal of p has the unit of time and is called the time constant (τ) of the first order system:

$$\tau = \frac{mc}{hA} \qquad (8.6)$$

As shown below, the transfer function can be used to derive the response of the system to any input such as a step, a ramp, or a sinusoidal input. The following derivation will also show that the same numerical value is obtained for the response time of a first order dynamic system whether we use a step, a ramp, or a sinusoidal input. Proceeding to derive the step response, we can write:

$$T_f(s) = \delta I(s) = \frac{a}{s} \qquad (8.7)$$

where a is the step amplitude. Substituting Equation 8.7 in 8.5, we will obtain:

$$T(s) = \frac{pa}{s\,(s + p)} \qquad (8.8)$$

The inverse Laplace transform of Equation 8.8 will give the step response of the system as follows:

$$O(t) = a\,(1 - e^{-\frac{t}{\tau}}) \quad where \quad \tau = \frac{1}{p} \qquad (8.9)$$

If we now perform an experiment in which the output of the system is measured for a step change in input, the data would resemble the curve shown in Figure 8.4. These data can now

AMS—DWG RSP001F
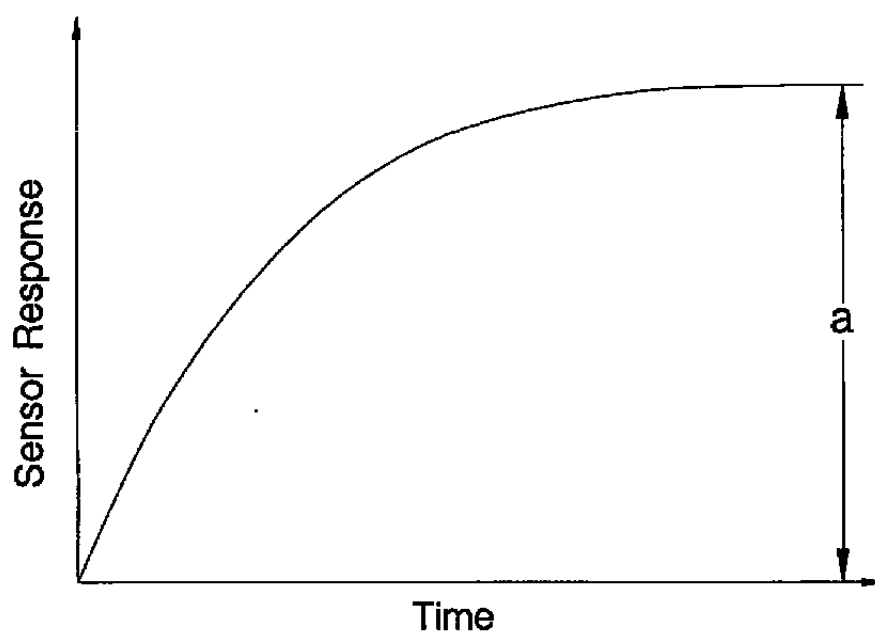
Figure 8.4. Step Response of a First Order System.

be fitted to Equation 8.9 to obtain the time constant (τ). However, fitting is not necessary in this simple case because Equation 8.9 can simply be solved for $t = \tau$ as:

$$O(t = \tau) = a(1 - e^{-1}) = 0.632\,a$$

$$O(t = \infty) = a \quad ; \quad a = final\ value$$

(8.10)

Equation 8.10 shows that the time constant of the system can be identified directly from the transient data shown in Figure 8.5. This is done by determining the time that is required for the system output to reach 63.2 percent of its final value.

The ramp response is obtained by substituting the Laplace transform of a ramp signal $\dfrac{r}{s^2}$ for $T_f\,(s)$ in Equation 8.5:

$$T(s) = \frac{rp}{s^2(s + p)}$$

(8.11)

where rp is a constant which we denote as k. An inverse Laplace transform of this equation results in:

$$O(t) = k\left[t - \tau + \tau e^{\frac{-t}{\tau}}\right]$$

(8.12)

A plot of this equation is shown in Figure 8.6. Note that when $t >> \tau$, the exponential term will be negligible and we can write:

$$O(t) = k\,(t - \tau)$$

(8.13)

That is, the asymptotic response of the system is delayed with respect to the input by a value equal to the step response time constant (τ).

AMS–DWG PXT025E
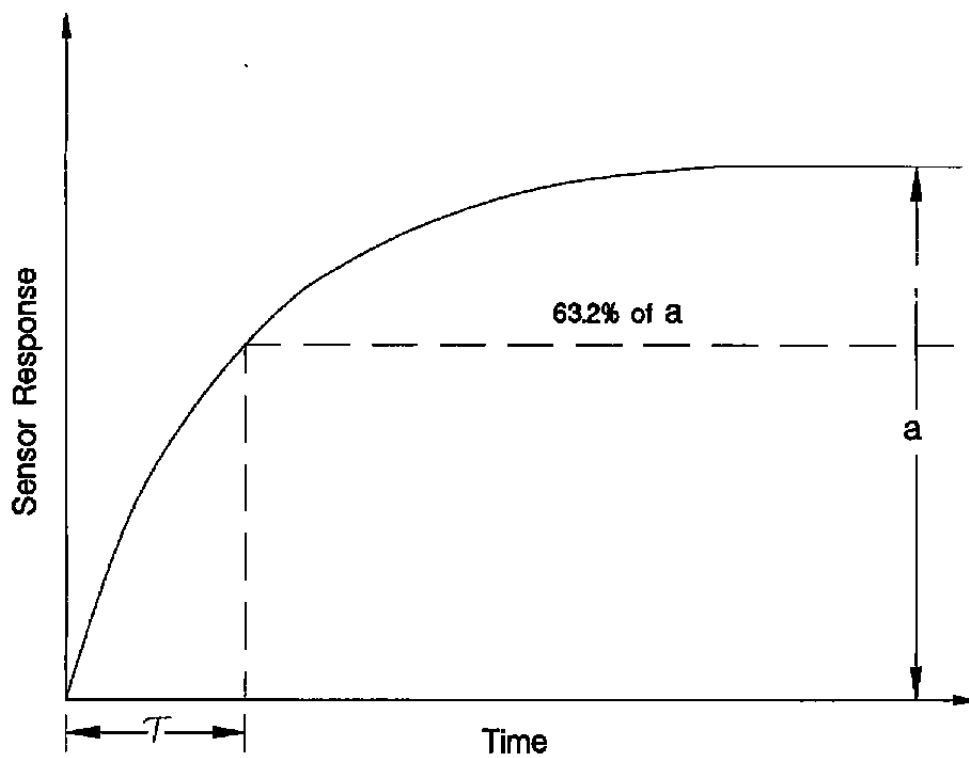
Figure 8.5. Determination of Time Constant from Step
Response of a First Order System.

AMS—DWG PXT022E
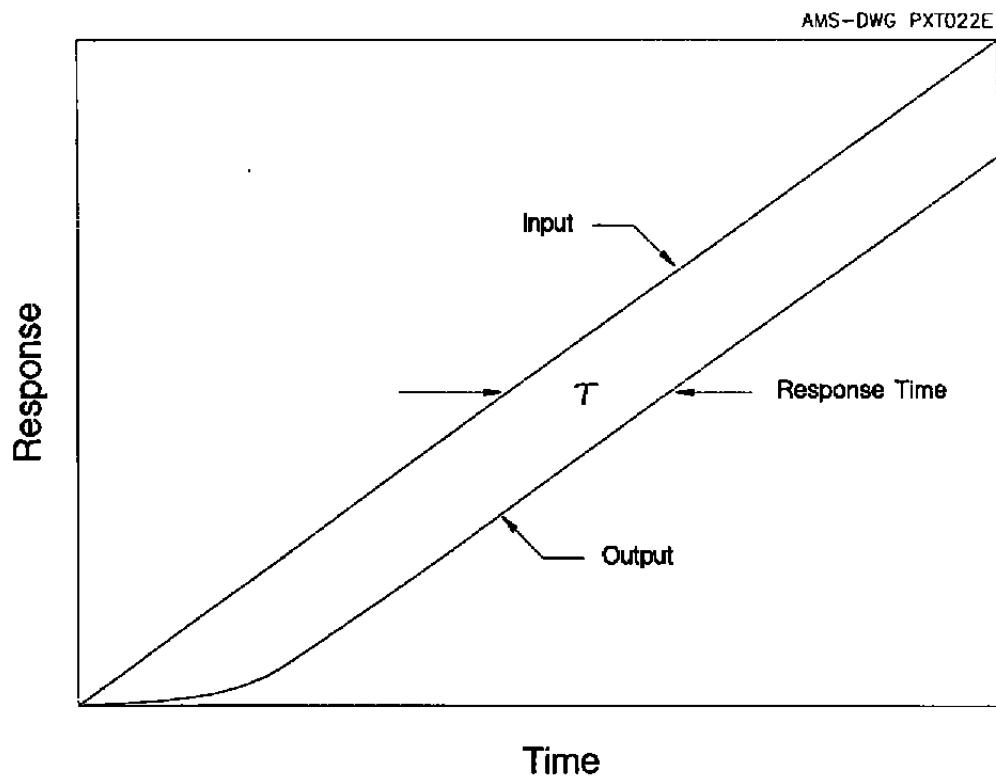
Figure 8.6. Illustration of Ramp Response.

For a sinusoidal input, the response time is expressed in terms of the reciprocal of the corner frequency of the frequency response plot (i.e., the break frequency of the Gain portion of the Bode plot). The corner frequency is denoted by the letter ω. We will show that $(\frac{1}{\omega})$ is equal to the time constant (τ) for a first order system. Substituting $j\omega$ for s in Equation 8.5 and writing τ for $(\frac{1}{p})$, we will obtain:

$$G(j\omega) = \frac{1}{j\omega\,\tau + 1} \tag{8.14}$$

where ω is the angular velocity in radians per second and $j = \sqrt{-1}$, a complex number. The magnitude of $G(j\omega)$ is:

$$|G| = \left[\frac{1}{\omega^2\tau^2 + 1}\right]^{\frac{1}{2}} \tag{8.15}$$

The corner frequency is the frequency at which $|G| = 0.707$. Substituting this in the above equation and solving for τ, we obtain $\tau = \frac{1}{\omega}$.

8.2   Characteristics of First Order Systems

A first order system is defined as a system that can be represented by a first order differential equation such as Equation 8.2. A first order system is also defined as a system that has only one pole in its transfer function such as Equation 8.5.

The response time of a first order system is expressed in terms of an index called time constant, ramp time delay, or frequency response, depending on how the index is measured.

If it is measured using a step input signal, the response time is usually expressed as time constant. If it is measured using a ramp input signal, it is called a ramp time delay; and if it is measured using a periodic signal such as a sinewave, it is called the frequency response of the first order system. A unique feature of a first order system is that its time constant, ramp time delay, and frequency response (expressed in terms of reciprocal of corner frequency), are numerically equal. Figure 8.7 presents a summary of the dynamic responses of a first order system for four different input signals. This includes the response for a nondeterministic input signal such as the random noise shown in the last item of Figure 8.7.

8.3   Definition of Time Constant

The time constant of a system in general is defined as the time required for the system output to reach 63.2 percent of its final value following a step change in input. Although this definition is based on the response of a first order system (Equation 8.10), it is conventionally used in defining the response time of temperature sensors such as thermocouples and RTDs that are not necessarily first order.

All references to the term time constant throughout this report correspond to the definition given above, regardless of the dynamic order of the system.

It should be noted that the normalized step response transients for two first order systems that have the same time constant are readily superimposed, while the step response transients for two higher order systems that pass the 63.2 percent mark at the same time may or may not have the same transient behavior (Figure 8.8). This indicates that a single time constant does not adequately characterize the dynamic response of systems that are not first order.

AMS-DWG PXT087C

Summary
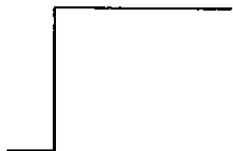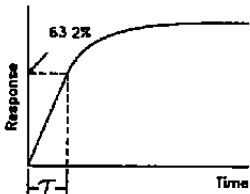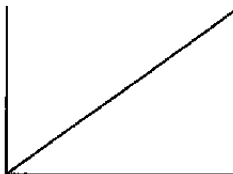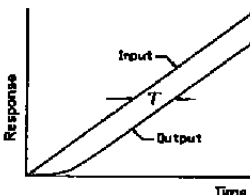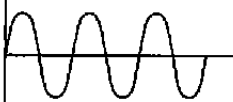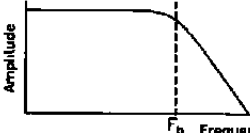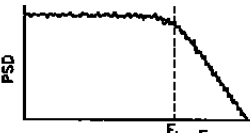
Input	Output	Result
	63 2% / Response / Time / T	Time Constant
	Input / T / Output / Response / Time	Ramp Time Delay
	Amplitude / F_b Frequency	Frequency Response $$T = \frac{1}{2\pi F_b}$$
	PSD / F_b Frequency	Response Time $$T = \frac{1}{2\pi F_b}$$

Figure 8.7. Transient Responses of a First Order System
for Various Input Signals.

71
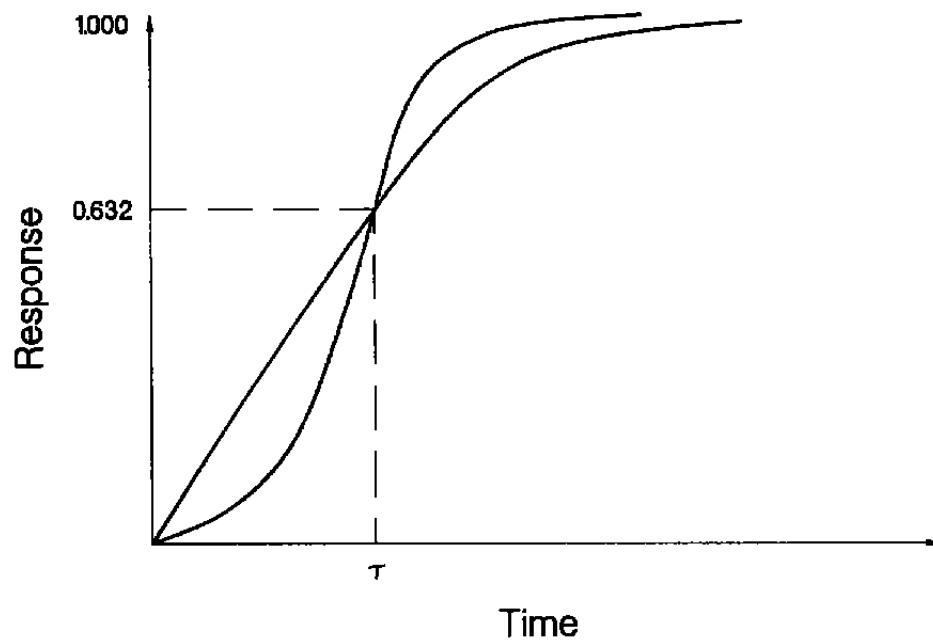
Figure 8.8. Possible Responses of Systems Higher than First Order.

8.4   Response of Higher Order Systems

Although some systems such as the simple thermal system discussed in Section 8.1 can

be approximated with a first order model, the transient behavior of most systems is generally

written in terms of higher order models. This includes thermocouples which should generally be

represented by the following transfer function:

$$G(s) = \frac{T(s)}{T_f(s)} = \frac{1}{(s - p_1) \, (s - p_2) \, \cdots \, (s - p_n)} \tag{8.16}$$

Where p_1, p_2, . . ., p_n are called the poles of the system transfer function. The poles are also

referred to as the modes of the system's response. The reciprocal of these poles are denoted

as τ_1, τ_2, . . ., τ_n, which are called modal time constants. The following derivations show that

the overall time constant of a system is obtained by combining its modal time constants.

The response of a higher order system to a step change in input is derived by substituting

$T_f(s) = \dfrac{1}{s}$ in Equation 8.16 and performing an inverse Laplace transform. This will give the

following:

$$T(t) = \frac{1}{(-p_1)(-p_2) \, \cdots \, (-p_n)} + \frac{e^{p_1 t}}{p_1 (p_1 - p_2) \, \cdots \, (p_1 - p_n)}$$

$$+ \frac{e^{p_2 t}}{p_2 (p_2 - p_1) \, \cdots \, (p_2 - p_n)} + \cdots \tag{8.17}$$

73

This may be written as:

$$T(t) = \frac{1}{(-p_1)(-p_2)\cdots(-p_n)}\left[1 + \frac{(-p_1)(-p_2)\cdots(-p_n)}{p_1(p_1-p_2)\cdots(p_1-p_n)}\,e^{p_1 t}\right.$$

$$\left. + \frac{(-p_1)(-p_2)\cdots(-p_n)}{p_2(p_2-p_1)\cdots(p_2-p_n)}\,e^{p_2 t} + \cdots \right] \tag{8.18}$$

Now we introduce the concept of modal time constants, $\tau_i = \dfrac{1}{p_i}$ or:

$$e^{p_i t} = e^{-t/\tau_i}. \tag{8.19}$$

We now proceed to calculate the steady state or the final value of the step response. Substituting the expression 8.19 in Equation 8.18, and evaluating the resulting equation at a time when the exponential terms have died out, we will obtain:

$$T(\infty) = \frac{1}{(-p_1)(-p_2)\cdots(-p_n)} \tag{8.20}$$

Thus:

$$\frac{T(t)}{T(\infty)} = 1 + \frac{\dfrac{1}{\tau_1\tau_2\cdots\tau_n}}{\dfrac{1}{-\tau_1}\left[\dfrac{1}{-\tau_1}+\dfrac{1}{\tau_2}\right]\cdots\left[\dfrac{1}{-\tau_1}+\dfrac{1}{\tau_n}\right]}\,e^{-\frac{t}{\tau_1}}$$

$$+ \frac{\dfrac{1}{\tau_1\tau_2\cdots\tau_n}}{\dfrac{1}{-\tau_2}\left[\dfrac{1}{-\tau_2}+\dfrac{1}{\tau_1}\right]\cdots\left[\dfrac{1}{-\tau_2}+\dfrac{1}{\tau_n}\right]}\,e^{-\frac{t}{\tau_2}} + \cdots \tag{8.21}$$

Now we proceed to determine the expressions that give the overall time constant (τ) of the system in terms of its modal time constants $(\tau_1, \tau_2, \tau_3, \ldots)$.

Due to the decaying nature of temperature sensor response curves, we can safely assume that the values of the modal time constants rapidly decrease as we go from τ_1 to τ_2 to $\ldots \tau_n$.

If we let τ_1 be the slowest time constant (largest in value) and evaluate the second exponential at $\dfrac{t}{\tau_1} = 1$, we obtain the following:

$\dfrac{\tau_1}{\tau_2}$	e^{-t/τ_2} (at $t = \tau_1$)
2	0.135
3	0.050
4	0.018
5	0.007

Since $\dfrac{\tau_1}{\tau_2}$ is typically about 5 or greater for a temperature sensor, the contribution of τ_2 is small by the time $t = \tau_1$. Since τ_1 has the most important effect on τ, we can also assert that τ_2 and higher terms have a small influence when $t = \tau$. Thus, we may write:

$$\frac{T(t)}{T(\infty)} \approx 1 + \frac{\dfrac{1}{\tau_1 \tau_2 \cdots \tau_n}}{\dfrac{1}{-\tau_1}\left[\dfrac{1}{-\tau_1} + \dfrac{1}{\tau_2}\right] \cdots \left[\dfrac{1}{-\tau_1} + \dfrac{1}{\tau_n}\right]} e^{-\frac{t}{\tau_1}} \qquad (8.22)$$

Now, we can set $\dfrac{O(\tau)}{O(\infty)} = 0.632$ and solve for τ to obtain:

$$e^{-\tau/\tau_1} = 0.368 \left(1 - \frac{\tau_2}{\tau_1}\right)\left(1 - \frac{\tau_3}{\tau_1}\right) \cdots \left(1 - \frac{\tau_n}{\tau_1}\right) \qquad (8.23)$$

AEDC-TR-91-26

or

$$\tau = \tau_1 \left[1 - \ln\left(1 - \frac{\tau_2}{\tau_1}\right) - \ln\left(1 - \frac{\tau_3}{\tau_1}\right) - \dots \ln\left(1 - \frac{\tau_n}{\tau_1}\right) \right] \qquad (8.24)$$

This is an important relationship in the Loop Current Step Response (LCSR) development. As will be seen later in Chapter 10, the overall time constant of a thermocouple is determined from the modal time constants that are readily obtained by fitting of the LCSR data.

For ramp response, we substitute $\frac{k}{s^2}$ for $T_f(s)$ in Equation 8.16, where k is the ramp rate:

$$T(s) = \frac{k}{s^2(s-p_1)(s-p_2)\dots(s-p_n)} \qquad (8.25)$$

The sensor response may be evaluated by inverse Laplace transformation. The partial fraction method gives:

$$O(s) = \frac{A_1}{p^2} + \frac{A_2}{p} + \frac{A_3}{p-p_1} + \frac{A_4}{p-p_2} + \dots \qquad (8.26)$$

The arbitrary constants A_is must be evaluated if the complete response is required. However, we are interested only in determining the ramp time delay. Consequently, the exponential terms are of no interest, and we can concentrate on A_1 and A_2. These may be evaluated to give the following result:

$$A_1 = k$$
$$A_2 = -k\left[\tau_1 + \tau_2 + \dots + \tau_n\right] \qquad (8.27)$$

76

Therefore

$$O(t) \sim k [t - (\tau_1 + \tau_2 + \ldots + \tau_n)]$$ (8.28)

In this case, we obtain:

$$Ramp\ Time\ Delay = \tau_1 + \tau_2 + \ldots + \tau_n$$ (8.29)

Equations 8.29 and 8.24 show that the time constant of a first order system is equal to the ramp time delay of the system and as the order of the system increases, the time constant and the ramp time delay slowly depart from one another. As shown in Figure 8.9, the time constant is always greater than the ramp time delay for higher than first order systems.

JJG008A-01C
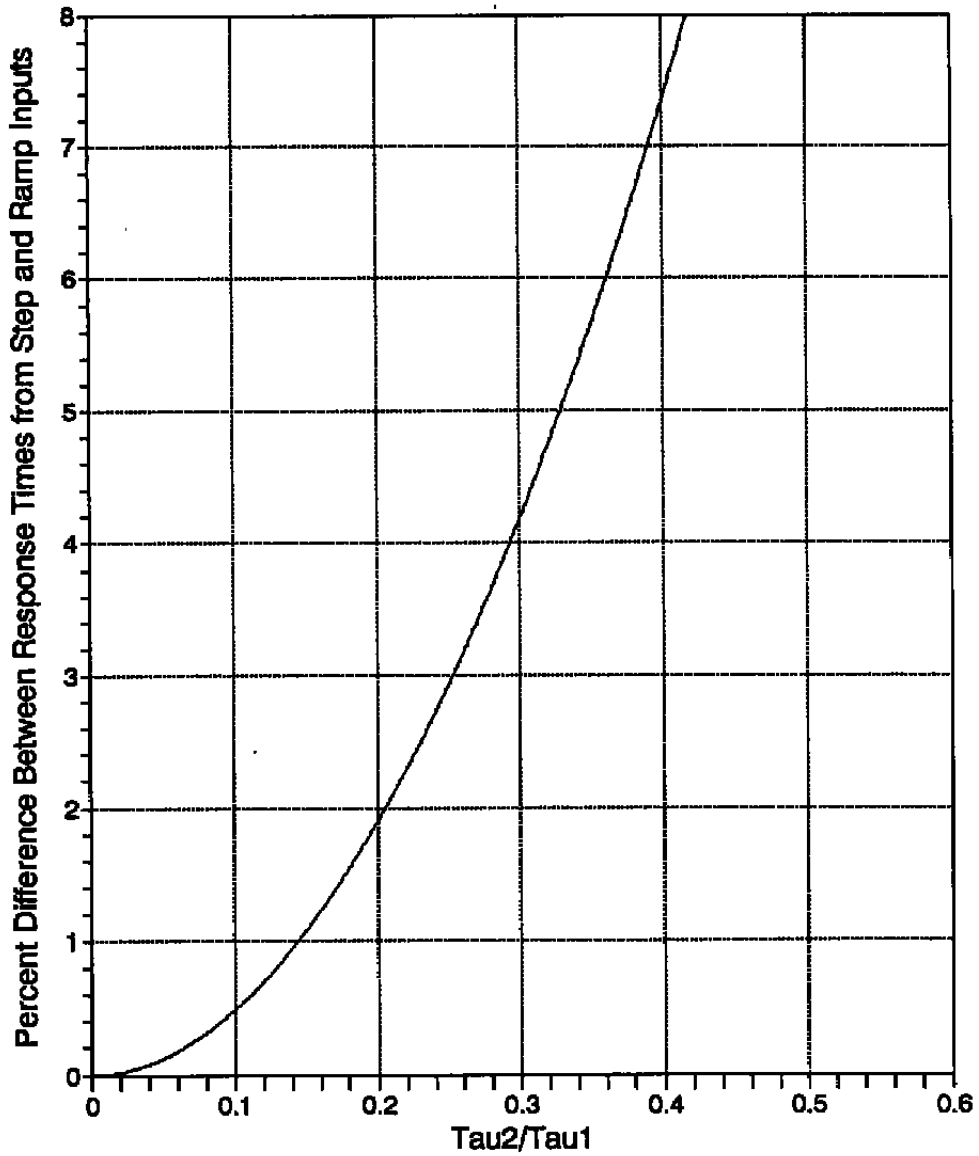
Figure 8.9. Relationship Between Time Constant
and Ramp Time Delay.

9. RESPONSE TIME TESTING METHODS

9.1 Plunge Test

The response time of a thermocouple is classically measured in a laboratory environment using a method called plunge test. In this test, the thermocouple is exposed to a sudden change in temperature and its output is recorded until it reaches steady state. The analysis of a plunge test to obtain the time constant of a thermocouple is simple. For example, if the thermocouple output transient is recorded on a strip chart recorder, the time constant is found by measuring the time that corresponds to 63.2 percent of the final value (Figure 9.1). It should be noted once again that although this definition of time constant is analytically valid only for a first order system, it is used conventionally for determining the response time of all temperature sensors regardless of the dynamic order. Therefore, all references to the term response time or time constant in this report correspond to this definition regardless of the type or size of the thermocouple, the test condition, or the test method being used (whether it is the plunge or the LCSR test).

The step change in temperature that is needed for response time testing is usually produced by plunging the thermocouple from one medium into another with a different temperature. The test is normally conducted in either water or air. Water testing may be accomplished by any number of methods. One method is to hold the thermocouple in room temperature air and then plunge it suddenly into warmer or cooler water. The temperature of the final medium, in this case the water, must be constant during the test. A similar method, which would not involve an effort to maintain the water temperature constant, is to heat the thermocouple in air above the water using a warm air blower, and then plunge it into room

PD: 25 M<15:04:54 =05 JUN 90 =SPD: 5 MM/S (200.0 MS/MM

Timing Signal

63.2% of a

Test Transient

a
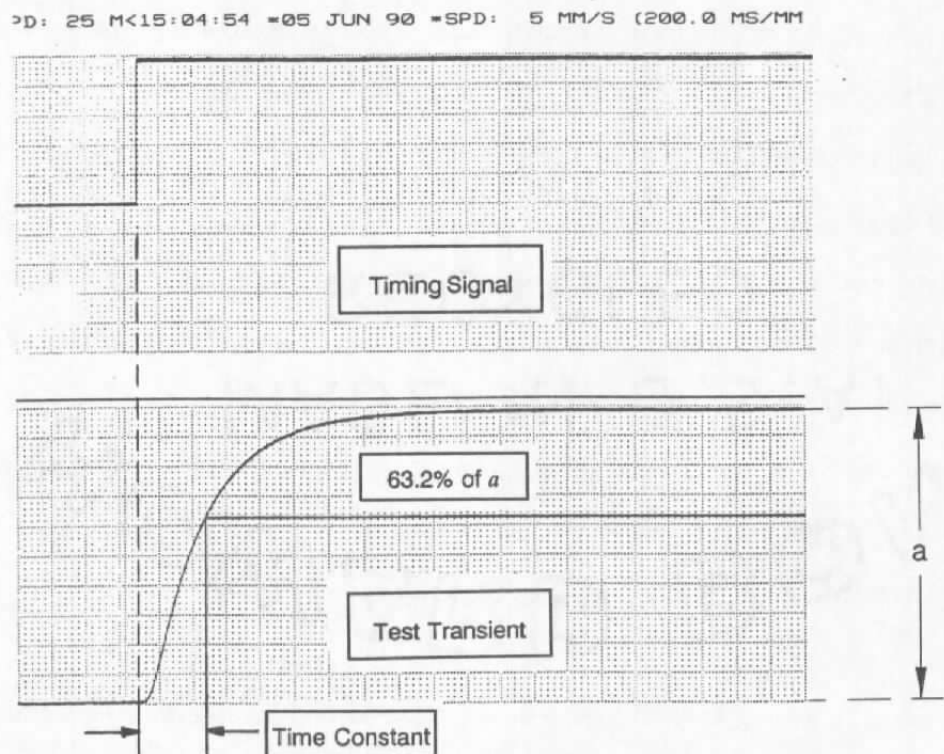
Time Constant

Figure 9.1. Determination of Thermocouple Time Constant
from an Actual Plunge Test Transient.

temperature water. Similar procedures are used for testing of thermocouples in air. The tests that were performed in air in this project involved heating the thermocouple with a warm air blower, and plunging it into an air stream at ambient temperature.

Figure 9.2 shows simplified schematics of the laboratory test equipment we used in this project to perform plunge testing in water and in air. This is followed by Figures 9.3 through 9.5 with photographs of the equipment.

The thermocouple time constant obtained by the plunge method is a relative index which should be accompanied by an expression of the test conditions. This is important because the response time of thermocouples is strongly dependent on the properties of the final medium in which they are plunged. The type of medium (air, water, etc.) and its flow rate, temperature, and pressure must always be mentioned with the response time results. The flow rate is usually the most important factor followed by temperature and then pressure. These parameters affect the film heat transfer coefficient on the thermocouple surface which is related to response time. Higher flow rates increase the heat transfer coefficient and reduce the response time. Temperature, however, has a mixed effect. On one hand, it acts in the same manner as flow, i.e., it increases the film heat transfer coefficient and reduces the response time. On the other hand, high temperatures can affect the material properties inside the thermocouple and either increase or decrease the response time. Pressure does not usually affect the time constant except for whatever effect it may have on the fluid properties that control the surface heat transfer coefficient.

81

AMS—DWG THC020E

Trigger
IN   OUT

Signal
Conditioning

DMM

Sensor

Hot Air
Blower

Timing Probe

Water

r

ω

Rotating
Tank

Velocity = $r \cdot \omega$

Ch. 1   Ch. 2

Strip
Chart
Recorder

Trigger
IN   OUT

Signal
Conditioning

DMM

Sensor

Hot Air
Blower

Fan

Air

Gage Pressure

Ch. 1   Ch. 2

Strip
Chart
Recorder
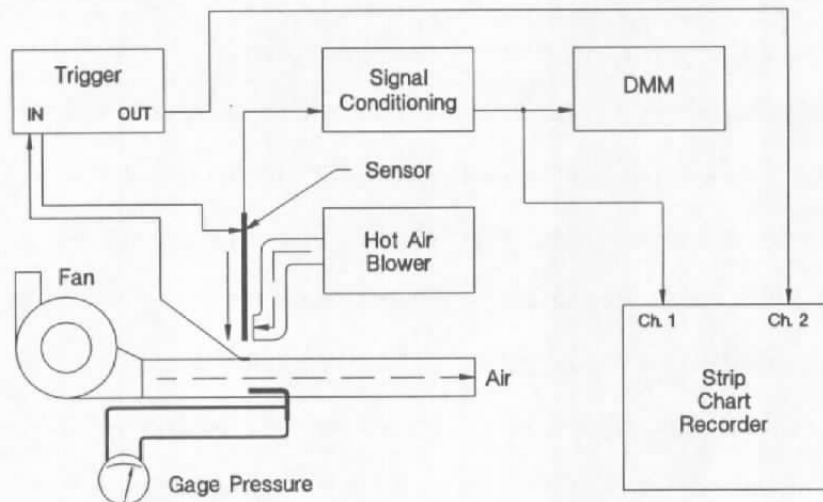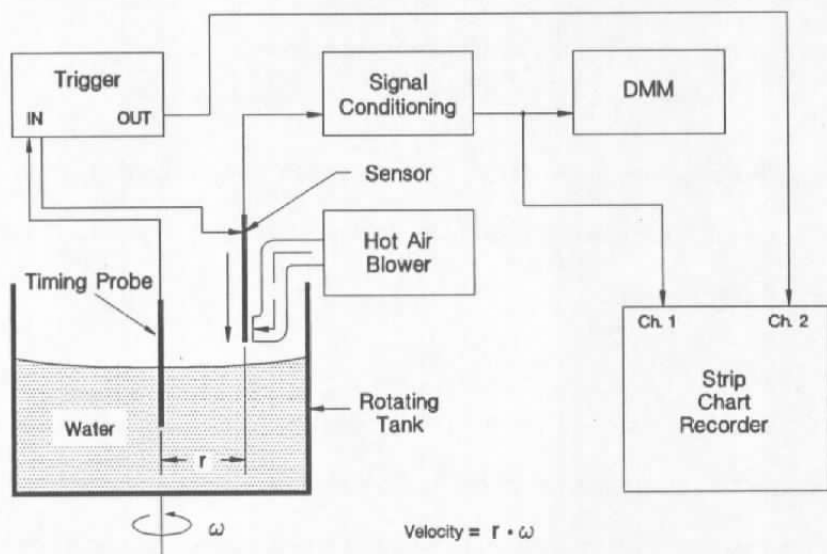
Figure 9.2. Equipment Setup for Laboratory Plunge
Tests in Water and Air.
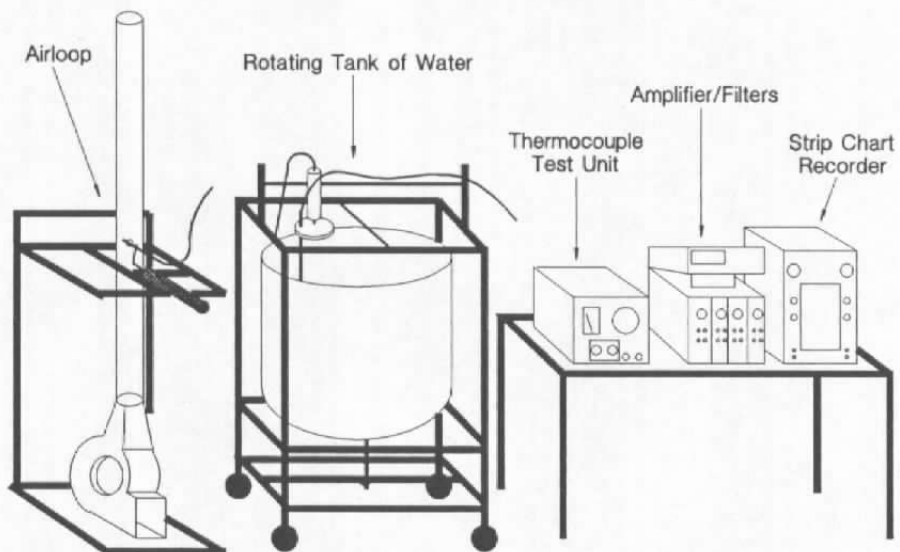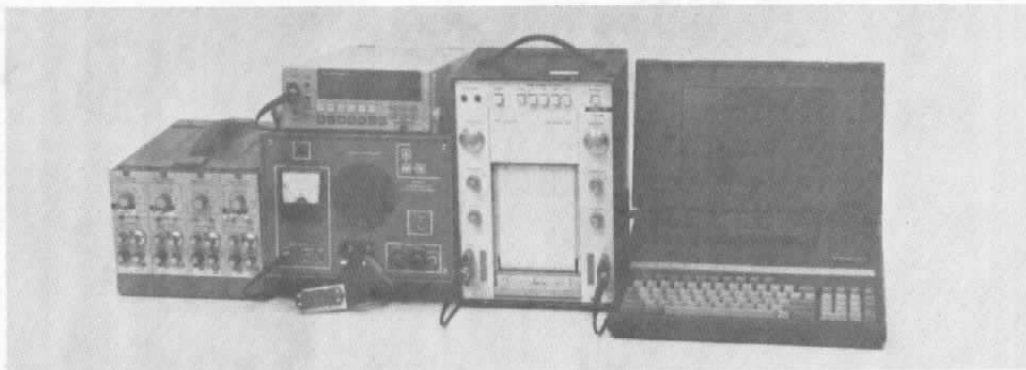
Figure 9.3. Laboratory Equipment for Response Time Testing of Thermocouples.
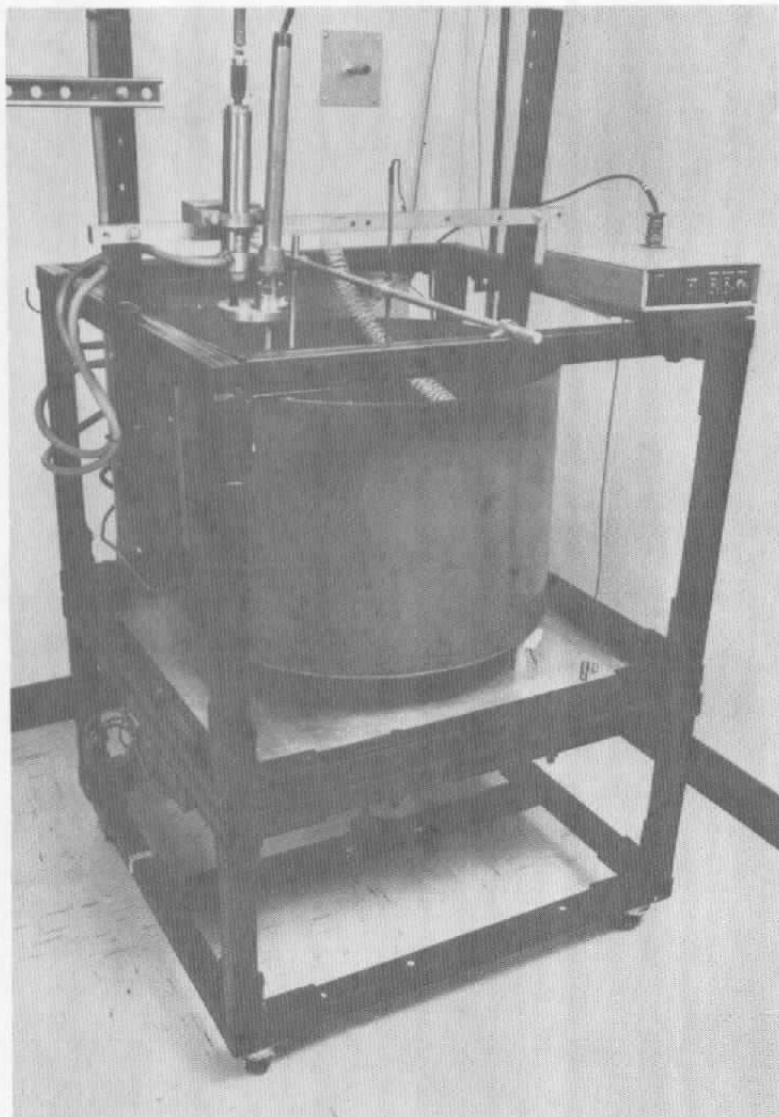
Figure 9.4. Rotation Tank of Water for Plunge Test.
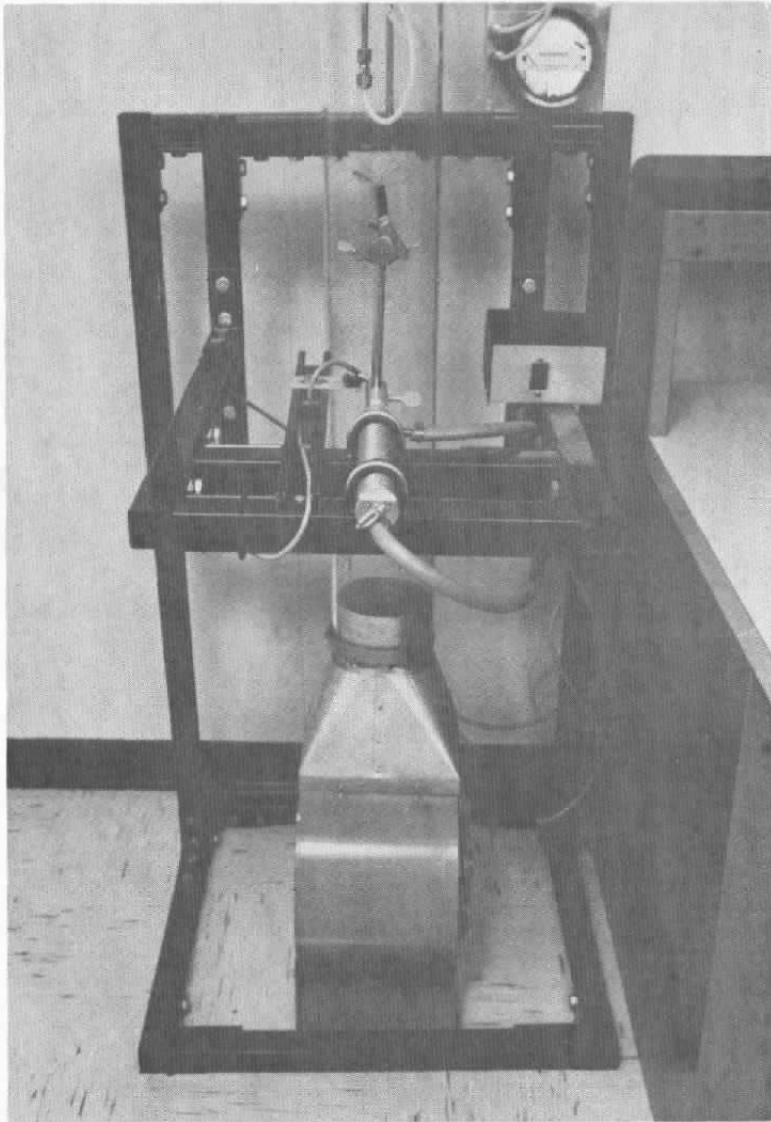
Figure 9.5. Air Loop for Response Time Testing
of Thermocouples.

85

9.2 Loop Current Step Response Test

Since the response time of a thermocouple is strongly affected by process conditions, laboratory measurements such as plunge tests in a reference condition cannot provide accurate information about the "in-service" response time of the thermocouple. Therefore, an in-situ method that can be implemented at process operating conditions must be used. The LCSR method was developed to provide the in-situ response time testing capability. The test is performed by heating the thermocouple internally by applying an electric current to its extension leads (Figure 9.6). The current is applied for a few seconds to raise the temperature of the thermocouple a few degrees above the ambient temperature. The current is then cut off and the thermocouple output is recorded as it cools to the ambient temperature (Figure 9.7). This transient, which is referred to as the LCSR transient, is predominantly due to the cooling of the thermocouple junction. The rate of the thermocouple cooling transient is proportional to its ability to dissipate the heat generated in its junction. Therefore, the LCSR data can be used with an analytical approach to identify the time constant of the thermocouple under the conditions tested. The analytical approach uses the LCSR data to establish the response of the sensor to any change in temperature. The validity of the LCSR test can be demonstrated by measuring time constants of a group of thermocouples by the plunge method in a laboratory and repeating the measurements in the same conditions using the LCSR method. This work was done in this project as described in Chapter 12 entitled, "LCSR Validation".

The LCSR testing of thermocouples can be performed using an AC or a DC current source to produce Joule heating, which is proportional to the current squared and is distributed along the whole length of the thermocouple. The Joule heating is given by I^2R where I is the applied current and R is the electrical resistance of the thermocouple wires involved. Since the electrical resistance of thermocouple circuits are small and distributed along the sensor, the heating current must be large enough to produce sufficient heating and provide a useful LCSR signal when the current is cut off. Depending on the size and length of the thermocouple and

AMS-DWG THC0030
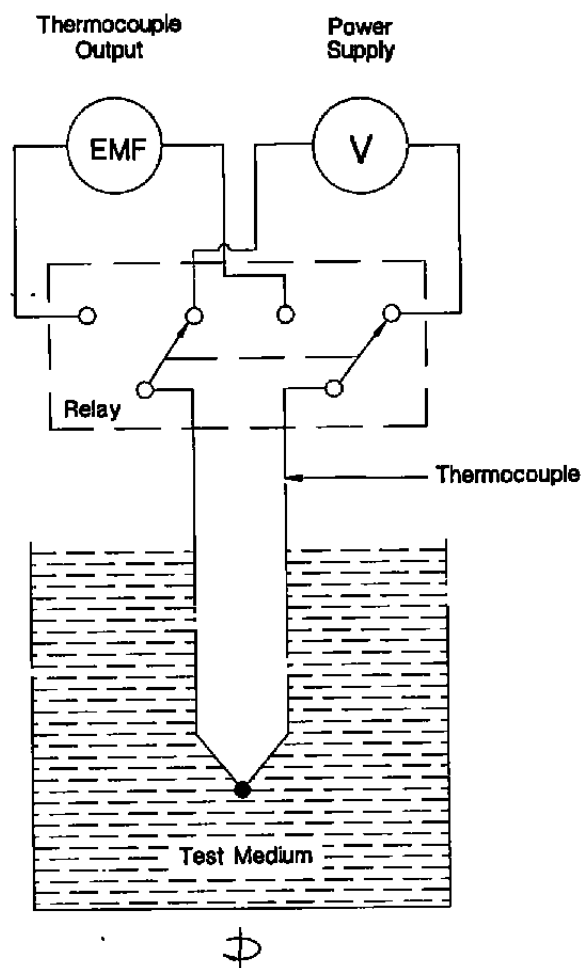
Figure 9.6. Simplified Schematic of LCSR Test Equipment.
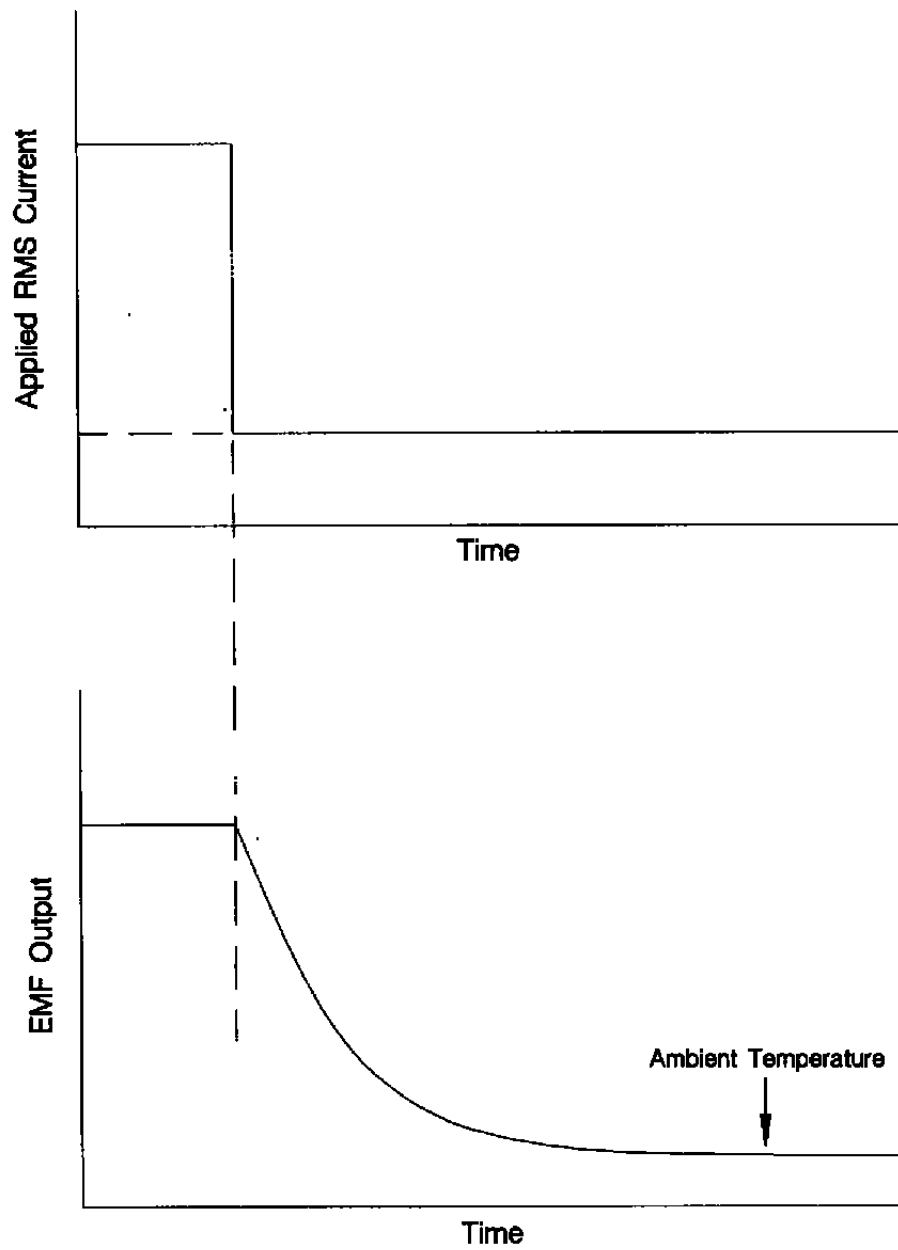
Figure 9.7. A Typical LCSR Cooling Transient.

Its extension wires, heating currents of approximately 0.3 to 3.0 amperes are usually used in LCSR testing of thermocouples as opposed to 30 to 60 milliamperes that is used in testing of Resistance Temperature Detectors (RTDs). This is because in RTDs, the resistance of the circuit is much higher and predominantly concentrated at the RTD's sensing filament.

In addition to Joule heating, the application of an electric current to a thermocouple produces Peltier heating or cooling depending on the direction of the applied current. Peltier effect can cause a problem if DC currents are used in LCSR testing of thermocouples. While Joule heating is uniformly distributed along the thermocouple wires, Peltier heating/cooling is concentrated at the junctions of all dissimilar metals in the thermocouple circuit. Consequently, if a DC current is used, all the junctions in the circuit that have accumulated Peltier heating/cooling during the LCSR test will produce temperature transients after the current is cut off. These transients are unrelated to the response of the thermocouple junction and can cause error in the LCSR results. Furthermore, the Peltier heating/cooling at the measuring junction will decay axially as opposed to radially. This is detrimental to the LCSR analysis which is based on the assumption of predominantly radial heat transfer. In Joule heating, the heat transfer from the junction is predominantly radial. This is because with Joule heating, in addition to the junction, the thermocouple wires will heat up during the LCSR test. When the current is cut off, the Joule heat at the junction can not go up through the wires much because the wires are approximately as hot as the junction itself. This forces most of the heat to decay radially. With Peltier heating/cooling, however, there is a temperature difference between the junction and the thermocouple wires when the current is cut off. Therefore, with Peltier, the heat can go up through the wires even though some of it will also dissipate radially.

To avoid the Peltier effect, AC currents are often used. The higher the frequency of the AC current, the lower is the Peltier effect. This is because the heating or cooling that is produced when the current is in a given direction is canceled by the heating or cooling that is produced when the direction of the current is reversed. In order to minimize or avoid the Peltier effect, we

have used a 1000 Hz current source in the LCSR test equipment that was developed in this project. Figure 9.8 illustrates the effects of Peltier heating or cooling on the LCSR test transient for a thermocouple[6].

Another phenomenon that may have a bearing on the LCSR testing of thermocouples is referred to as the magnetic effect. The magnetic effect is a problem mostly with the type K (Chromel/Alumel) thermocouples due to the Alumel wire which is Ferromagnetic. The magnetic effect which is also called Ettingshausen-Nernst (EN) effect describes the combined effects of temperature, applied current and magnetic fields on the voltage produced in thermocouple circuits. The effect depends on the orientation of the magnetic field and the temperature gradient along thermocouple wires. A magnetic field placed around the thermocouple can change the Seebeck coefficient of the wires by interfering with the transport of electrons in the metal. In a study conducted by Kollie, et. al.[7], it was shown that type K thermocouples placed in a magnetic field can have temperature indication errors of as much as ± 150 percent at 100°C. This error occurred due to an interaction of temperature gradient and magnetic field impressed on thermocouples during heat transfer experiments at the Oak Ridge National Laboratory.

Shepard & Carroll[6] found that the magnetic effect can cause a non-thermal transient with a 63.2 percent decay time of about 50 milliseconds on the LCSR signals for type K thermocouples tested with a 1000 Hz of AC current. Apparently the magnetic transient occurs due to the LCSR heating current magnetizing the Alumel wire in the thermocouple. This transient which is not related to response time of the thermocouple, results from the decay of a magnetic field after the current is cut off. The direction of the magnetic transient (positive or negative) was found to vary with the phase of the AC current at the instant when the current is cut off in a LCSR test. Figure 9.9 illustrates the potential results of the magnetic effect on a LCSR signal. It also illustrates the explanation provided by Shepard[6] that this effect may be described in terms of magnetic domain flipping and relaxation in the Alumel wire.
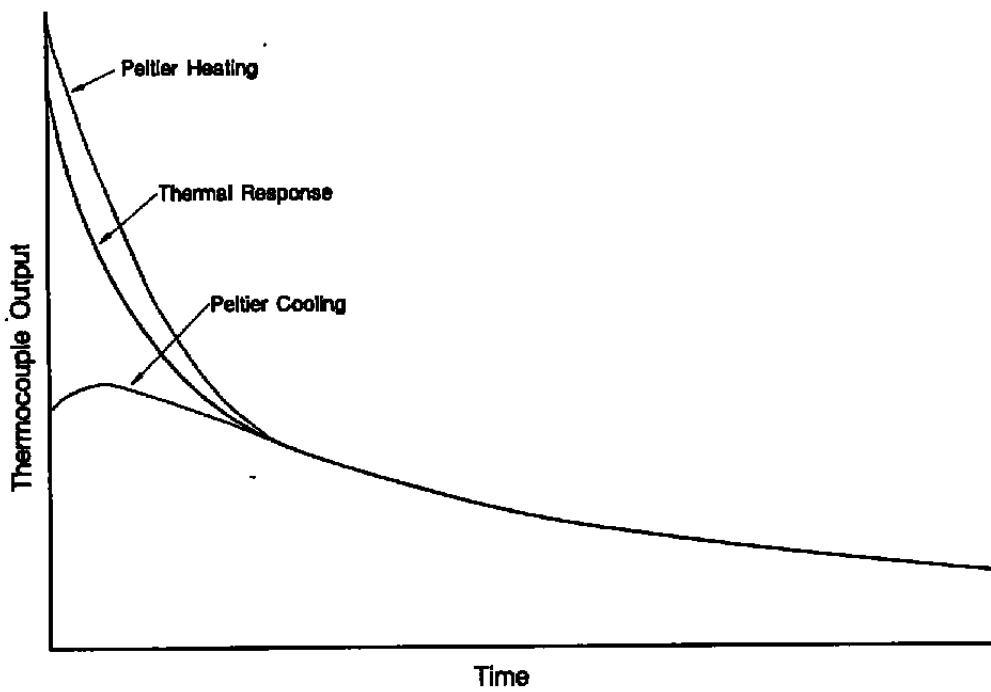
Figure 9.8. Peltier Effect on LCSR Test Transients.

91
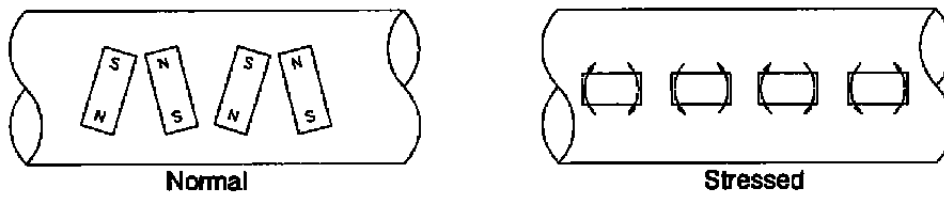
a) Orientation of magnetic dipole in Alumel
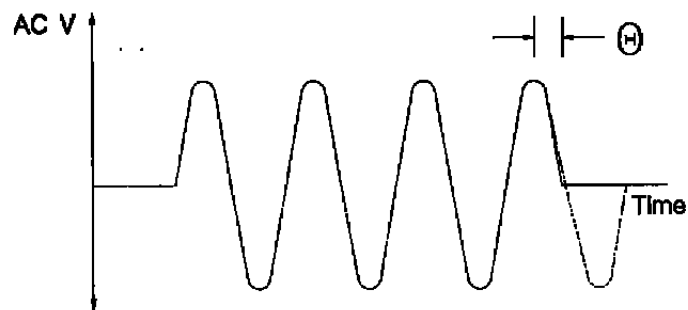
b) AC Current for LCSR
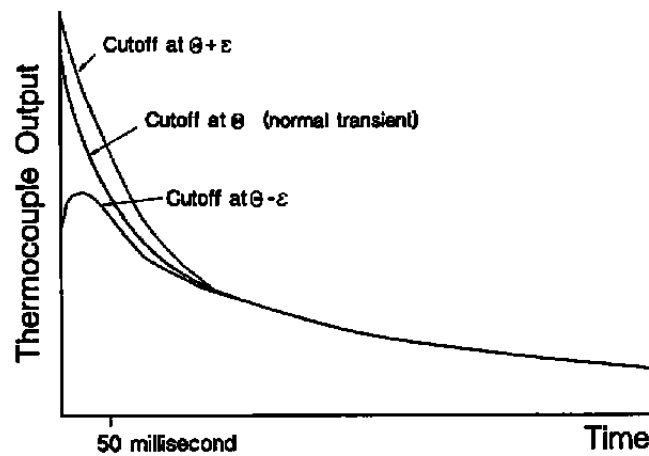
c) Response when the current is cutoff

Figure 9.9. Illustration of Magnetic Effect on LCSR
Transients for Type K Thermocouples.

Shepard & Carroll[6] found that the magnetic effect in type K thermocouples is measurable below the Curie temperature of Alumel wire, which is about 160°C, and that the effect vanishes above 160°C. This has been confirmed by placing the Alumel coil in a furnace and observing that the magnetic EMF appears and disappears as the coil temperature was varied above the Curie temperature. Shepard & Carroll have concluded that the magnetic EMF can be prevented in a LCSR test by a ramp shut off of the heating current rather than a sudden interruption. More specifically, they used a procedure by which the LCSR heating current was first ramped down about 10 percent at each cycle, for 10 cycles of a 1000 Hz heating signal, and then cut off. We did not use this approach or any other approach in the design of the equipment developed in this project. This decision was made after much deliberation and a series of laboratory tests to address the question. Based on the results of our discussions and the laboratory tests, we concluded that we can neglect the magnetic effect because it is only a problem with type K thermocouples, and the 50 milliseconds magnetic decay time is small compared to the nominal response time of most common sizes of type K thermocouples.

10. LOOP CURRENT STEP RESPONSE THEORY

10.1 Background

The Loop Current Step Response (LCSR) test is based on the principle that the output of a thermocouple to a step change in temperature induced inside the thermocouple can be converted to give the equivalent response for a step change in temperature outside the thermocouple (Figure 10.1). This is possible because the transfer function that represents the response to an external step change in temperature is related to that for an internal step change in temperature as follows:

$$G_{Plunge} = \frac{1}{(s - p_1)(s - p_2) \cdots} \tag{10.1}$$

$$G_{LCSR} = \frac{1}{(s - p_1)(s - p_2) \cdots} \, [(s - z_1)(s - z_2) \cdots] \tag{10.2}$$

Where G_{Plunge} represents the response that will be obtained in a plunge test and G_{LCSR} represents the response that will be obtained in a LCSR test. It is clear that the plunge response is a subset of LCSR response meaning that if LCSR response is known, the $p_1, p_2, \ldots$ will be known and can be used to obtain G_{Plunge}. The derivations that follow are carried out to show how we arrived at Equations 10.1 and 10.2 given above.

10.2 Heat Transfer Analysis of a Thermocouple System

The derivation of the LCSR and plunge test transfer functions given as G_{LCSR} and G_{Plunge} above are based on the assumption that the heat transfer between the thermocouple junction and the surrounding media is one dimensional (radial). With this assumption, the heat transfer
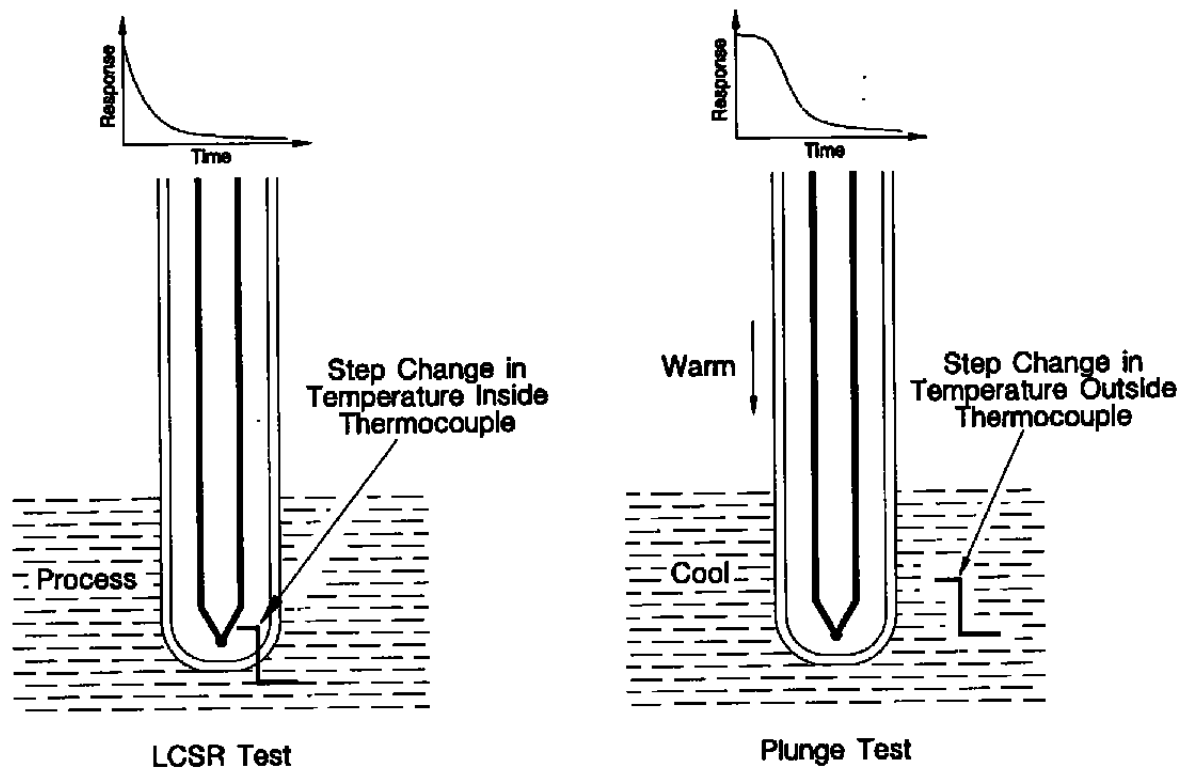
Figure 10.1. Comparison of LCSR Method With Plunge Test.

between the hot junction and the medium (fluid) surrounding the thermocouple may be represented by a lumped parameter network such as the one shown in Figure 10.2. For this network, the transient heat transfer equation for node i is written as[8]:

$$mc \frac{dT_i}{dt} = \frac{1}{R_1}(T_{i-1} - T_i) - \frac{1}{R_2}(T_i - T_{i+1}) \qquad (10.3)$$

where m and c are the mass and specific heat capacity of material in the node, and R_1 and R_2 are the heat transfer resistances. Equation 10.3 may be rewritten as:

$$\frac{dT_i}{dt} = a_{i,i-1} T_{i-1} - a_{i,i} T_i + a_{i,i+1} T_{i+1} \qquad (10.4)$$

where

$$a_{i,i-1} = \frac{1}{mcR_1}$$

$$a_{i,i} = \frac{1}{mc}\left(\frac{1}{R_1} + \frac{1}{R_2}\right) \qquad (10.5)$$

$$a_{i,i+1} = \frac{1}{mcR_2}.$$

The nodal equations may be applied to a series of nodes, starting with the node closest to the center ($i = 1$) and ending with the node closest to the surface ($i = n$):
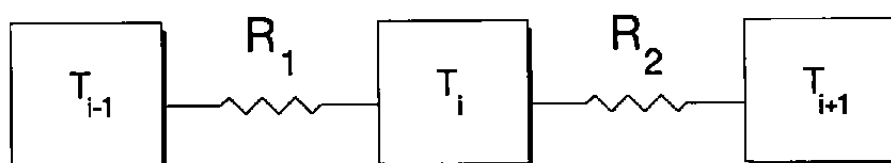
Figure 10.2. Lump Parameter Representation for
LCSR Analysis.

$$\frac{dT_1}{dt} = -a_{11} T_1 + a_{12} T_2$$

$$\frac{dT_2}{dt} = a_{21}T_1 - a_{22}T_2 + a_{23}T_3$$

$$\frac{dT_3}{dt} = a_{32}T_2 - a_{33}T_3 + a_{34}T_4 \qquad (10.6)$$

$$\cdot$$
$$\cdot$$
$$\cdot$$

$$\frac{dT_n}{dt} = a_{n,n-1}T_{n-1} - a_{n,n}T_n + a_{nF}T_F$$

where

T_i = temperature of the ith node (measured relative to the initial fluid temperature).
T_F = change of fluid temperature from its initial value.

These equations may be written in matrix form:

$$\frac{d\bar{x}}{dt} = A\bar{x} + \bar{f} T_F \qquad (10.7)$$

where

$$\bar{x} = \begin{bmatrix} T_1 \\ T_2 \\ T_3 \\ \cdot \\ \cdot \\ \cdot \\ T_n \end{bmatrix} \quad A = \begin{bmatrix} -a_{11} & a_{12} & 0 & 0 & 0 & 0 \\ a_{21} & -a_{22} & a_{23} & 0 & 0 & 0 \\ 0 & a_{32} & -a_{33} & a_{34} & 0 & 0 \\ 0 & \cdot & \cdot & \cdot & \cdot & \cdot \\ 0 & \cdot & \cdot & \cdot & \cdot & \cdot \\ 0 & \cdot & \cdot & \cdot & \cdot & \cdot \\ 0 & \cdot & \cdot & \cdot & a_{n,n-1} & -a_{n,n} \end{bmatrix} \quad \bar{f} = \begin{bmatrix} 0 \\ 0 \\ 0 \\ \cdot \\ \cdot \\ \cdot \\ a_{nF} \end{bmatrix} \qquad (10.8)$$

98

Laplace transformation gives:

$$[sI - A]\,\bar{x}(s) = \bar{f}\,T_F(s) + \bar{x}(t = 0).$$

(10.9)

The solution for the temperature at the central node, x_1 (s), is found by Cramer's rule:

$$T_1(s) = \frac{B(s)}{|sI-A|}$$

(10.10)

where

$$B(s) = \begin{bmatrix} T_1(0) & a_{12} & 0 & . & . & 0 \\ T_2(0) & (s+a_{22}) & -a_{23} & 0 & . & . \\ T_3(0) & -a_{32} & (s+a_{33}) & -a_{33} & . & . \\ . & . & . & . & . & . \\ . & . & . & . & . & 0 \\ . & . & . & . & . & 0 \\ [T_n(0) + a_n T_F(s)] & 0 & 0 & 0 & ... & -a_{n,n-1}(s+a_{n,n}) \end{bmatrix}$$

(10.11)

This Laplace transform is general for one-dimensional problems and its accuracy depends on the number of nodes used. Equation 10.9 is solved below for two different initial conditions, one initial condition to correspond to the LCSR test and the other to correspond to the plunge test. In the LCSR test, the temperature in the center node (hot junction of thermocouple) is not ambient at time t = 0, while for the plunge test, the temperature at the center node is ambient at t = 0.

10.3   LCSR Equation

For the LCSR test, $\bar{x}\,(t\,=\,0)$ is the initial temperature distribution, and it is a vector with
all entries nonzero, meaning that the first column of $B(s)$ in matrix 10.11 has all nonzero entries.

Evaluation of the determinants, $B(s)$ and $|sI - A|$, in Eq. 10.10 gives:

$$G(s) = \frac{T_1(s)}{T_F(s)} = K \frac{(s - z_1)(s - z_2) \ldots (s - z_{n-1})}{(s - p_1)(s - p_2) \ldots (s - p_n)} \qquad (10.12)$$

where each z_i is a zero (a number that causes $T_1(s)$ to equal zero), and p_i is a pole (a number
that causes $T_1(s)$ to equal infinity) and K is a constant gain factor that can be set equal to unity
to simplify the equation. The response $T_1(t)$ for a step change is obtained using the residue
theorem (assuming all distant poles):

$$T_1(t) = \frac{(-z_1)(-z_2) \ldots (-z_{n-1})}{(-p_1)(-p_2) \ldots (-p_n)} + \frac{(p_1 - z_1)(p_1 - z_2) \ldots (p_1 - z_{n-1})}{(p_1 - p_2)(p_1 - p_3) \ldots (p_1 - p_n)} e^{p_1 t}$$

$$+ \frac{(p_2 - z_1)(p_2 - z_2) \ldots (p_2 - z_{n-1})}{(p_2 - p_1)(p_2 - p_3) \ldots (p_2 - p_n)} e^{p_2 t} + \ldots \quad . \qquad (10.13)$$

This may be rewritten as

$$T(t) = A_0 + A_1 e^{p_1 t} + A_2 e^{p_2 t} + \ldots$$

$$A_0, A_1, A_2, \ldots = f(p_1, p_2, \ldots z_1, z_2, \ldots) . \qquad (10.14)$$

Equation 10.12 is referred to as the LCSR transfer function (G_{LCSR}) and Equation 10.14
is referred to as the equation for the LCSR transient. If the data for a LCSR test is mathematically

fit to Equation 10.14, the values of p_1, p_2, ... can be identified and used to construct the plunge test transient.

10.4 Plunge Test Equation

For a step perturbation of fluid temperature, $T_F(s)$ is nonzero, but $\bar{x}$ ($t = 0$) has all zero entries because the initial temperature distribution is flat and equal to the initial fluid temperature. In this case, the first column of $B(s)$ contains all zeros, except for the last entry.

In this case, $B(s)$ from matrix 10.10 may be written as:

$$B(s) = \begin{bmatrix} 0 & a_{12} & 0 & \cdot & \cdot & & \cdot \\ 0 & (s+a_{22}) & -a_{23} & 0 & \cdot & & \cdot \\ 0 & -a_{32} & (s+a_{33}) & -a_{34} & \cdot & & \cdot \\ \cdot & \cdot & \cdot & \cdot & \cdot & & \cdot \\ \cdot & \cdot & \cdot & \cdot & \cdot & & \cdot \\ \cdot & \cdot & \cdot & \cdot & \cdot & 0 \\ a_{nF}T_F(s) & 0 & 0 & 0 & \cdot & & -a_{n,n-1}(s+a_{n,n}) \end{bmatrix} \tag{10.15}$$

Using the Laplace expansion method for evaluation of the determinants, we obtain:

$$B(s) = a_{nF}T_F(s)(-1)^{n+1} \begin{vmatrix} -a_{12} & 0 & 0 & 0 & \cdots \\ (s+a_{22}) & -a_{23} & 0 & 0 & \cdots \\ -a_{32} & (s+a_{33}) & -a_{34} & 0 & \cdots \\ 0 & -a_{43} & (s+a_{44}) & -a_{45} & \cdots \\ \cdot & \cdot & \cdot & \cdot & \cdots \\ \cdot & \cdot & \cdot & \cdot & \cdots \\ \cdot & \cdot & \cdot & \cdot & \cdots \end{vmatrix} \tag{10.16}$$

This is a lower diagonal matrix, and its determinant is the product of the diagonals:

$$B(s) = a_{nF} T_F(s)(-1)^{n+1} (a_{12} a_{23} a_{34} \cdots) . \qquad (10.17)$$

Therefore:

$$T_1(s) = \frac{a_{nF} T_F(s)(-1)^{n+1}}{(s-p_1)(s-p_2) \cdots (s-p_n)} \qquad (10.18)$$

and the transfer function $\dfrac{T_1(s)}{T_F(s)}$ is:

$$G(s) = \frac{K}{(s-p_1)(s-p_2) \cdots (s-p_2)} \qquad (10.19)$$

where K is a constant that can be set equal to unity to simplify the equation. By using the residue theorem, we obtain the following expression for the fluid temperature step change (Laplace transform of a unit step, i.e., $T_F(s) = \dfrac{1}{s}$:

$$T_1(t) = \frac{1}{(-p_1)(-p_2) \cdots (-p_n)} + \frac{1}{p_1(p_1-p_2)(p_1-p_3) \cdots (p_1-p_n)} e^{p_1 t}$$
$$+ \frac{1}{p_2(p_2-p_1)(p_2-p_3) \cdots (p_2-p_3)} e^{p_2 t} + \cdots \qquad (10.20)$$

This equation may be written as:

$$T_1(t) = B_0 + B_1 e^{p_1 t} + B_2 e^{p_2 t} + \cdots$$
$$B_0, B_1, B_2 \cdots = f(p_1, p_2, \cdots) \qquad (10.21)$$

The following observations can be made about the fluid temperature step change (plunge) case:

1.   The exponential terms $(p_1, p_2, \ldots)$ are the same as those of the LCSR result. This is expected since the exponents depend only on the heat transfer resistances and heat capacities, and these are the same in both cases.

2.   The coefficients that multiply the exponentials are determined by the values of the poles but not of the zeros. Therefore, a knowledge of the poles alone is sufficient to determine these coefficients and the exponentials.

10.5   LCSR Transformation Procedure

The results of the derivations carried out above are used with the following procedure to

convert the LCSR transient to give the equivalent plunge test transient:

1.   Perform a LCSR test and sample the data with a computer. Figure 10.3 shows a laboratory LCSR transient for a thermocouple tested in air. Normally, the LCSR transient starts at a high output value when the LCSR test begins and decreases as the thermocouple cools to the ambient temperature. However, it is customary to invert the LCSR transient and show it from low to high as displayed in Figure 10.3.

2.   Fit the LCSR data to the following equation and identify the p_i's. The A_i's do not have to be identified.

$$T(t) = A_0 + A_1 e^{p_1 t} + A_2 e^{p_2 t} + \ldots \quad (10.22)$$

3.   Use the p_i's identified above in Equation 10.20 to construct the temperature response that would have occurred if a fluid temperature step had been imposed.

4.   Use the transient identified in step 3 to obtain the time constant of the thermocouple by determining the time that it takes for the transient to reach 63.2 percent of its final steady state value. Another approach, which is more often used to obtain the time constant, involves substituting the $p_1, p_2, \ldots$ (or $\tau_1, \tau_2, \tau_3, \ldots$) in Equation 8.24 to obtain the time constant directly. This equation is repeated here:
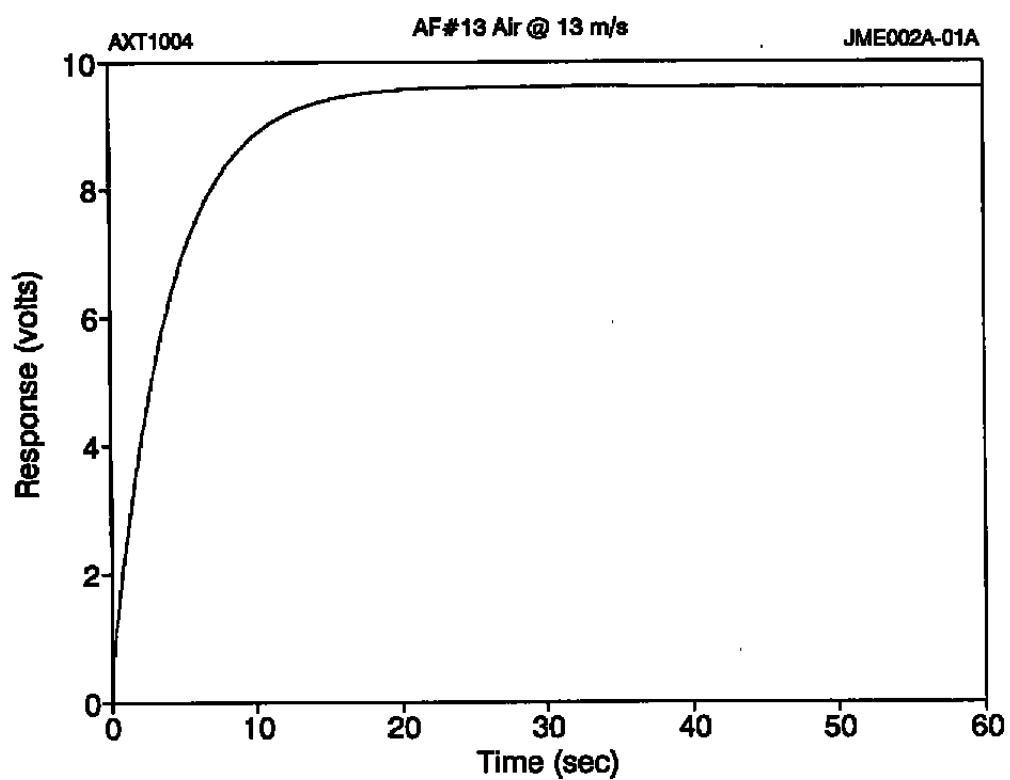
Figure 10.3. LCSR Transient from a Laboratory Test
of a Sheathed Thermocouple.

$$\tau = \tau_1 [1 - \ln(1 - \frac{\tau_2}{\tau_1}) - \ln(1 - \frac{\tau_3}{\tau_1}) \ldots] \qquad (10.23)$$

10.6 Two Dimensional Heat Transfer

The approach used above can be followed to analyze the thermocouple heat transfer based on a two dimensional model.[8] The reader may consult Reference 8 for a derivation of the two dimensional equation. The key results of the two dimensional analysis is that, unlike the one dimensional case, the step response results have zeros in the transfer function as well as poles. That is, the poles identified by the LCSR test are not all that is needed to construct the plunge test results. However, experience with typical thermocouples in typical installations has shown that the errors due to a minor departure from one dimensional assumptions are often not significant.

11. EFFECT OF PROCESS CONDITIONS ON RESPONSE TIME

This chapter presents a method that can be used to measure the response time of a thermocouple in a convenient medium in a laboratory and use the information to estimate the response time in another medium or in a different test condition. This method was originally developed for selection of thermocouples to measure the temperature of liquid sodium in certain class of nuclear power reactors. In this application, it was crucial to know in advance that the selected thermocouples to be installed in the reactor will have a good chance of meeting the response time requirements when the reactor begins operation. The method has also been used by sensor manufacturers in qualification testing of prototype sensors that are designed to satisfy specific response time requirements. The method is not a replacement for the Loop Current Step Response test. Rather, it is a tool for obtaining a rough estimate for the response time that can be expected from a thermocouple when it is installed in a process under known operating conditions and installation details.

11.1 Technical Background

The response time of a thermocouple consists of an internal component and a surface component. The internal component depends predominantly on the thermal conductivity (k) of materials inside the thermocouple while the surface component depends on the film heat transfer coefficient (h). The internal component is independent of the process conditions except for the effect of temperature on material properties inside the thermocouple. The surface component is predominantly dependent on the process conditions such as flow rate, temperature, and to a lesser extent, the process pressure. These parameters affect the film heat transfer coefficient which increases as the process parameters such as flow rate and temperature are increased.

106

Figure 11.1 illustrates how the response time of a thermocouple may decrease as .is increased.

In this illustration, the effect of temperature on material properties inside the sensor is neglected.

Another factor that should be considered in the study of process effects on response time

is the ratio of internal heat transfer resistance to the surface heat transfer resistance. This ratio

is called the Biot Modulus (N_{Bi}) which is given by:

$$N_{Bi} = \frac{\text{internal heat transfer resistance}}{\text{surface heat transfer resistance}} = \frac{h r_o}{k}$$

If the Biot Modulus is large, then the response time may change very little as h is

increased, but if Biot Modulus is small, the response time will be very sensitive to changes in h

especially in poor heat transfer media where h is small. Figure 11.2 shows the response time

of two sensors in room temperature water as a function of flow rate. One of the sensors was

tested inside a thermowell and the other one was tested without a thermowell. It is apparent that

the response time versus flow rate does not improve as much for the sensor with the thermowell.

This is because the internal resistance of the sensor-thermowell combination dominates its

surface resistance, while the internal and surface resistances of the sensor without the

thermowell are closer to one another.

11.2   Response Time Versus Heat Transfer Coefficient

As shown in Figure 11.1, the response time of a thermocouple decreases as the heat

transfer coefficient is increased.   In order to derive the correlation between the heat transfer

AMS-DWG GRF022A
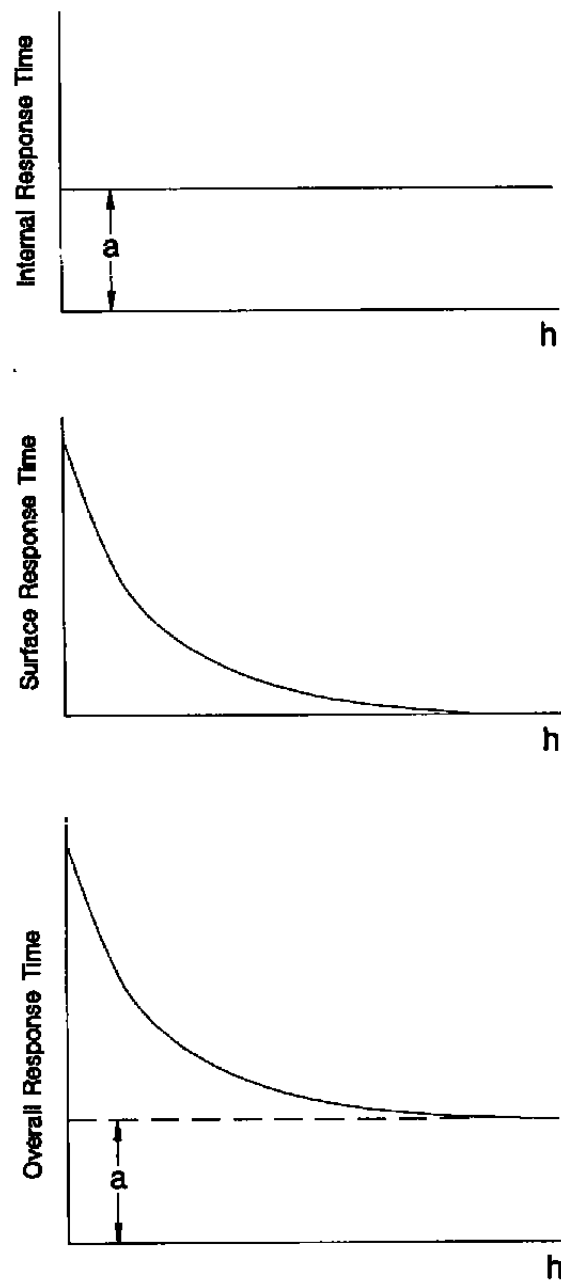
Figure 11.1. Changes in Internal and Surface Components of Response
Time as a Function of Heat Transfer Coefficient.

MEH002A-01B
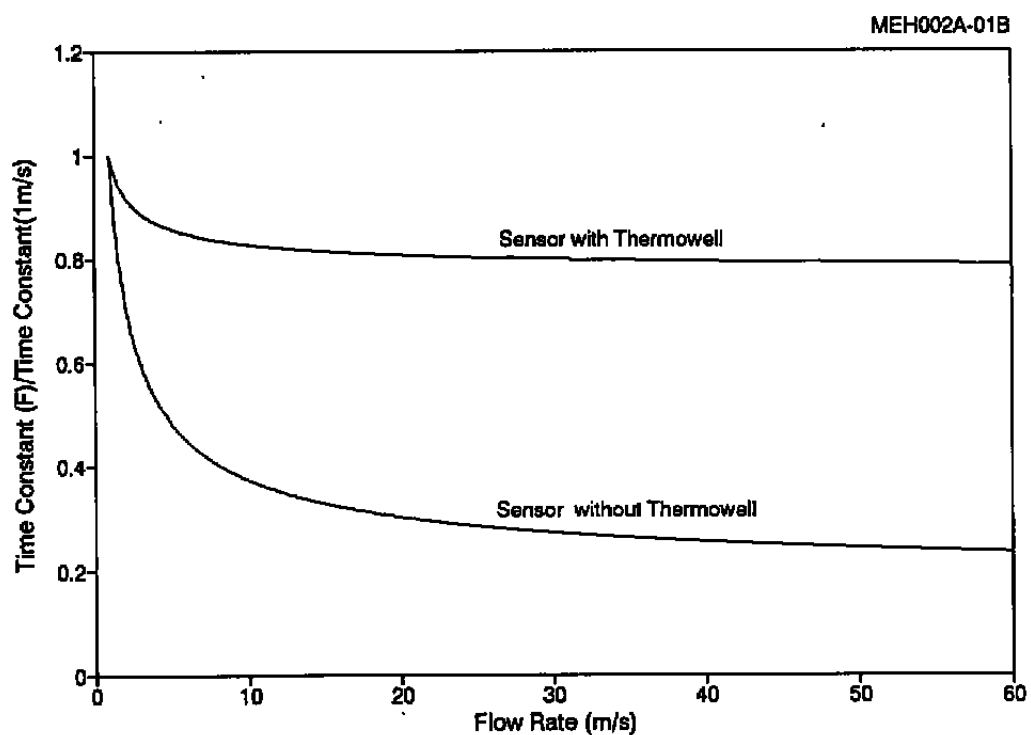
Figure 11.2. Response-Versus-Flow Behavior of a Sensor
Tested With and Without Its Thermowell.

coefficient and response time, we recall Chapter 8 where we showed that the time constant (τ)

of a thermocouple may be written as:

$$\tau = \frac{mc}{UA} \qquad (11.1)$$

In this equation m and c are the mass and specific heat capacity of the sensing portion, and U

and A are the overall heat transfer coefficient and the affected surface area of the thermocouple.

Note that we used the overall heat transfer coefficient, U, as opposed to the film heat transfer

coefficient, h, which was used in Chapter 8. The overall heat transfer coefficient accounts for the

heat transfer resistance both inside the sensor and at the sensor surface. More specifically, we

can write:

$$UA = \frac{1}{R_{tot}} = \frac{1}{R_{int} + R_{surf}} \qquad (11.2)$$

where :

R_{tot} = total heat transfer resistance
R_{int} = internal heat transfer resistance
R_{surf} = surface heat transfer resistance.

For a homogeneous cylindrical sheath, the internal and surface heat transfer resistances

may be written as follows for a single-section lumped model[9]:

$$R_{int} = \frac{\ln (r_o/r_i)}{2\pi kL} \qquad (11.3)$$

$$R_{surf} = \frac{1}{2\pi hLr_o} \qquad (11.4)$$

where :

r_o = outside radius of thermocouple
r_i = radius at which the junction is located
k = thermal conductivity of sensor material
L = effective heat transfer length
h = film heat transfer coefficient.

Substituting Equation 11.3 and 11.4 in Equation 11.1 and 11.2 yields :

$$\tau = \frac{mc}{UA} = mc \left[\frac{\ln(r_o/r_i)}{2\pi kL} + \frac{1}{2\pi hLr_o} \right] \tag{11.5}$$

Since $m = \rho \pi r_o^2 L$ we can write :

$$\tau = \frac{\rho c r_o^2}{2k} \left[\ln (r_o/r_i) + \frac{k}{hr_o} \right] \tag{11.6}$$

where ρ is the density of the material in the sensor. Note that the second term in Equation 11.6 is reciprocal of the Biot Modulus ($N_{Bi} = hr_o/k$).

Writing Equation 11.6 in terms of two constants C_1 and C_2, we will obtain :

$$\tau = C_1 + C_2 / h \tag{11.7}$$

where :

$$C_1 = \frac{\rho c r_o^2}{2k} \ln (r_o/r_i) \tag{11.8}$$

$$C_2 = \frac{\rho c r_o}{2} \tag{11.9}$$

Equation 11.7 can be used to estimate the response time of a thermocouple after it is installed in a process based on response measurements made in a laboratory. The procedure is to make laboratory response time measurements in at least two different heat transfer media (with different values of h) and identify C_1 and C_2. Once C_1 and C_2 are identified, Equation 11.7 can be used to estimate the response time of the thermocouple in process media for which the value of h can be estimated based on the type of media and its temperature, pressure, and flow conditions. A useful application of Equation 11.17 is in estimating the response time of a thermocouple at a given process flow rate based on response time measurements in a laboratory flow loop. This application is described below.

11.3 Response Time Versus Flow Correlation

A correlation for response time versus fluid flow rate is derived here by determining the relationship between the heat transfer coefficient (h) in Equation 11.7 and fluid flow rate (u).

The heat transfer coefficient is obtained using general heat transfer correlations involving the Reynolds number, Prandtl number, and Nusselt number which have the following relationship:

$$Nu = f(Re,\ Pr) \qquad\qquad (11.10)$$

In this equation, $Nu = hD/K$ is the Nusselt number, $Re = Du\rho/\mu$ is the Reynolds number, and $Pr = C\mu/K$ is the Prandtl number. These heat transfer numbers are all dimensionless and their parameters are defined as follows :

h = film heat transfer coefficient
D = sensor diameter
K = thermal conductivity of process fluid
u = average velocity of process fluid
ρ = density of process fluid
μ = viscosity of process fluid
C = specific heat capacity of process fluid

For the correlation of Equation 11.10, several options are available in the literature for flow past a signal cylinder. One of the common correlations is that of Rohsenow & Choi[10], and the other is from Perkins & Leppert[11]. The Rohsenow & Choi correlation is :

$$Nu = 0.26 \ Re^{0.6} \ Pr^{0.3} \quad for \quad 1,000 < Re < 50,000 \qquad (11.11)$$

and the Perkins & Leppert correlation is :

$$Nu = 0.26 \ Re^{0.5} \ Pr^{1/3} \quad for \quad 40 < Re < 10^5 \qquad (11.12)$$

The second correlation covers a wider range of Reynolds numbers and is probably more suited for air, while the first correlation is more suited for water. Substituting Equation 11.11 or 11.12 in Equation 11.10 will yield :

$$h = C_1' u^{0.6} \qquad or \qquad h = C_2' u^{0.5} \qquad (11.13)$$

where C_1' and C_2' are constants and u is the fluid flow rate. Substituting the relations given by 11.13 in Equation 11.7, we will obtain the correlation between the response time and fluid flow rate:

$$\tau = C_1 + C_3 \ u^{-0.6} \qquad (11.14)$$

or

$$\tau = C_1 + C_4\, u^{-0.5} = C_1 + \frac{C_4}{\sqrt{u}} \tag{11.15}$$

Either one of the above two equations may be used to estimate the response time of a thermocouple as a function of flow rate. In this project, we have used equation 11.14 in the response versus flow experiments described later in this report. Others have used Equation 11.15 for diagnosis of very low liquid and gas flows using a thermocouple as a flow sensor. This is important because most flow sensors are not sensitive enough at very low liquid or gas flow rates while thermocouple response times are very sensitive at low flow rates and can therefore be used to detect very small changes at low flows. Figure 11.3 shows experimental results for detecting small changes at low flows using a differential pressure sensor for flow indication and a thermocouple[12].

With either of the two Equations 11.14 or 11.15, one can make measurements at two or more flow rates in water or other convenient media in a laboratory and identify the two constants of the response versus flow correlation for the thermocouple in hand. Once these constants are identified, they can be used to estimate the response time of the thermocouple in other media for which the flow rate (u) is known.

11.4   General Effects of Temperature on Response Time

Unlike flow, the effect of temperature on response time of a thermocouple can not be estimated with great confidence. This is because temperature can either increase or decrease the response time of a thermocouple. Temperature affects both the internal and the surface components of the response time. Its effect on the surface component is similar to that of the

114

AMS—DWG THC061B
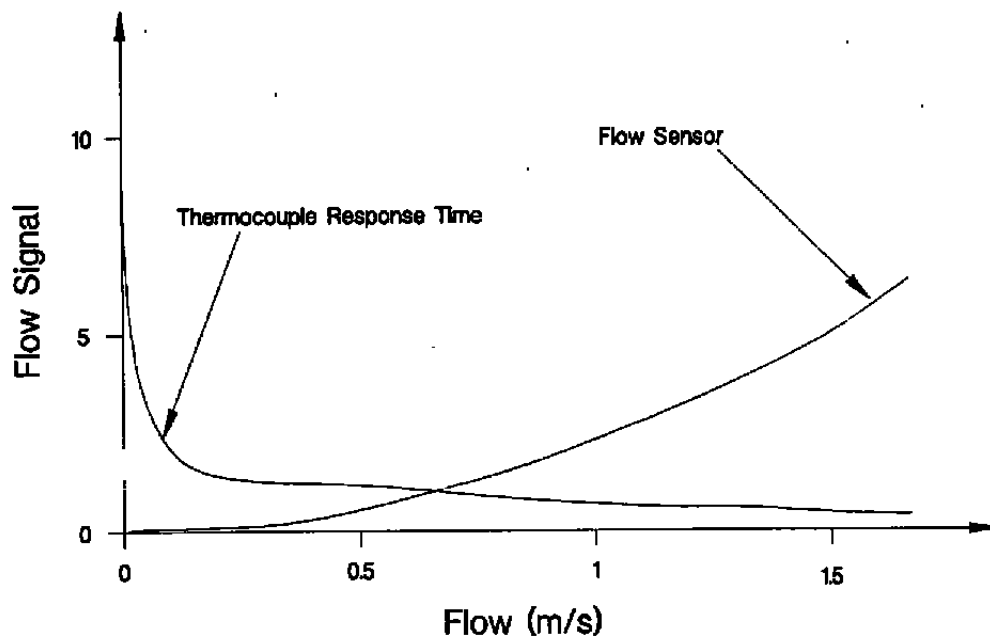
Figure 11.3. Thermocouple Response Time for Detection
of Small Changes at Low Flows.

flow. That is, as temperature is increased, the film heat transfer coefficient (h) generally increases and causes the surface component of response time to decrease. However, the effect of temperature on the internal component of response time is more subtle. High temperatures can cause the internal component of response time to either increase or decrease depending on how temperature may affect the properties and the geometry of the material inside the thermocouple. Due to differences in the thermal coefficient of expansion of materials inside the thermocouple and the sheath, the insulation material inside the thermocouple may become either more or less compact at higher temperatures. Consequently, the thermal conductivity of the thermocouple material and therefore the internal response time can either increase or decrease. Furthermore, voids such as gaps and cracks in the thermocouple construction material can either expand or contract at high temperatures and cause the internal response time to either increase or decrease depending on the size, the orientation, and the location of the void. At high temperatures, the sheath sometimes expands so much that an air gap is created at the interface between the sheath and the insulation material inside the thermocouple. In this case, the response time can increase significantly with temperature.

In experiments conducted by Carroll and Shepard[2] in a Sodium loop at the Oak Ridge National Laboratory (ORNL), more than a dozen insulated junction type K sheathed thermocouples with Magnesium Oxide (MgO) insulation were tested for the effect of temperature on response time. All these thermocouples were found to have a larger response time at higher temperatures. Figure 11.4 shows two examples of the ORNL results. The thermocouples in the ORNL experiments were all 0.16 cm in outside diameter and were tested in flowing Sodium

AMS—DWG GRF025C
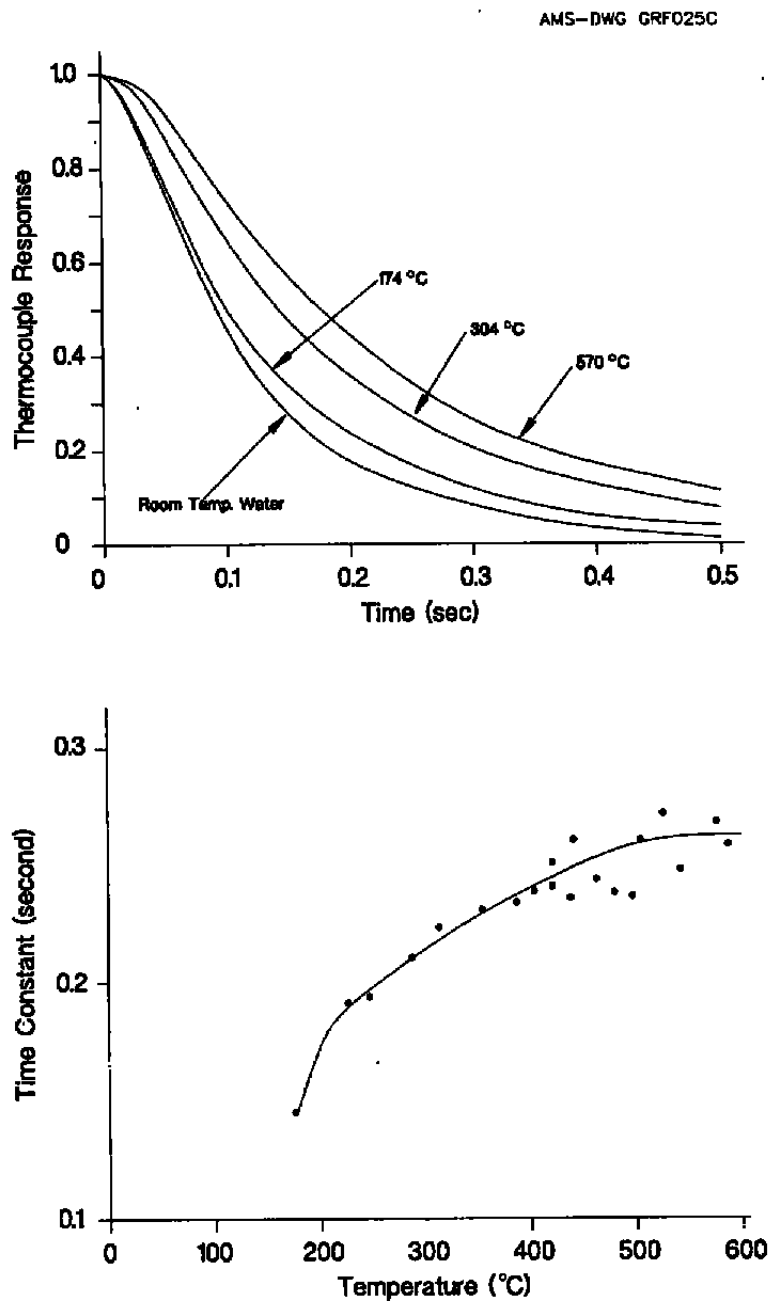
Figure 11.4. Examples of Effect of Temperature on Response
Time of Sheathed Thermocouples.

at approximately 0.6 cm per second. It was further determined by ORNL that the effect of temperature on response time of different thermocouples is different. It was confirmed that the effect of temperature on an identical group of thermocouples is different from one thermocouple to another. Therefore a general response time versus temperature relationship could not be determined for thermocouples tested by ORNL.

The above discussions demonstrate that the only way to obtain the actual response time of a thermocouple under process operating temperature conditions is to use the Loop Current Step Response (LCSR) method. However, when it is impossible or impractical to perform a LCSR test, and a rough estimate of response time suffices, the information which we have presented in this chapter can be used in lieu of an in-situ test.

11.5 Effect of Temperature on Heat Transfer Coefficient

In this section, we will show how to account for the effect of temperature on the surface component of response time. Neglecting the effect of temperature on the internal component of response time, the term C_1 in Equation 11.14 will be unchanged. Therefore, we only need to account for the effect of temperature on the second term of Equation 11.4.

For a given reference flow rate, it can be shown that the second term of Equation 11.4 is affected by temperature as follows[9] :

$$C_3(T_2) = C_3(T_1) \frac{h(T_1)}{h(T_2)} \tag{11.16}$$

118

Therefore, if we know the value of constant C_3 at room temperature (approximately 21°C or 70°F), we can find its value at temperature (T_2) if $h(70°F)/h(T_2)$ is known. Based on Equation 11.11 (Rohsenow & Choi correlation), we can write :

$$\frac{h(70°F)}{h(T)} = (4.3612)K(T)^{-0.7}\mu\,(T)^{0.3}\,\rho\,(T)^{-0.6}C_p\,(T)^{-0.3} \qquad (11.17)$$

From the Perkins and Leppert correlation:

$$\frac{h(70°F)}{h(T)} = (3.3603)K(T)^{-2/3}\mu(T)^{1/6}\,\rho(T)^{-0.50}C_p(T)^{-1/3} \qquad (11.18)$$

A plot of Equations 11.17 and 11.18 for water is shown in Figure 11.5.

The data in Figure 11.5 are for a pressure of approximately 140 bars ($\approx$ 2000 psi). However, since the properties of water are not strongly dependent on pressure, the data should hold for pressures of up to about $\pm$ 30% of 140 bars. Note that there is a large difference between the two curves in Figure 11.5 arising from the use of two different heat transfer correlations.
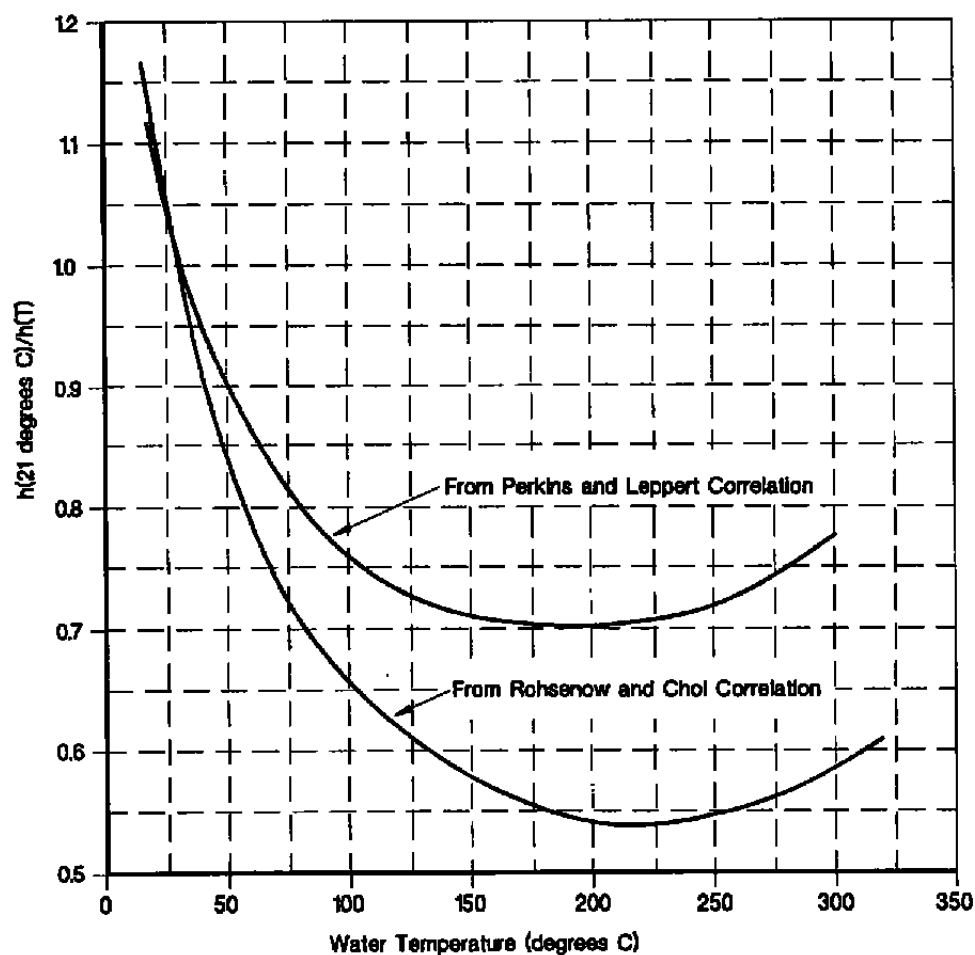
Figure 11.5. Correlations for Determining the Effect of Temperature on Thermocouple Response Time.

120

12. LCSR VALIDATION

A major portion of the research conducted in this project was concentrated on experimental validation of the Loop Current Step Response (LCSR) method for in-situ response time testing of thermocouples of the types and sizes of interest to the Air Force. The key results of the validation work are summarized in this chapter and the details are presented in Volume II under a separate cover. A listing of the representative thermocouples that were included in the validation work and their pertinent characteristics are given at the end of this chapter.

The validation work described here was essential to establish the LCSR testability of thermocouples and determine the accuracy of the response time results obtained by the LCSR method. More specifically, the following questions had to be addressed for types J, K, E, and T thermocouples with wire or sheath outside diameters ranging from approximately 0.1 to 6 millimeters:

1. The optimum heating times and the current levels needed to generate suitable LCSR signals.

2. The characteristics (e.g., gain and frequency response) of amplifiers and filters to be used in LCSR testing.

3. The optimum sampling rates and the total sampling times that should be used in digitizing the LCSR signals for computer analysis.

4. The best mathematical fitting algorithms and computer fitting methods to be programmed into a microprocessor for automatic analysis of LCSR data.

5. The effect of long extension wires and thermocouple connectors on LCSR signals.

6. The accuracy of the response time results obtained from LCSR testing of thermocouples in liquid and gaseous process media.

7. The minimum current levels that can be used to perform a LCSR test on a thermocouple.

The last question was addressed in light of a specific concern expressed by the Air Force for testing of those thermocouples that can not be given high electrical currents for the fear that they could cause an explosion and for other process installation concerns. To accommodate these concerns, the test equipment that has been developed in this project is equipment with a programmable power supply that can be programmed to automatically limit the amount of electrical currents that are used in the LCSR tests. This is discussed in more detail in Volume III.

Based on the results of the validation research conducted in this project, it has been concluded that the thermocouples of interest to the Air Force are in-situ testable by the LCSR method and the average accuracy of the test results is about 20 percent. This exceeds the Air Force requirement for the accuracy of the response time results. The Air Force has specified that in-situ response time results that are within a factor of two of the true response times of installed thermocouples are acceptable. It has been determined that when long extension wires and multiple connectors are not involved, accuracies of as good as 10 percent can be expected in LCSR results when optimum test currents, heating times, sampling rates, and sampling times are used and the data is properly analyzed.

The equipment, procedures and training instructions that have been developed in this project are intended to provide all that is needed to conduct an accurate LCSR test and obtain correct response time results for common thermocouple types and sizes as installed in liquid and

122

gaseous process media. The project did not specifically address the response time testing of thermocouples that are embedded in solids or attached to solid surfaces. However, much of the research and equipment development work completed in this project is useful in developing a capability for response time testing of thermocouples used in media other than liquids and gases.

12.1 Validation Results in Laboratory Conditions

The validation of the LCSR method involves a plunge test followed by a LCSR test performed under the same test conditions on each thermocouple. The LCSR data is analyzed and the response time results for the thermocouple is compared with that of the corresponding plunge test to establish the validity and the accuracy of the LCSR method. For resistance temperature detectors (RTDs), the sensor is said to be testable by the LCSR method if the difference between its plunge test and LCSR test results is generally less than 10 percent[13]. For thermocouples, however, a difference of 20 to 30 percent is usually used as the threshold for expressing LCSR testability depending on the thermocouple, the test conditions, the length of extension wires, the number of connectors in the circuit, and the maximum current levels that can be used to perform the LCSR test.

Table 12.1 presents typical validation results for representative thermocouples tested in the laboratory in room temperature water flowing at 1 meter per second (m/s). The reasonable agreement between the plunge and the LCSR test results shown in Table 12.1 indicates that these thermocouples are in-situ testable by the LCSR method. The same type results are listed in Table 12.2 from testing of thermocouples in room temperature air flowing at 14 m/s. Again, the agreement between the results of the two tests are reasonable in most cases, indicating that the LCSR method is valid for these thermocouples as installed in flowing air.

TABLE 12.1

LCSR Validation Results in Water

Tag Number	Outside Diameter (mm)	Response Time (sec) Plunge	LCSR
		TYPE E	
44	6	1.9	1.6
27	5	1.9	1.8
29	3	1.4	1.3
43	2	0.3	0.4
		TYPE J	
46	6	1.8	1.5
36	5	1.4	1.1
38	3	1.8	1.4
40	2	0.4	0.4
		TYPE K	
4	6	2.7	2.7
7	5	2.7	2.4
9	3	0.7	0.6
13	2	0.3	0.2

Above results are from plunge and LCSR tests in room temperature water flowing at 1 meter/second.

TABLE 12.2

LCSR Validation Results in Air

Tag Number	Outside Diameter (mm)	Response Time (sec)	
		Plunge	LCSR
TYPE E			
51	Exposed Junction	1.1	0.8
43	2	3.9	4.5
29	3	10.6	12.1
27	5	17.1	22.3
44	6	23.9	32.6
TYPE J			
52	Exposed Junction	1.3	1.2
40	2	3.2	3.8
38	3	9.9	12.1
36	5	17.5	21.3
46	6	24.9	35.9
TYPE K			
22	Exposed Junction	0.5	0.3
13	2	3.7	3.9
9	3	10.0	11.3
7	5	17.1	23.0
4	6	25.2	29.7

Above results are from plunge and LCSR tests in room temperature air flowing at 14 meters/second.

Note that the thermocouple dimensions given in the tables mentioned above and in the rest of this report are approximate values that were converted from the English units and presented here in round numbers.

The results in Table 12.1 and 12.2 are shown graphically in Figure 12.1. This is followed by Figure 12.2 which shows the step response of a thermocouple from a laboratory plunge test. The signal on the top of Figure 12.2 indicates the time when the thermocouple was exposed to a sudden change in temperature, and the signal on the bottom shows the transient response of the thermocouple to the step change in temperature. The combination of the two signals as shown in Figure 12.2 is referred to as plunge test data or plunge test transient. The response time of the thermocouple is obtained directly from this data by simply measuring the time from when the step change in temperature is imposed, to the time when the thermocouple reaches 63.2 percent of its final steady state value.

Typical LCSR transients for testing of thermocouples in water and air are shown in Figure 12.3. These are inverted and normalized LCSR cooling transients. All LCSR transients shown hereafter in this report are inverted and in most cases are normalized for ease of comparison. The details of how LCSR tests are conducted and further laboratory validation results for different thermocouple sizes and test conditions are presented comprehensively in Volume II.

The laboratory plunge tests conducted in this project were based mostly on the methods prescribed by the American Society for Testing and Materials (ASTM). The ASTM methods for response time testing of industrial RTDs and thermocouples are outlined in two standards:
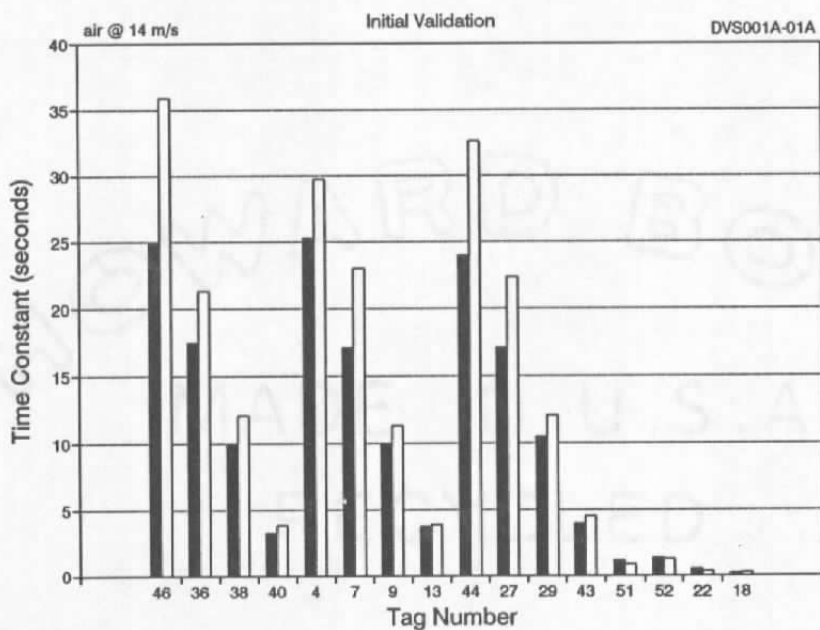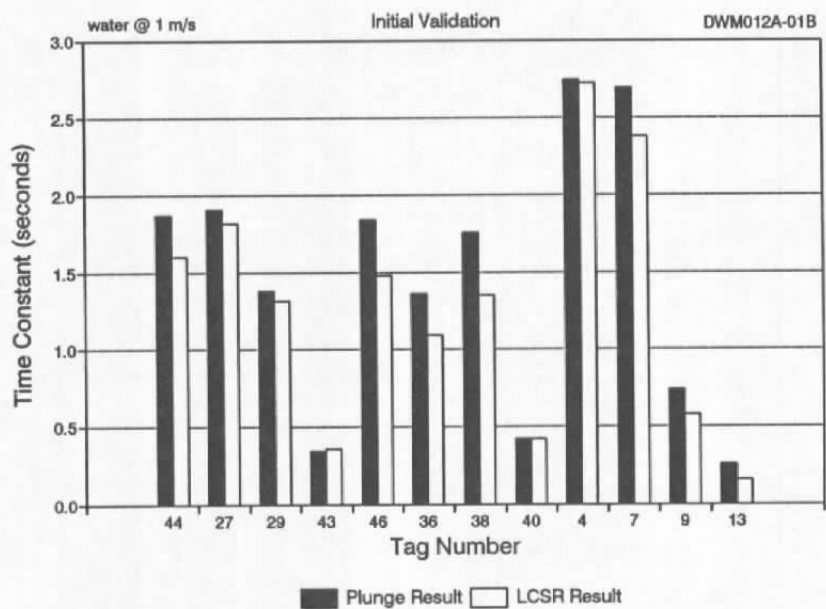
Figure 12.1. LCSR Validation Results in Water and Air.

127

'D: 25 M<15:04:54 *05 JUN 90 *SPD: 5 MM/S (200.0 MS/MM)
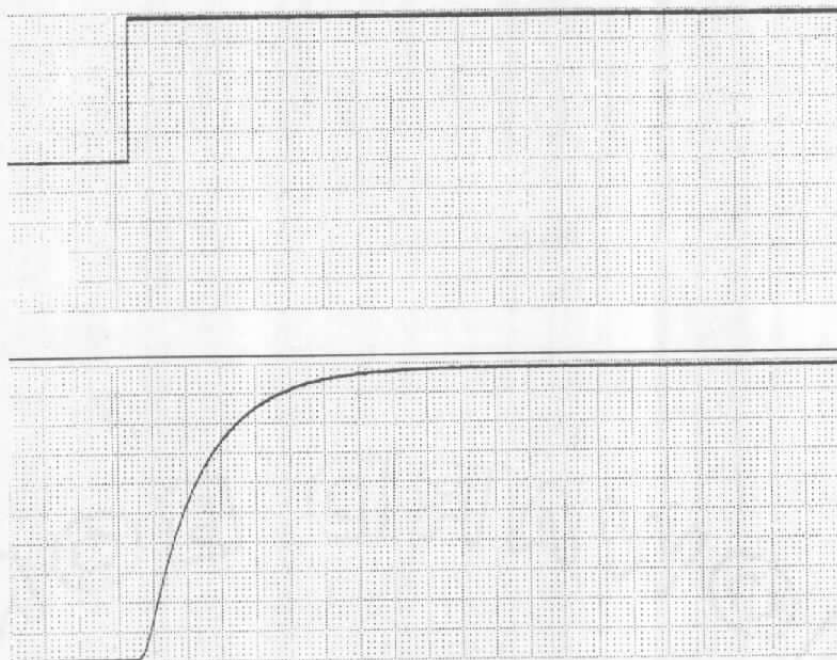
Figure 12.2. A Typical Plunge Test Transient.
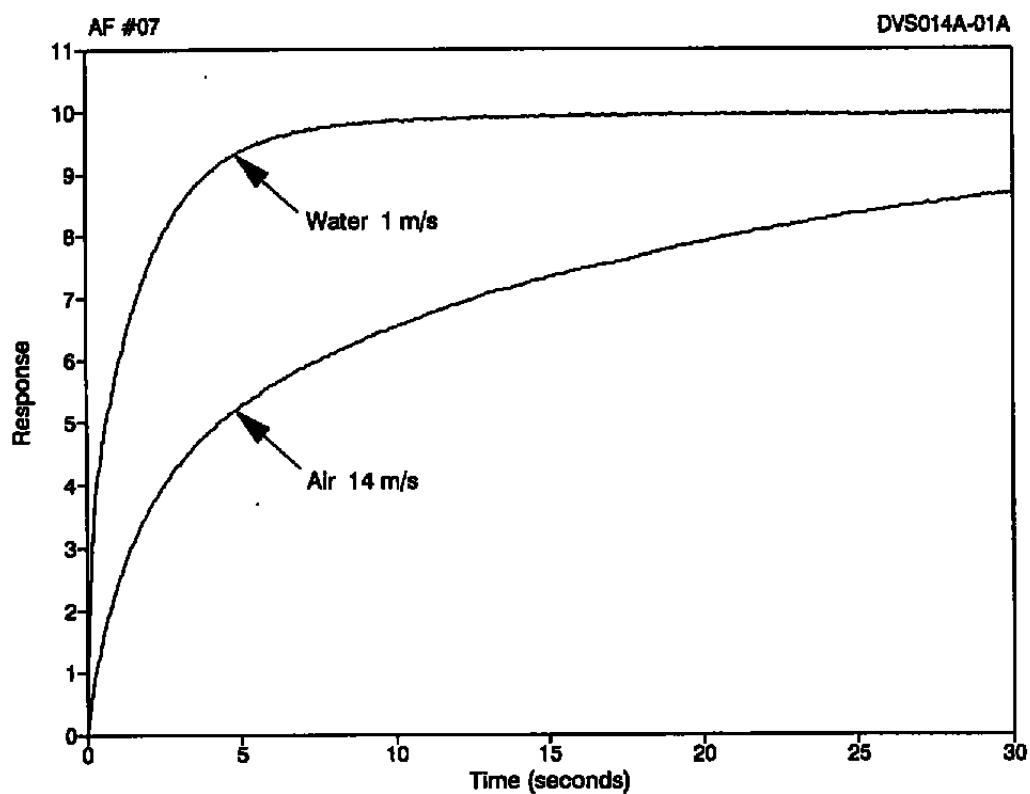
Figure 12.3. Typical LCSR Transients in Water and Air.

1. ASTM Standard E839-89 entitled, "Standard Test Methods for Sheathed Thermocouples and Sheathed Thermocouple Material".

2. ASTM Standard E644-86 entitled "Standard Methods for Testing Industrial Resistance Thermometers".

These Standards are published in the annual book of ASTM standards[14,15]. There is no standard for LCSR testing of thermocouples. The only standard that relates to the LCSR method is that of the Instrument Society of America (ISA) for RTDs[16]. Referred to as ISA Standard 67.06, this standard outlines the acceptable methods for response time testing of safety-related sensors in nuclear power plants. It includes the LCSR method for in-situ response time testing of RTDs as installed in nuclear power plants.

12.2 Validation Results in Wind Tunnels

Since many aerospace applications involve temperature measurements in high air velocities, some LCSR validation tests were performed at flow rates beyond what could be generated in the laboratory air loop that was constructed for this project. Thus, the high flow tests were performed in the subsonic and supersonic wind tunnels at the Mechanical and Aerospace Engineering Department at the University of Tennessee in Knoxville (UT). In the subsonic tunnel, a system was set up to permit plunge testing, but in the supersonic tunnel, plunge tests could not be performed. Therefore, the thermocouples that were selected for the supersonic tests were plunge tested in the AMS laboratory and their response time results were extrapolated to the supersonic flow conditions using the guidelines given in Chapter 11.

Table 12.3 presents the results of the LCSR validation tests performed in the subsonic wind tunnel for three air flow rates. The results for 60 and 100 miles per hour velocities are presented graphically in Figure 12.4. The reasonable agreements between the plunge and the LCSR results testify to the validity of the LCSR method for testing of these thermocouples.

TABLE 12.3

LCSR Validation Results in
Subsonic Wind Tunnel

Tag Number	Response Time (sec)	
	Plunge	LCSR
27 m/sec ≈ 60 miles/hr		
14	1.4	1.2
15	0.7	0.8
16	1.7	1.5
22	0.4	0.5
29	8.0	9.1
40	2.5	4.4
45 m/sec ≈ 100 miles/hr		
14	1.2	2.0
15	0.4	0.3
16	1.1	1.0
22	0.3	0.4
40	2.2	3.0
55 m/sec ≈ 123 miles/hr		
29	6.0	6.3
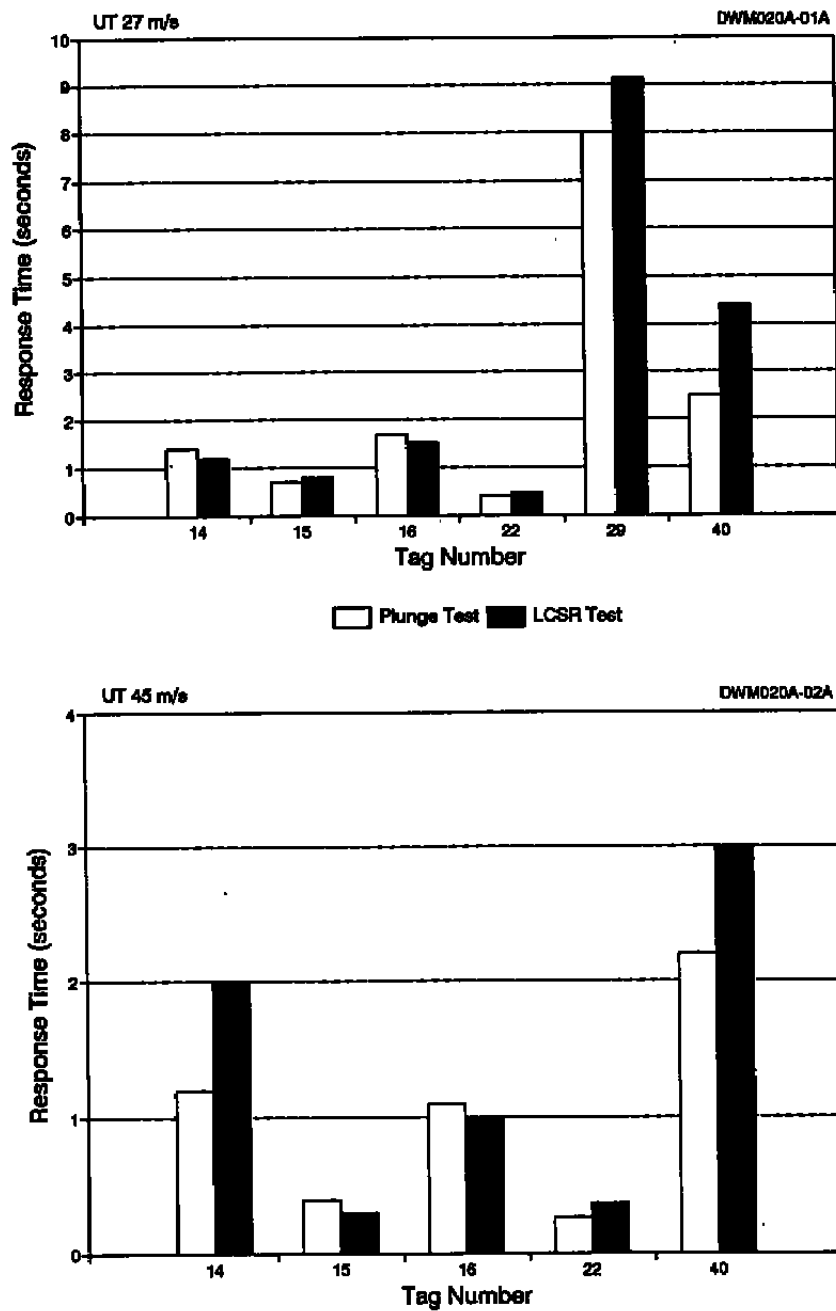
Figure 12.4. Representative Results of LCSR Validation
Tests in Subsonic Wind Tunnel.

The results from the tests in the supersonic tunnel are given in Table 12.4. These results are from the LCSR tests in the supersonic tunnel at Mach 2. The reasonable agreement between the plunge and LCSR results shown in Table 12.4 indicates that the LCSR method is valid for these thermocouples at supersonic flow conditions. Typical LCSR transients for two of the thermocouples tested in the supersonic wind tunnel are given in Figure 12.5.

12.3 LCSR Software Qualification

In Chapter 10, we covered the theory of the LCSR method and presented the analysis procedure for obtaining the response time of a thermocouple using the LCSR data. The analysis is needed because the LCSR data is obtained by internal heating of a thermocouple while the response time of interest should result from a step change in temperature outside the thermocouple. Therefore, the LCSR data must be converted by a mathematical fitting procedure implemented on a computer to transform the LCSR data to an equivalent plunge test transient and yield the response time of the thermocouple tested. The details of the mathematical equations and procedures for the transformation of LCSR data were covered in Chapter 10.

Three independent algorithms were developed in this project and tested for computer analysis of LCSR data for various thermocouples. These developments took advantage of our earlier work on LCSR analysis of Resistance Temperature Detectors (RTDs) in nuclear power plant applications. An analysis technique and a software package called "Time Series Fitting or TSFIT" that had been developed for RTDs was found to be equally useful for thermocouples. The results of LCSR analysis with the TSFIT package are shown in Table 12.5 and compared with the results of two other techniques implemented in two computer codes called LST-SQ and

TABLE 12.4

LCSR Validation Results in Supersonic Wind Tunnel
(Mach 2)

Tag Number	Response Time (sec) @ 14 m/sec Plunge	Response Time (sec) @ Mach 2 Plunge*	LCSR
18	0.14	0.05	0.05
20	0.16	0.05	0.04
22	0.49	0.06	0.06
23	0.50	0.06	0.08

* *Extrapolated from laboratory measurements.*
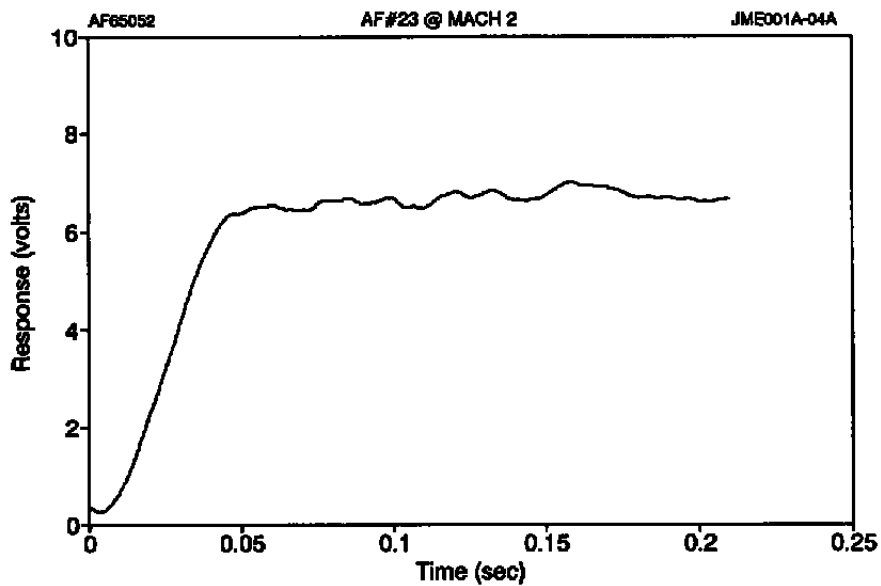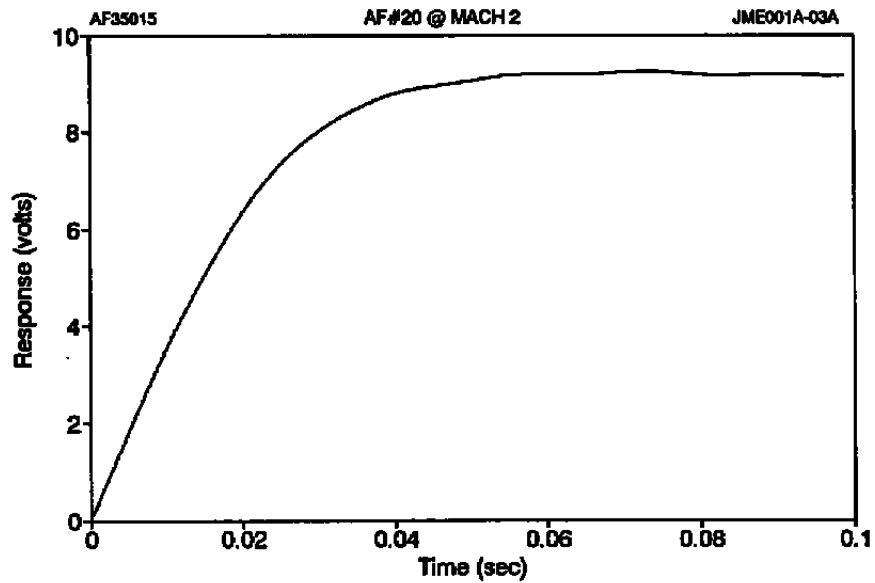
Figure 12.5. Typical LCSR Transients from Tests in Supersonic Wind Tunnel.

TABLE 12.5

Results of LCSR Software Qualification

Tag Number	Response Time by Plunge (sec)	Response Time (sec) by LCSR Test		
		TSFIT	LST-SQ	XTCA9
		Water @ 1 m/s		
4	2.7	2.6	2.4	2.1
7	2.7	2.4	2.2	3.2
9	0.7	0.6	0.5	0.5
13	0.3	0.2	0.2	0.2
27	1.9	2.0	1.7	1.6
29	1.4	1.2	1.2	1.8
36	1.4	1.2	1.0	0.7
38	1.9	1.7	2.1	2.3
38	1.8	1.4	1.8	1.6
40	0.4	0.5	0.3	0.3
43	0.3	0.4	0.3	0.3
44	1.9	1.7	2.1	0.16
46	1.8	1.5	1.5	1.2
		Air @ 14 m/s		
7	17.1	27.0	26.0	26.1
7	17.1	19.7	17.2	26.6
13	0.3	0.3	0.3	0.2
27	17.1	18.4	16.5	34.2
36	17.5	22.6	20.2	62.7
36	17.5	22.8	20.5	39.4
36	17.5	18.2	30.0	20.8

XTCA9. The results are given for both plunge tests and LCSR tests in room temperature water flowing at 1 m/s and in room temperature air flowing at 14 m/s. The results for the tests in water are shown graphically in Figure 12.6. Based on these and other similar results produced during the project, it was determined that the TSFIT is the most suitable approach and it was therefore selected for use in the microprocessor-based LCSR test analyzer that has been developed in this project. The details of development of the LCSR analyzer are given in Volume III.

12.4   LCSR Noise Reduction

The LCSR transient for a thermocouple may contain both high frequency and low frequency noise. For the purpose of this discussion, we define high frequency noise as those electrical and other interferences with frequencies of 10 Hz or higher, and low frequency noise as the low amplitude fluctuations of less than 10 Hz which often result from temperature fluctuations in the process.

The high frequency noise is removed with a Low-Pass (LP) electronic filter. The LP filter must be set at a frequency that is low enough to adequately remove the extraneous noise, and at the same time is high enough to ensure that it will not eliminate any useful portion of the thermocouple signal. The following equation provides a guide for where the LP filter should be set at:

$$\tau = \frac{1}{2\pi F} \qquad \text{or} \qquad F = \frac{1}{2\pi \tau} \qquad\qquad (12.1)$$

137
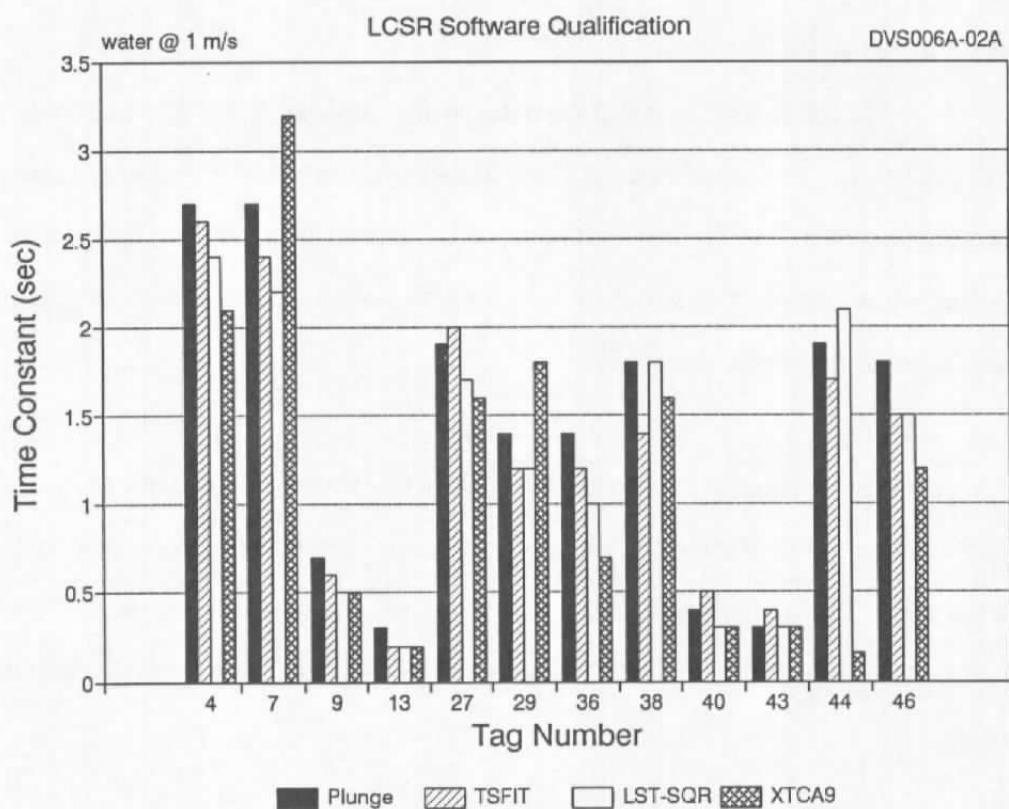
Figure 12.6. LCSR Software Qualification Results.

where τ is the expected response time of the thermocouple (in seconds) and F is a its corresponding frequency response or corner frequency in Hz. The LP filter should be set at about 10 to 20 times the frequency response (F) depending on the roll off rate or sharpness of the LP filter. Figure 12.7 shows two LCSR transients with and without filtering. Note how the high frequency noise that is apparent on the top transient in Figure 12.7 is not present in the filtered transient at the bottom.

12.5   Averaging of LCSR Data

To reduce the effect of low frequency noise, the LCSR test is repeated 10 to 30 times and the raw data is simply averaged to provide a smooth transient to facilitate the analysis and yield accurate results. Figure 12.8 shows three LCSR transients as follows: a single transient, an average of 10 transients, and an average of 20 transients. Note that averaging can effectively eliminate the low frequency noise on the LCSR data, and that the average of 10 single LCSR transients is usually adequate, as apparent in the case shown in Figure 12.8. Most of the LCSR transients that are shown in this report are the average of 10 data sets.

A key point in implementation of an averaging scheme is the identification of the exact beginning of the LCSR transient. It is important for the LCSR transients that are averaged to start at the same time into the data or the averaged transient would be distorted and will give incorrect results.
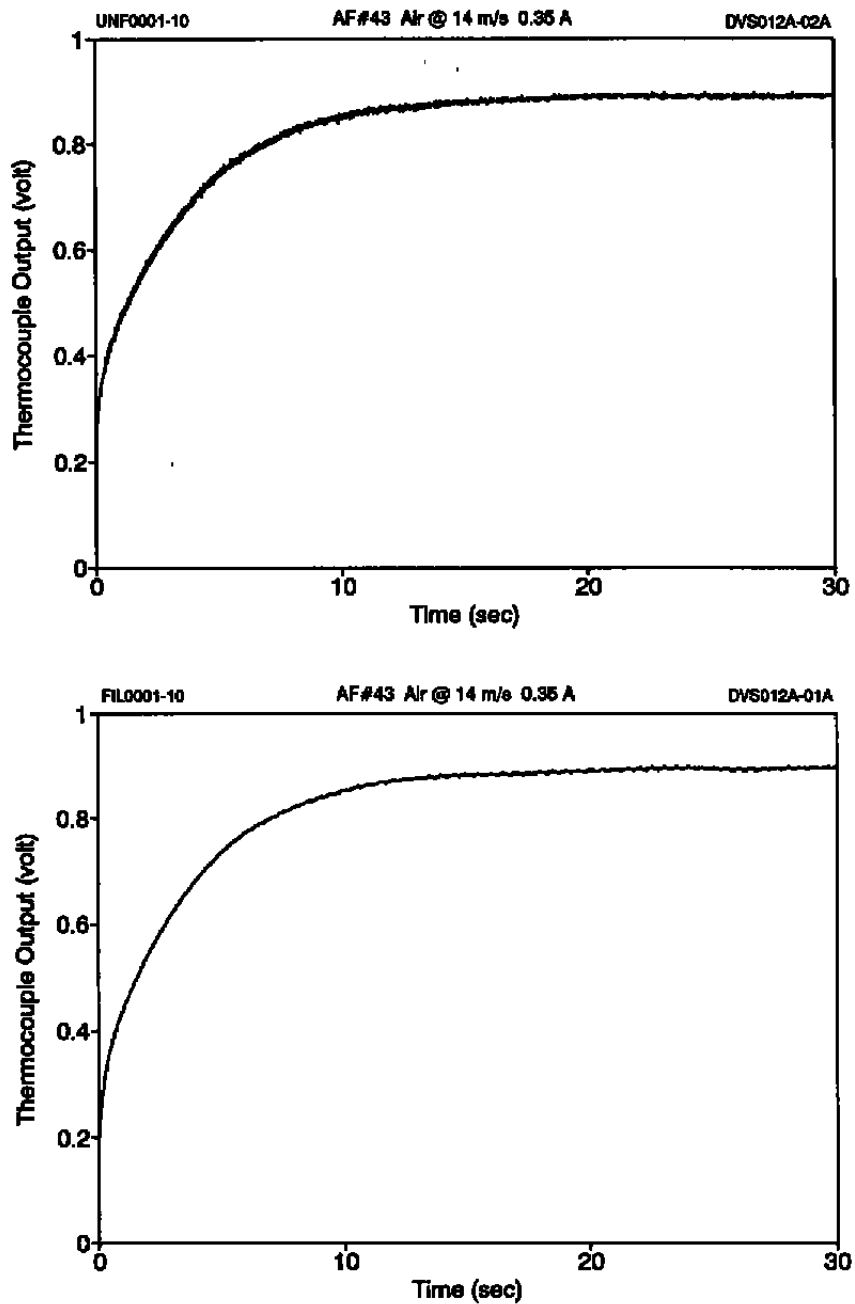
Figure 12.7. LCSR Transients With and Without Filtering.
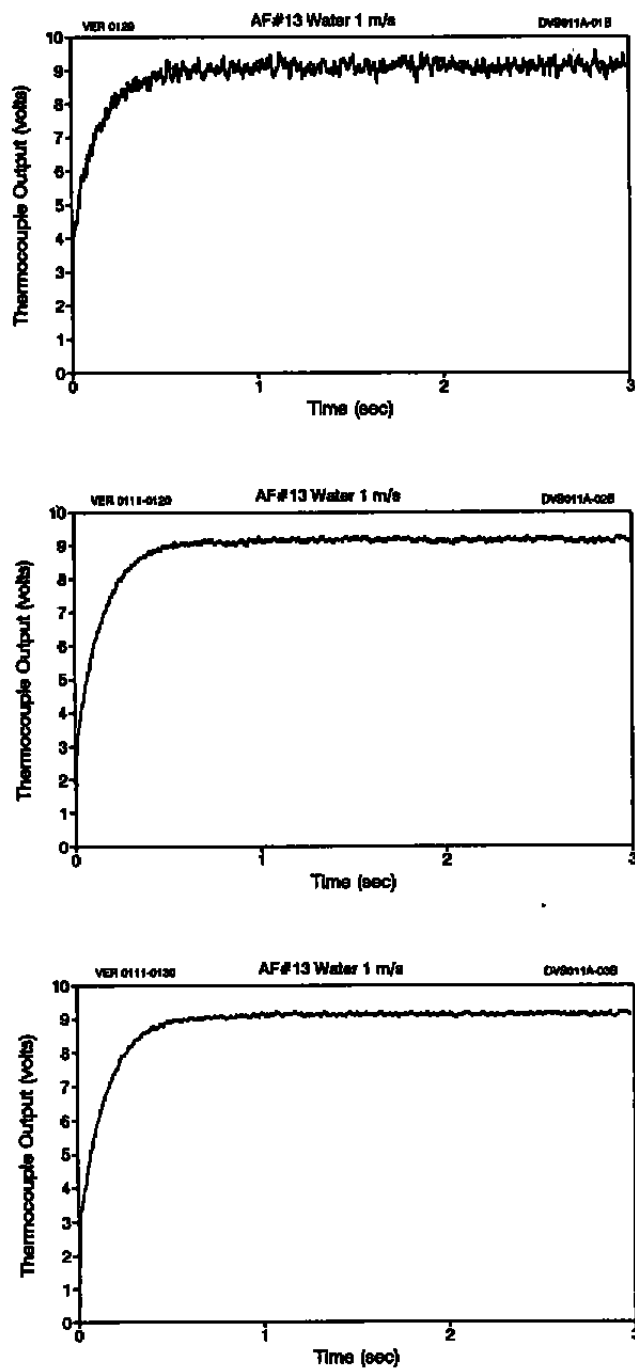
Figure 12.8. A Single Raw LCSR Transient (top), Average of 10 Transients (Middle), and Average of 20 Transients (Bottom).

12.6   LCSR Parameter Optimization

A number of parameters are involved in performing a LCSR test and analyzing the data. These parameters must be set at correct values to yield accurate LCSR results. The challenge is that these parameters are often interactive meaning that a change in one affects one or more of the others.

The LCSR data for a thermocouple that is expected to have a response time in the neighborhood of 0.10 seconds is sampled much faster and for a much shorter length of time than the data for a thermocouple that is expected to have a 10 second response time. The optimum values for these two parameters depend on the expected response time of the thermocouple under the condition that it is tested. Several other parameters are involved in a LCSR test. A description of these parameters and how to properly select them is presented below.

- **Heating Current**. The LCSR test of a thermocouple requires a heating current of about 0.3 to 3.0 amperes depending on the size (diameter) of the thermocouple, the length of the extension wires, and the process conditions in which the thermocouple is used. The rule-of-thumb is to start with a small current and increase it as necessary to obtain a reasonable LCSR transient. Figure 12.9 shows three raw transients that are labeled as reasonable, borderline, and not acceptable for accurate response time determination.

  A number of remedies are available for improving the quality of a LCSR transient. The first and usually the most effective remedy is to use a higher heating current if possible. Figure 12.10 shows how the quality of a LCSR is improved by increasing the heating current while keeping the other test parameters constant.

  There are two problems with using high heating currents. One is safety, and the other is the possibility of creating large temperature gradients in the thermocouple extension wires and connectors. A large gradient together with any inhomogeneity in the thermocouple circuit can result in EMF transients that are not related to the thermocouple junction, but are superimposed on the LCSR signal.
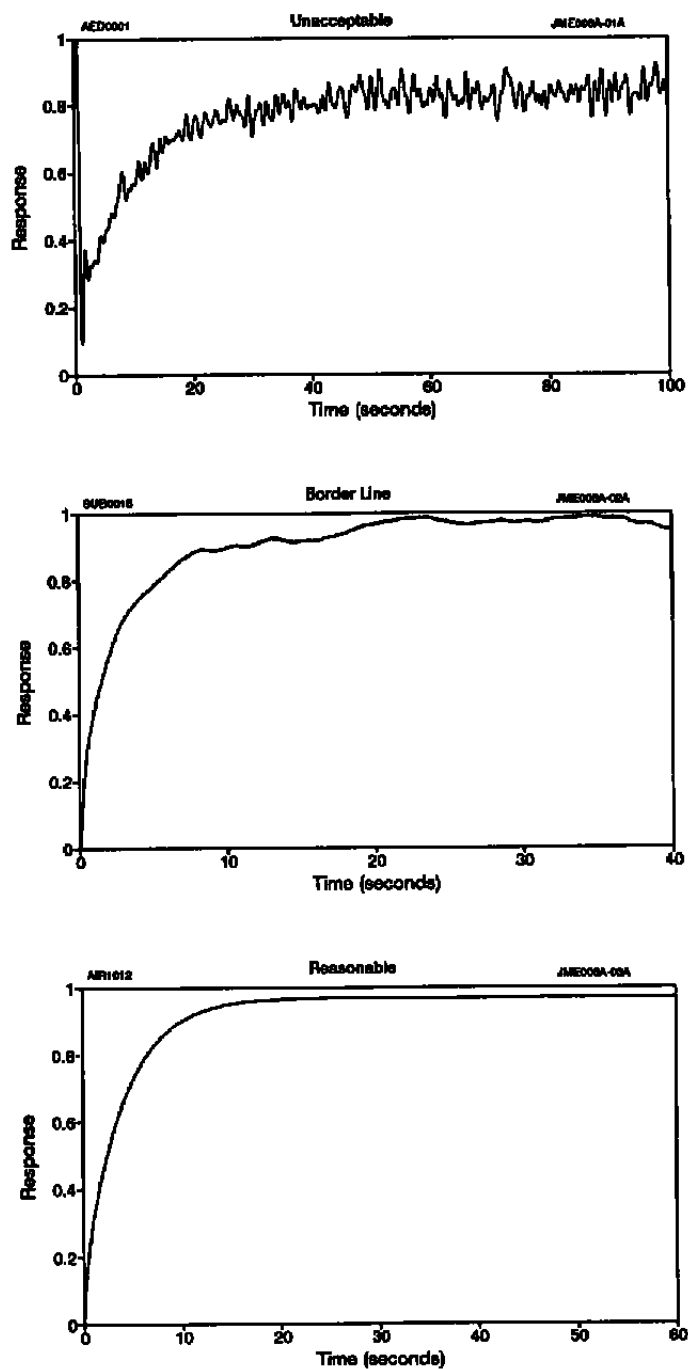
Figure 12.9. LCSR Transients of Varying Quality.

Figure 12.10. Quality of LCSR Transient Versus Applied Current.

Another remedy is to use a small heating current but a large amplifier gain to improve the dynamic range of the LCSR transient. The problem with a large gain is the possibility of introducing high frequency noise on the LCSR signal. This problem can be resolved using a low-pass filter as was explained in Section 12.4. above. There is always a trade off between the heating current, the amplifier gain, and the low pass filter setting. Another parameter that is highly linked with the heating current is the heating time as described below.

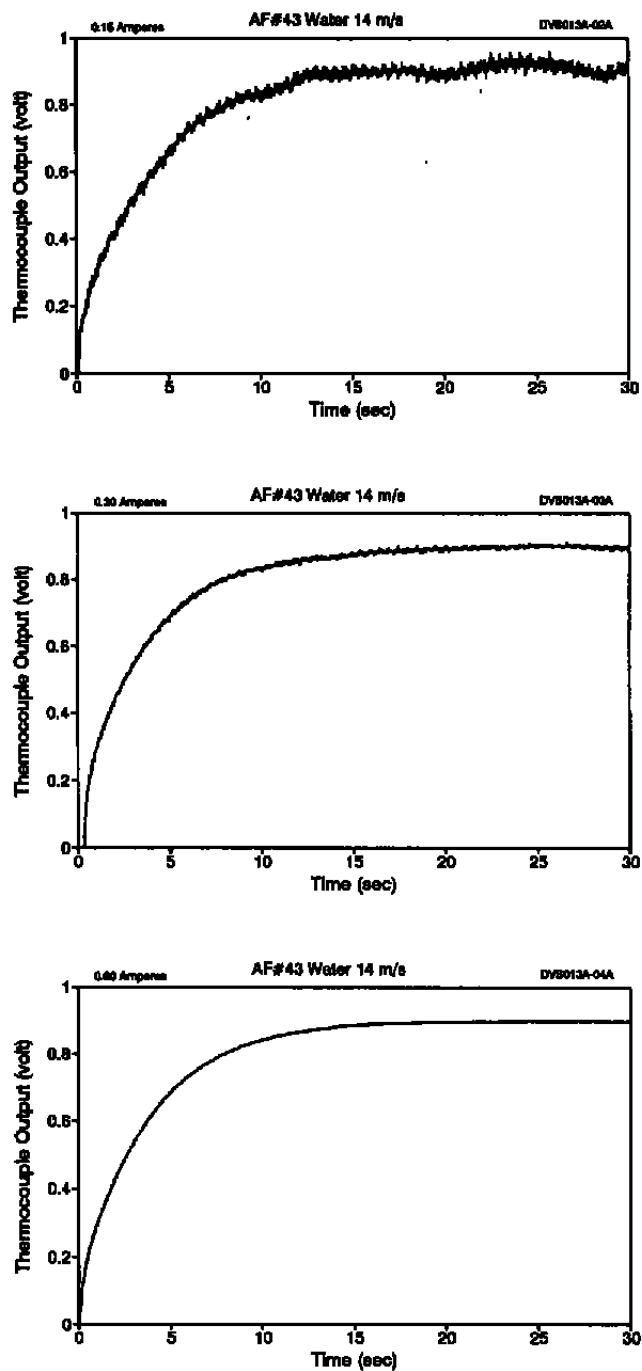- **Heating Time.** The amount of LCSR heating in a thermocouple depends not only on the applied current, but also on the heating time. Generally, the heating time should be long enough to allow the thermocouple junction to reach steady state. A good rule is to apply the heating current for about 5 to 10 times the expected response time of the thermocouple under the conditions of the test. Longer heating times do not usually have an adverse effect on the LCSR data except when there is an inhomogeneity in the thermocouple circuit. In this case, a long heating time can produce large temperature gradients that can adversely affect the LCSR transient when the current is cut off. More specifically, the effect can manifest itself in terms of an upward or downward drift on the steady state portion of the LCSR transient.

In the experiments that were conducted in this project, heating times of 5 to 15 seconds were used. A series of experiments were performed specifically to address the effect of heating currents and heating times on the LCSR results. Key results of these experiments are summarized graphically in Figure 12.11 for 5 and 15 second heating times. These results are from LCSR testing of thermocouples in room temperature water flowing at 0.6 m/s. They are shown for three current levels: low current, medium current, and high current. The current levels were 0.25, 0.5, and 1.0 amperes for thermocouples with 23, 24, and 30 gage wires, and 0.75, 1.0, and 1.5 amperes for thermocouples with 18 and 20 gage wires. The data in Figure 12.11 are given in terms of percent difference between the LCSR results and the corresponding plunge test results.

- **Amplifier Gain.** In LCSR testing of thermocouples, it is usually desirable to have signal amplitudes of near 10 volts even though signal amplitudes as low as 1 volt are often acceptable. In the laboratory LCSR tests that were conducted in this project, depending on the thermocouple being tested and the test conditions, the required amplifier gains were 20,000 to 500,000 for a 10 volt signal. The lower gains were used for the small diameter thermocouples, and the higher gains were used for large diameter thermocouples. For the tests in air, smaller gains were usually adequate, but for the tests in water, larger gains were generally required. This is because in the air tests, due to poor heat transfer, thermocouples heat up more for the same amount of current than they do in water.

- **Low-Pass Filter Setting.** The LCSR test equipment for thermocouples often require a low-pass (LP) filter. The LP filter is required to remove the high
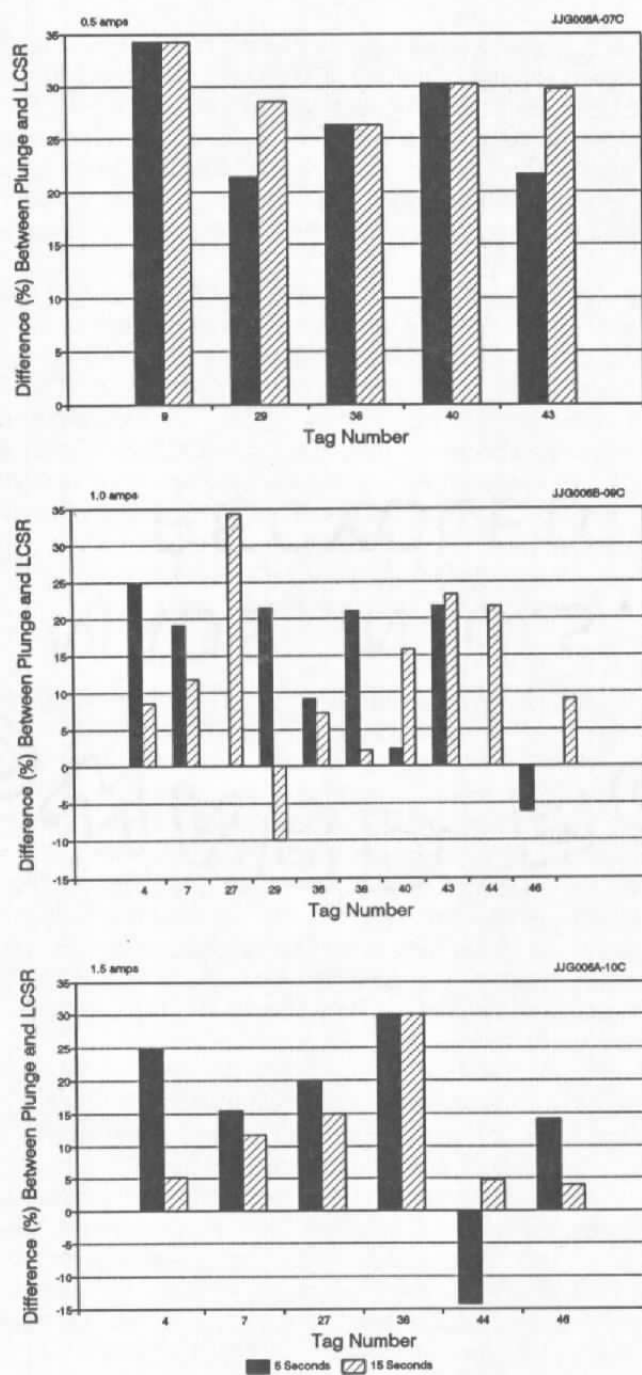
Figure 12.11. Differences Between the LCSR and Plunge Test Results
for Three Levels of LCSR Heating Currents.

frequency noise which is often present on the LCSR signals due to high amplifier gains that are usually necessary for the LCSR tests. Furthermore, thermocouples are inherently susceptible to electrical noise pick up which contaminate the LCSR data and interfere with a successful analysis. The high frequency noise should be removed using a low-pass filter that is properly set for the application in hand. The filter setting depends on the amplitude and frequency of the interfering noise. In the laboratory tests that were conducted in this project, LP filter setting of 10 to 30 Hz were often used depending on the size of the thermocouple, the heating current, and the test conditions.

- **Sampling Rate.** A 12-bit analog-to-digital converter (also referred to as A to D, ADC, or A/D) was used in all the LCSR tests that were conducted in this project and in the test equipment that was developed. The A/D was adjusted for 0 to 10 volt range for the LCSR signals. Depending on the expected response time of the thermocouple being tested, sampling intervals of 0.005 to 0.1 seconds (10 to 200 Hz) were used. The smaller sampling intervals were used in testing of the faster thermocouples and the larger sampling rates were used in testing the slower thermocouples. Although it was not attempted in the project, the use of a 16-bit A/D could have helped reduce the high amplifier gains that are required for LCSR testing of thermocouples.

- **Total Number of Samples.** The total number of points that are sampled in a LCSR test depends on the sampling rate and the time that it takes for the LCSR transient to reach steady state. The product of the sampling rate and the total number of points sampled should exceed the time that it takes for the LCSR signal to reach steady state. This time is referred to as sampling time which ranges from a few seconds to several tens of seconds, depending on the size of the thermocouple being tested and the test conditions. The tests in air generally required longer sampling time and/or large sampling rates than the tests in liquids.

- **Number of LCSR Transients to Average.** The high frequency noise and low frequency fluctuations that usually exist on the LCSR signal must be removed or minimized to yield accurate response time results. The high frequency noise is removed by a low-pass filter, and the low frequency fluctuations are minimized by averaging a group of identical tests on the same thermocouple. Since the low frequency fluctuations usually originate from the process due to random temperature fluctuations, an ensemble averaging can reduce the fluctuations without affecting the dynamic characteristics of the data.

The number of single LCSR transients that are averaged together depends on the amount of fluctuations on the data. In the experiments that were conducted in this project, 10 LCSR transients were found to be adequate in most cases even though 20 transients were sometimes used. In field tests, it may be necessary to repeat the LCSR test as many as 30 times and average the single transients to obtain a smooth data set for optimum analysis. The test equipment that was developed in this project can readily be programmed to repeat the tests automatically for the number repeats specified by the user.

12.7   LCSR Difficulties

Both AMS and the Oak Ridge National Laboratory (ORNL)[2,6], who have worked extensively on LCSR testing of thermocouples, have had a common difficulty arising for inherent inhomogeneities that are sometimes present in thermocouple circuits. The inhomogeneities can exist in the extension wires, connectors, or even inside the thermocouple itself.

Shepard and Carroll[6] noted that each LCSR transient for a thermocouple is the resultant of three separate transients illustrated in Figure 12.12.   In this figure, trace 1 illustrates the cooling transient of the thermocouple junction which we wish to measure.   Trace 2 illustrates a transient due to an inhomogeneity in the circuit, and trace 3 is from the magnetic effect that may be present at the LCSR output of a type K thermocouple.   In Figure 12.12, traces 2 and 3 are exaggerated to make the point more clear.   In actuality, these traces are not nearly as large in amplitude as they are shown.

In testing of a type K thermocouple in stagnant and stirred water, ORNL obtained two widely different LCSR transients as illustrated in Figure 12.13.   This probably occurred due to an inhomogeneity in the thermocouple circuit producing a transient that competes with the LCSR transient.   When the water is stagnant, the LCSR transient dominates because it is apparently much slower and larger in amplitude than the interfering transient.   When the water is stirred, the interfering transient dominates because the junction transient is faster and decays much quicker than that of the interfering transient.   An investigation into these types of effects revealed, in one instance, that the inserts in the connectors of a thermocouple were manufactured with a wrong alloy.

Similar results have been observed by AMS as illustrated in Figure 12.14 and 12.15.   In each of these two figures, the resultant transient is illustrated on the top and its potential

AMS—DWG GRF024A
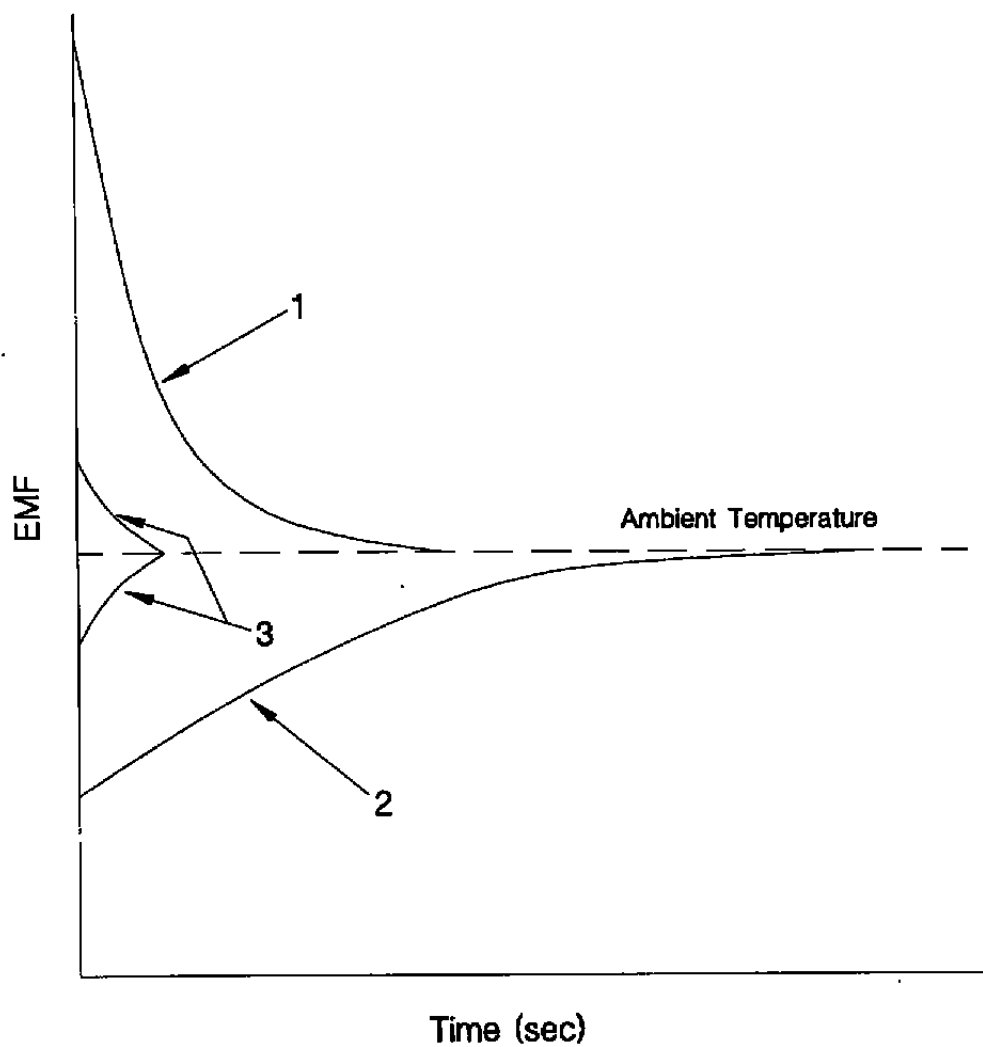
Figure 12.12. Illustration of Potential Components of a LCSR Test Transient.

AMS—DWG GRF023A
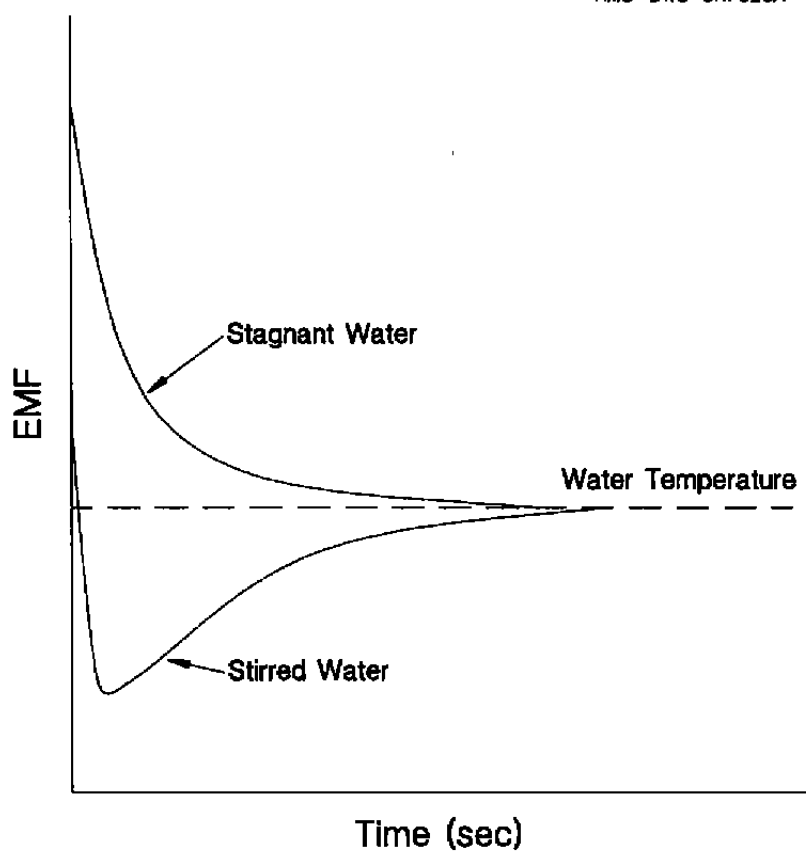
Figure 12.13. Illustration of Unusual LCSR Transients for a Thermocouple in Stagnant and Stirred Water.

AMS—DWG GRF021C
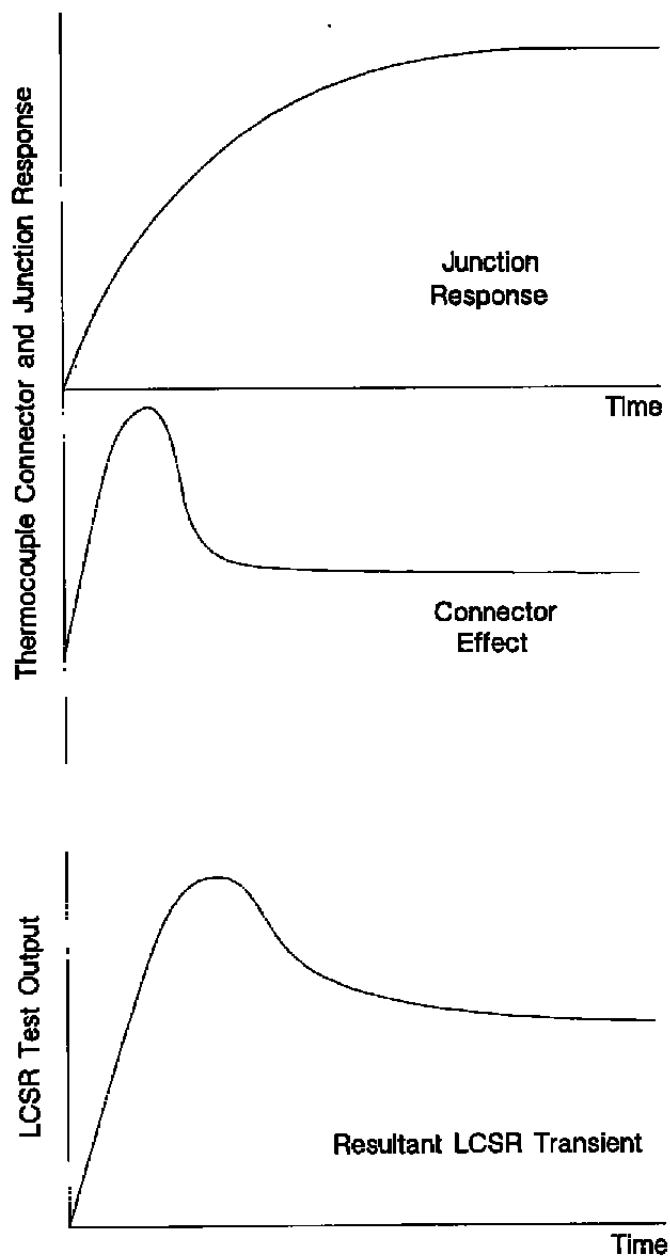
Figure 12.14. Illustration of Possible LCSR Transients for Thermocouple
Circuits With Gross Inhomogeneities.
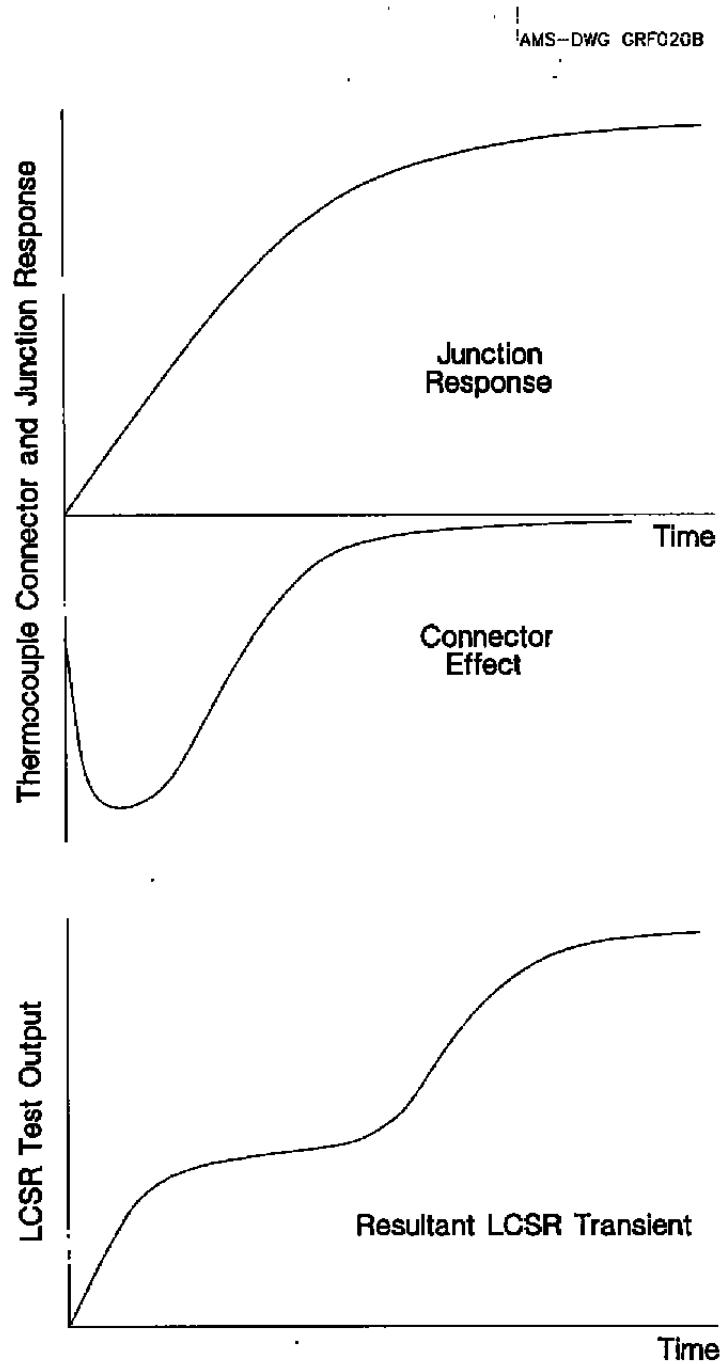
Figure 12.15. Illustration of Possible LCSR Transients for Thermocouple
Circuits With Gross Inhomogeneities.

components are shown on the bottom. Two actual LCSR transients showing the two most commonly observed inhomogeneity effects are presented in Figure 12.16. These data are from LCSR testing of thermocouples in laboratory conditions.

12.8 LCSR Test for Detection of Thermocouple Inhomogeneities

There is a positive aspect to the LCSR difficulties discussed above. That is, the ability of the LCSR test as a method for diagnosis of gross inhomogeneities in thermocouple circuits. In an experiment conducted in the early 1980's at the Argonne National Laboratory in Chicago, the author and others were involved in LCSR testing of a group of thermocouples that were being prepared for installation into a nuclear radiation experiment. The unusual LCSR transients that were initially observed in these thermocouples provided a clue that there was a problem in the thermocouple circuits. Further investigations revealed that the thermocouples were inadvertently reversed in their connectors during installation. The problem was corrected and the thermocouples were LCSR tested successfully. Figure 12.17 shows two LCSR transients for a thermocouple that was first installed in its connector correctly and then reversed to show how the LCSR can reveal the problem.

12.9 Effect of Extension Wire and Connectors

Long extension wires and connectors sometimes present problems in LCSR testing of installed thermocouples. The problem is often exasperated by inhomogeneities in the extension wires or in the connectors where the extension wires are attached to the thermocouple wires. The effect of connectors on LCSR signals were covered in Phase I as documented in our Phase I report[17].
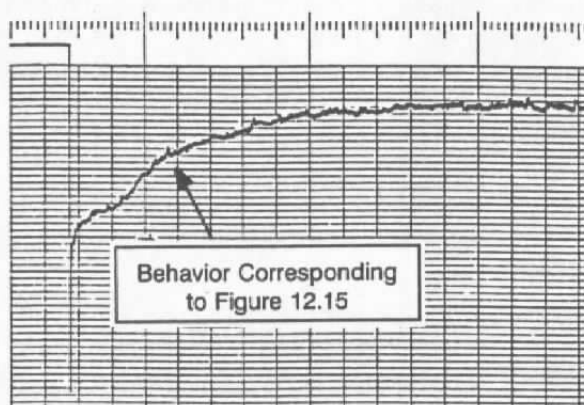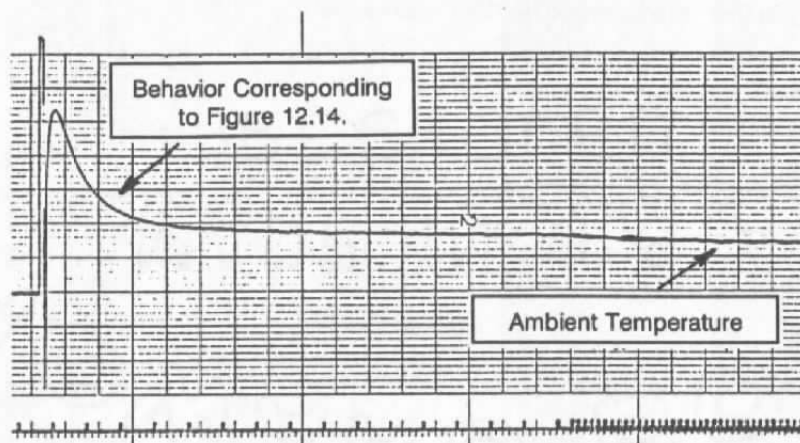
Figure 12.16. Actual LCSR Transients for Thermocouples With
Circuit Inhomogeneities.
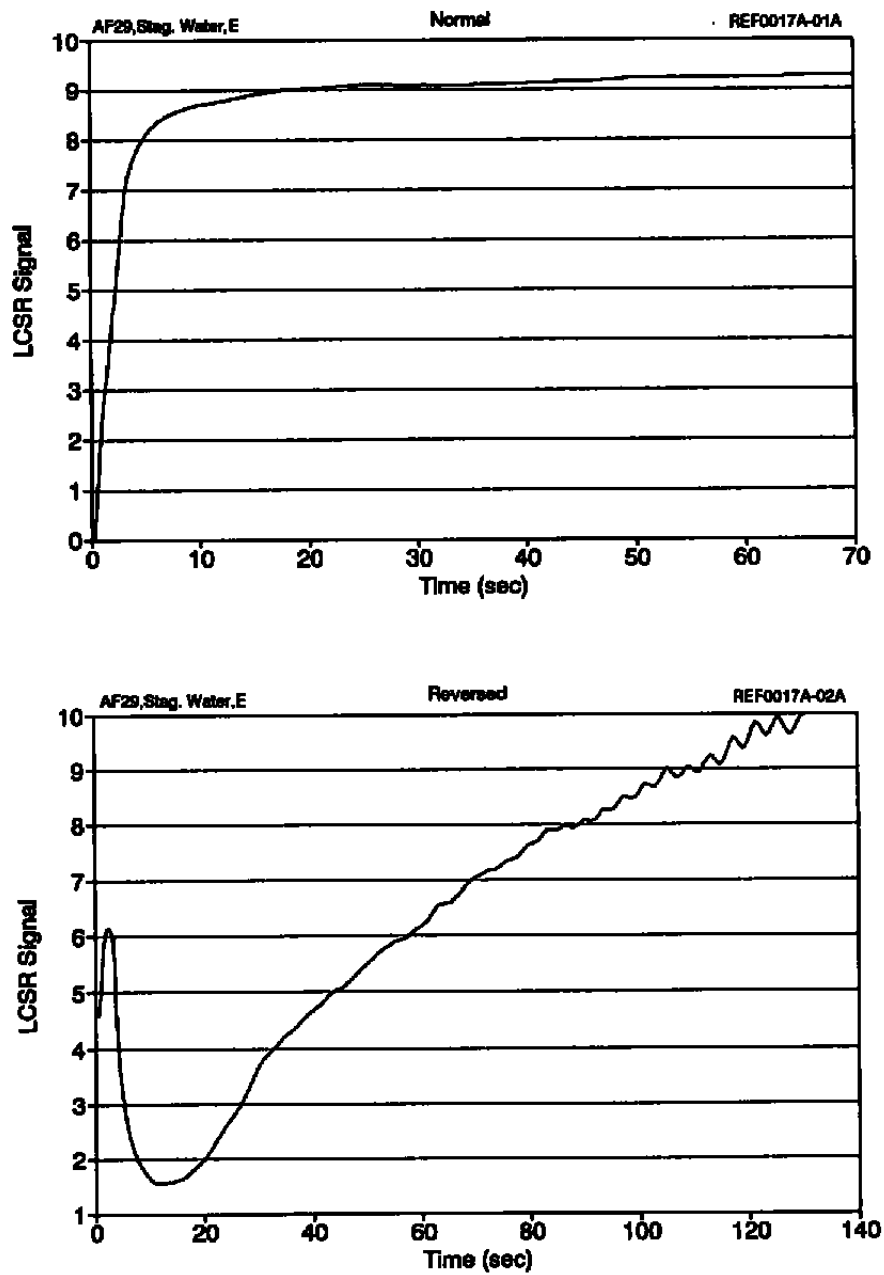
Figure 12.17. LCSR Transients for a Normal and a Reversed Installation of a Thermocouple into its Connector.

The effect of extension wires on the results of the LCSR tests and other difficulties that may be encountered in LCSR testing of thermocouples are discussed in detail in Volume II. Also shown in Volume II are experimental results with different types and lengths of thermocouple extension wires. An example of such results is shown in Figure 12.18 for a group of thermocouples tested in water. These data represent the percent differences between the results of LCSR and plunge tests performed under the same conditions with three different lengths of thermocouple extension wires. Note that there is not a good correlation between the LCSR error (present difference between the results of plunge and LCSR tests) and the length of the extension wires. That is, the accuracy of the LCSR test results is not always adversely affected by increasing the length of the extension wires.

.

12.10 Harmful Effects of LCSR Test

LCSR method is generally a safe test if it is performed properly and with adequate care. However, there is some potential for harmful effects to the thermocouple circuits and electrical hazard for the test personnel. These should be taken into account and guarded against in the LCSR process. In the three years that this project was actively pursued at AMS, there was no incident during the LCSR experiments even though many engineers and technicians worked on this project.

Volume II presents the results of experiments performed to assess the potential for damage to the extension wires or the insulation of the wires from LCSR testing. The data from these experiments have revealed that the LCSR test does not normally jeopardize the health and integrity of the wires as long as the LCSR current levels and heating times are maintained at a reasonable level.
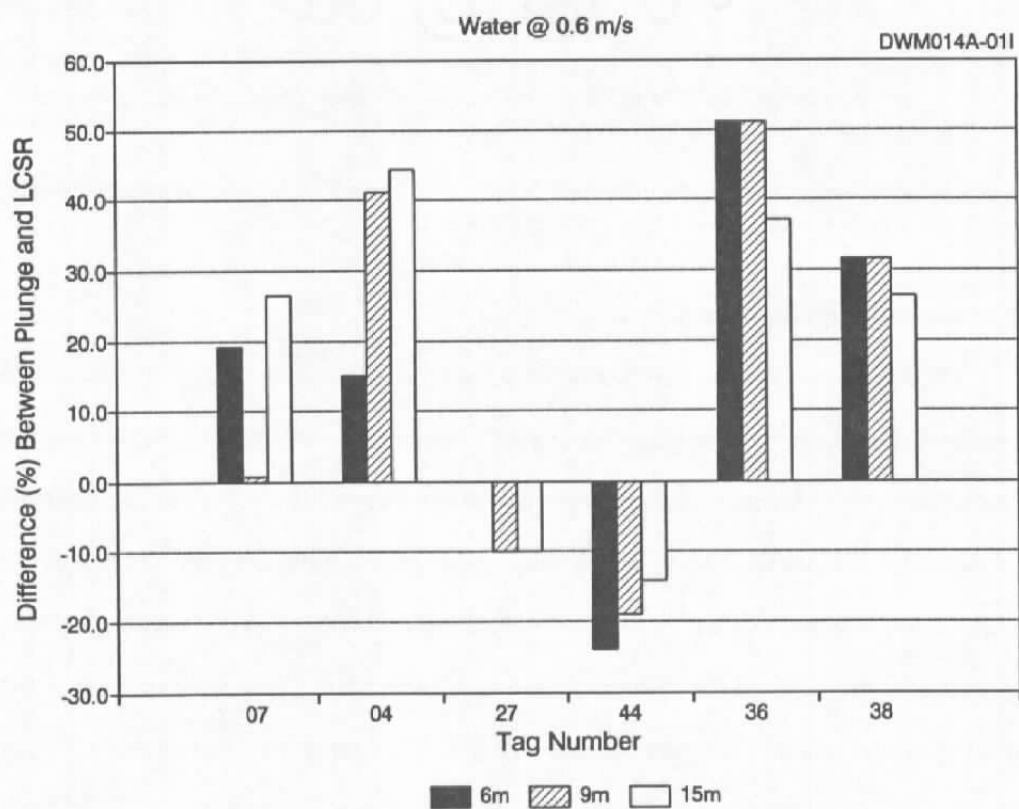
Figure 12.18. Error of LCSR Results Due to Extension Wires.

It is important for the users of the LCSR method to be aware of the heating that is produced in the thermocouple circuits during the LCSR test. It is also important to point out that the LCSR test sometimes involves potentially harmful electrical currents that must not come into contact with the test personnel when the thermocouple is under test. The equipment and procedures that were developed in this project have been designed with safety in mind. The safety features of the equipment are described in Volume III. Two examples of these features are:

1. An option for the user to program the AC power supply in the equipment for a limited current output.

2. A safety cover on the cold junction copper blocks in the equipment that turns the current off when the cover is removed.

12.11 Description of Project Thermocouples

Table 12.6 presents a listing of most of the thermocouples that were included in the tests described in this chapter. A tag number was assigned to each thermocouple to facilitate the presentation of the research data we produced in the project. Most of these thermocouples and the extension wires that were used in the project were purchased from Omega Engineering Incorporated, located in Stamford, Connecticut, USA. There was no particular reason for the types, sizes, physical configurations, and the manufacturer of the thermocouples that were selected for the project other than the fact that these thermocouples comply with the types and sizes that were specified by the Air Force for this project.

12.12 Effect of Heating Time on LCSR Results

We mentioned earlier that the LCSR heating time does not play a major role in the quality and accuracy of the LCSR test results. Of course, the heating time must be long enough to

TABLE 12.6

Listing of Thermocouples Used in the Project

Number	Type	Gage	O.D. (in)	Loop R	IR
AF#1	K Quick-Disconnect	18	1/4	0.61	200 K
AF#2	K Quick-Disconnect	18	1/4	0.53	40 M
AF#3	K Quick GND-JNC	18	1/4	0.45	n/a
AF#4	K Quick-Disconnect	18	1/4	0.65	25 M
AF#5	K Quick-Disconnect	18	1/4	∞	>100G
AF#6	K Quick-Disconnect	20	3/16	0.69	200 K
AF#7	K Quick-Disconnect	20	3/16	0.66	500 M
AF#8	K Trans 36"	20	3/16	2.27	1.5 M
AF#9	K Quick-Disconnect	23	1/8	1.46	10 M
AF#10	K Quick-Disconnect	23	1/8	1.67	15 M
AF#11	K Quick-Disconnect	23	1/8	1.58	1 M
AF#12	K Trans 40" Bent	23	1/8	3.55	n/a
AF#13	K Quick-Disconnect	30	1/16	5.11	4 M
AF#14	K Quick-Disconnect		Flex	1.72	n/a
AF#15	K Quick-Disconnect		Flex		n/a
AF#16	K Quick-Disconnect		Flex	1.2	n/a
AF#17	K Quick-Disconnect		Flex	4.63	n/a
AF#18	K Q-mini EXP-JNC		0.053	113.4	200 K
AF#19	K No CON EXP-JNC		0.053		
AF#20	K Q-mini EXP-JNC		0.052	111.4	150 K
AF#21	K Q-mini GND-JNC		0.053	284	n/a
AF#22	K Q-mini EXP-JNC		0.16	11.6	200 K
AF#23	K Q-mini EXP-JNC		0.16	10.9	350 K
AF#24	K Q-mini GND-JNC		0.052	14	n/a
AF#25	K Q-mini GND-JNC		0.052	13	n/a
AF#26	E Trans 40"	20	3/16	2.87	40 M
AF#27	E Quick-Disconnect	20	3/16	0.79	35 M
AF#28	E Quick-Disconnect	20	3/16	0.77	10 M
AF#29	E Quick-Disconnect	23	1/8	1.57	30 M
AF#30	E Trans 51"	20	1/8	4.38	90 M

159

TABLE 12.6 (continued)

Number	Type	Gage	O.D. (In)	Loop R	IR
AF#31	E Quick-Disconnect	30	1/16	6.15	300 M
AF#32	T Trans 40"	20	3/16	1.62	13 M
AF#33	T Quick GND-JNC	20	3/16	0.47	n/a
AF#34	T Quick-Disconnect	20	3/16	0.41	5 M
AF#35	T Quick-Disconnect	30	1/16	3.07	10 G
AF#36	J Trans 29"	20	3/16	1.47	10 G
AF#37	J Quick-Disconnect	20	3/16	1.03	6.5 M
AF#38	J Quick-Disconnect	24	1/8	1.28	6 M
AF#39	J Trans 51"	20	1/8	2.76	10 M
AF#40	J Quick-Disconnect	30	1/16	3.29	1.2 M
AF#41	E Dual PH assmb.		1/4	0.5	10 G
AF#42	T Dual PH assmb.		1/4	0.45	n/a
AF#43	E Quick-Disconnect	30	1/16	6.9	20 M
AF#44	E Quick-Disconnect	18	1/4	0.85	400 K
AF#45	E Quick-Disconnect	30	1/16	7.2	7 G
AF#46	J Quick-Disconnect	18	1/4	0.6	1.5 M
AF#47	J Quick-Disconnect	30	1/16	3.75	10 G
AF#48	J Quick-Disconnect	30	1/16	4.0	20 G
AF#49	K Quick-Disconnect	30	1/16	5.8	20 M
AF#50	K Quick-Disconnect	30	1/16	5.8	20 G
AF#51	E Quick EXP-JNC	30	1/16	6.3	4.0 M
AF#52	J Quick EXP-JNC	30	1/16	3.7	1.2 M

OD: Outside Diameter.

IR: Insulation Resistance.

allow one thermocouple to reach steady state above the temperature of the surrounding medium. During this project, we determined that a heating time of between 5 to 15 seconds is generally adequate for the thermocouples that were involved in this project (see Table 12.6) and under the laboratory conditions in which they were tested. Figure 12.19 shows the LCSR errors for heating times of 5 and 15 seconds. The errors represent the percent difference between the thermocouple time constants obtained by the plunge and LCSR tests under the same conditions. The results in Figure 12.19 indicate the magnitude of errors are generally the same for either 5 or 15 seconds of heating meaning that any heating time in the 5 to 15 second range is adequate for LCSR testing of these thermocouples in water.
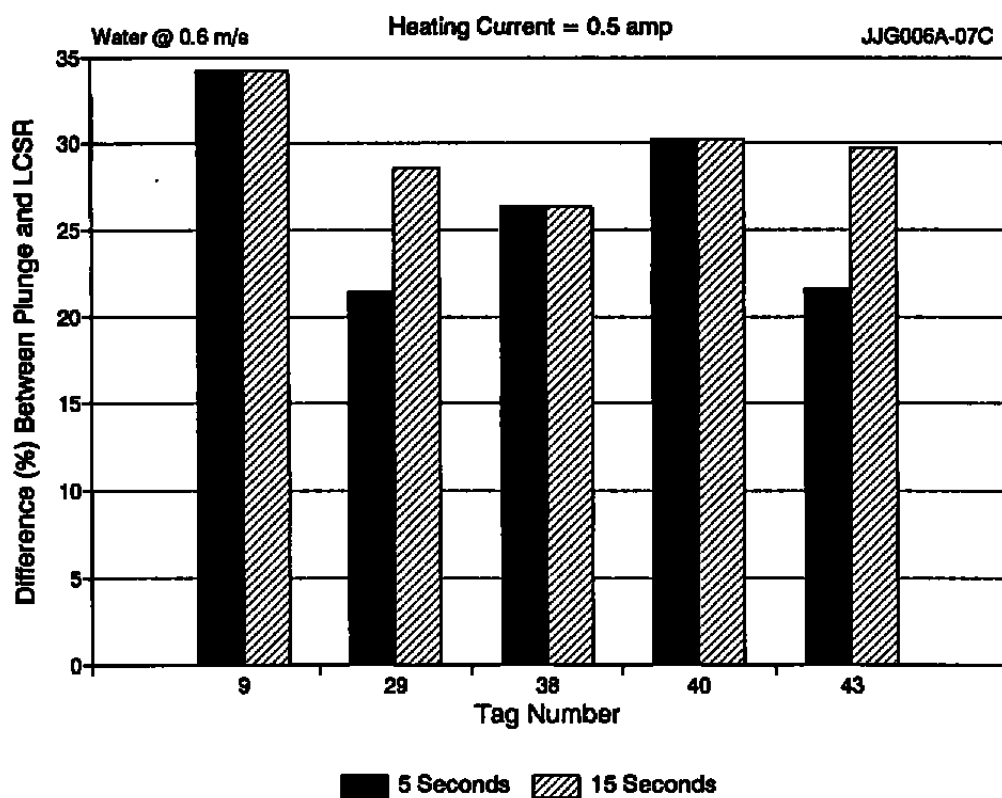
Figure 12.19. Optimum Heating Times for LCSR Testing of Thermocouples.

13. LCSR TEST INSTRUMENT

A photograph of the LCSR test instrument that was developed in this project is shown in Figure 13.1. This instrument can be used to perform both the LCSR test and the associated data analysis. The details of how this equipment was developed including its operations and maintenance manual, manufacturing procedure, and parts list are given in Volume III. The key points regarding the development and operation of the instrument are presented in this chapter.

The LCSR test instrument as shown in Figure 13.1 consists of two separate units. One is used to perform the LCSR test and generate the raw data, and the other is used to analyze the data and display the results. The first unit is named ETC-2, and the second unit is named ESA-1.

A photograph of ETC-2 is shown in Figure 13.2. This unit is an upgraded version of ETC-1 which was used in the Phase I project. A major difference between ETC-1 and ETC-2 is in the LCSR signal conditioning amplifiers and filters. In ETC-2, the amplifiers and filters are built into the unit, while in ETC-1, the signal conditioning equipment were used as separate equipment outside the unit.

A photograph of ESA-1 is shown in Figure 13.3. Both the front and back panels of the unit are shown. The ESA-1 was completely designed and assembled at AMS as a major part of this Phase II effort for AEDC. A block diagram of ESA-1 is presented in Figure 13.4. This unit is basically a diskless microcomputer with an Intel 386, 20 MHz microprocessor module. The system was designed and developed specifically for LCSR data acquisition and data analysis

Figure 13.1. Complete LCSR Test Instrument.
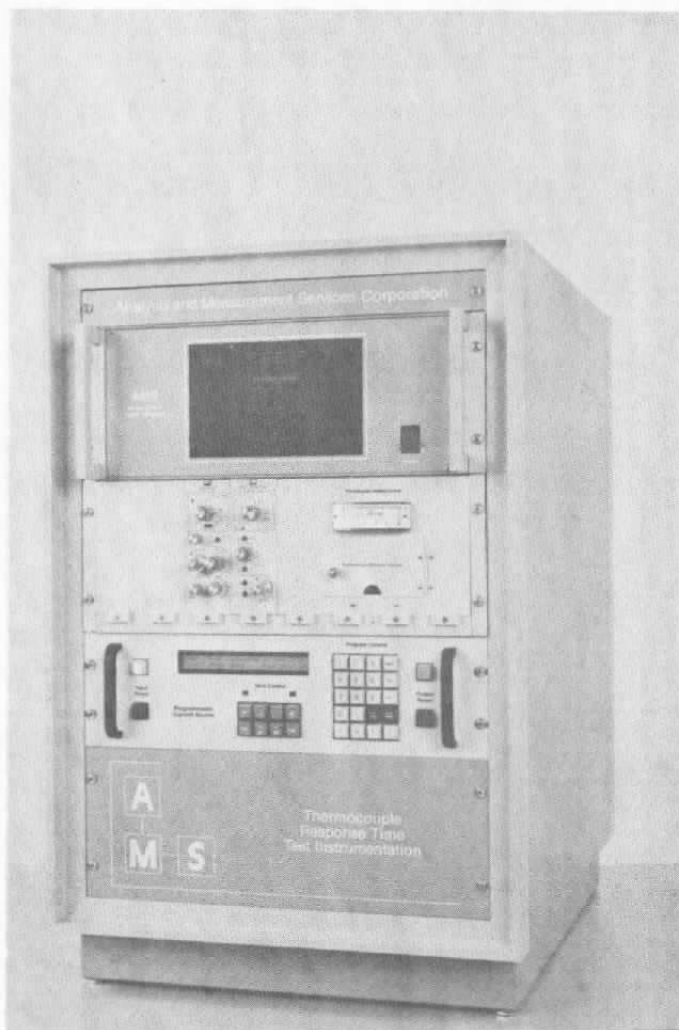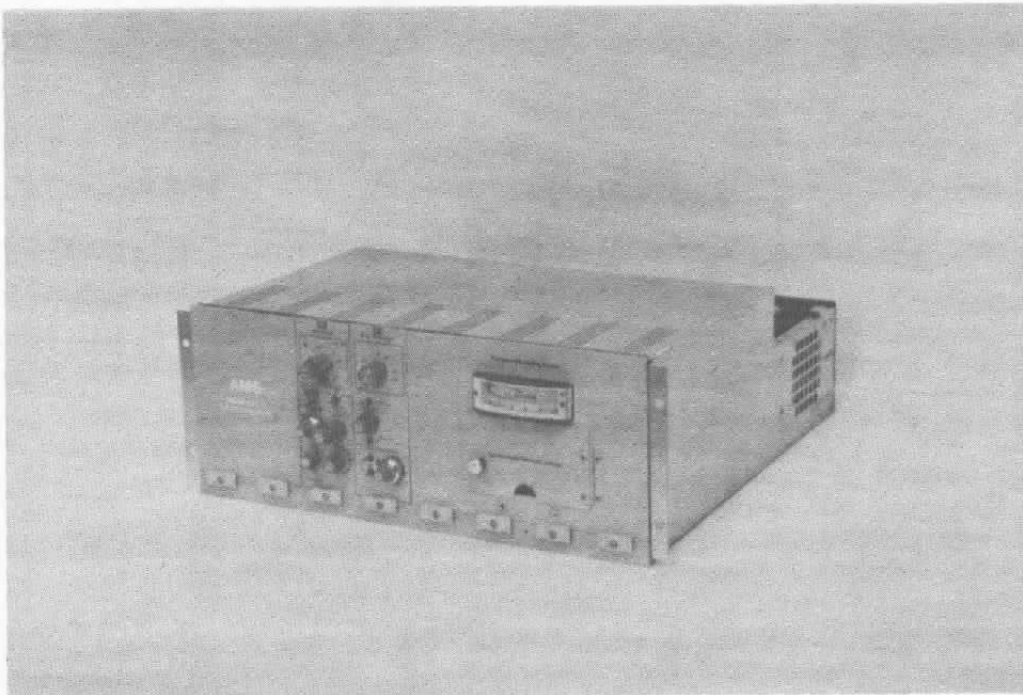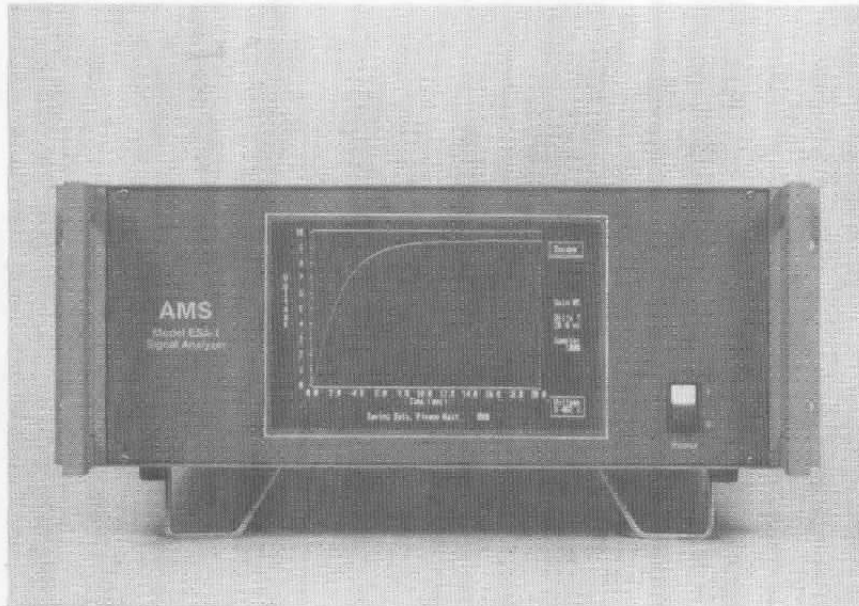
Figure 13.2. LCSR Signal Generator ETC-2.

FRONT PANEL
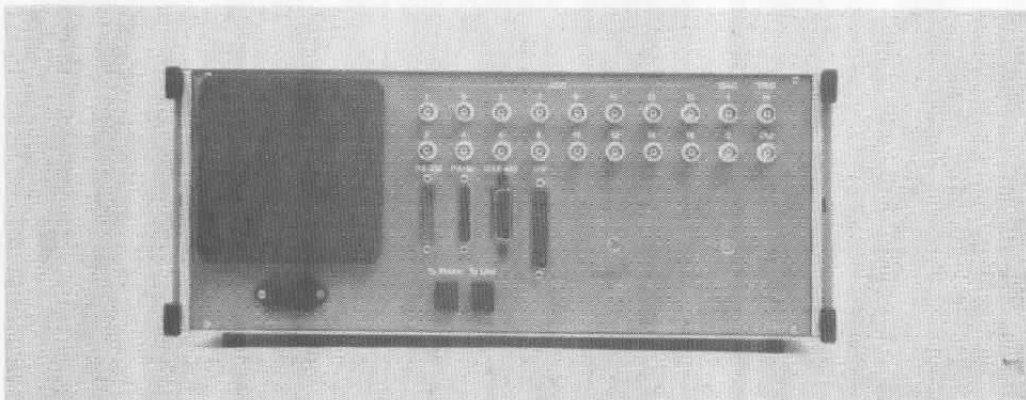
BACK PANEL

Figure 13.3. LCSR Test Analyzer ESA-1.
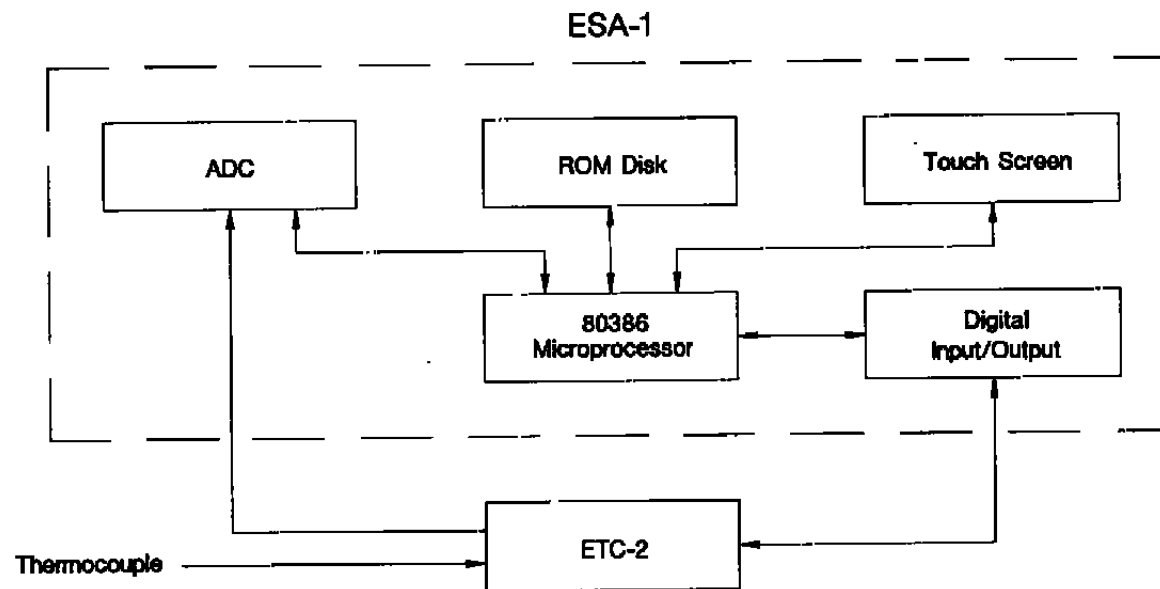
ESA-1

Figure 13.4. Block Diagram of LCSR Test Analyzer.

for thermocouples. It interacts with the ETC-2 to perform the LCSR test and analyze the data. A block diagram of ESA-1 together with ETC-2 is provided in Figure 13.5. In this configuration, the system can perform the LCSR test, sample the data in real time through the A/D, and store the data in the ESA-1 memory. The system can then analyze the data and display the response time of the thermocouple tested. A copy of a LCSR transient as displayed on the front panel of the ESA-1 is shown in Figure 13.6. The system can provide a hard copy of the data and the results if it is connected to a printer or a plotter.

A complete LCSR test of a thermocouple including 10 repeats, averaging, and analysis requires approximately 30 minutes.

Although the ESA-1 has been designed specifically for the LCSR test, it can be easily adapted for other data acquisition and data analysis purposes. To accomplish this, all that would be needed is to replace the software cartridge in the unit. Any new controls such as switches and knobs and new indicators that may be needed for a new application can easily be built into the software and displayed on the touch screen on the front panel of the unit. The unit does not have a keyboard and all communications with the system are through the touch screen. A front view photograph of the ESA-1/ETC-2 system is shown in Figure 13.7 with a LCSR transient and the corresponding response time results displayed on the touch screen.

An important addition to the ESA-1 could be hardware and software for testing of steady state characteristics of installed thermocouples. This would be useful to assess the steady state health, reliability, and accuracy of installed thermocouples in addition to measuring their response time. Further discussions on this point are provided in Chapter 18.

Figure 13.5. Block Diagram of LCSR Signal Generator (ETC-2) and Signal Analyzer (ESA-1).

Figure 13.6. LCSR Transient as Displayed on the Front Panel of ESA-1.

Figure 13.7. Front View of LCSR Test Instrument.

13.1 Description of Individual Components of LCSR Test Instrument.

A summary of important characteristics of the main components of the LCSR test instrument is present in this section. The details are provided in Volume III.
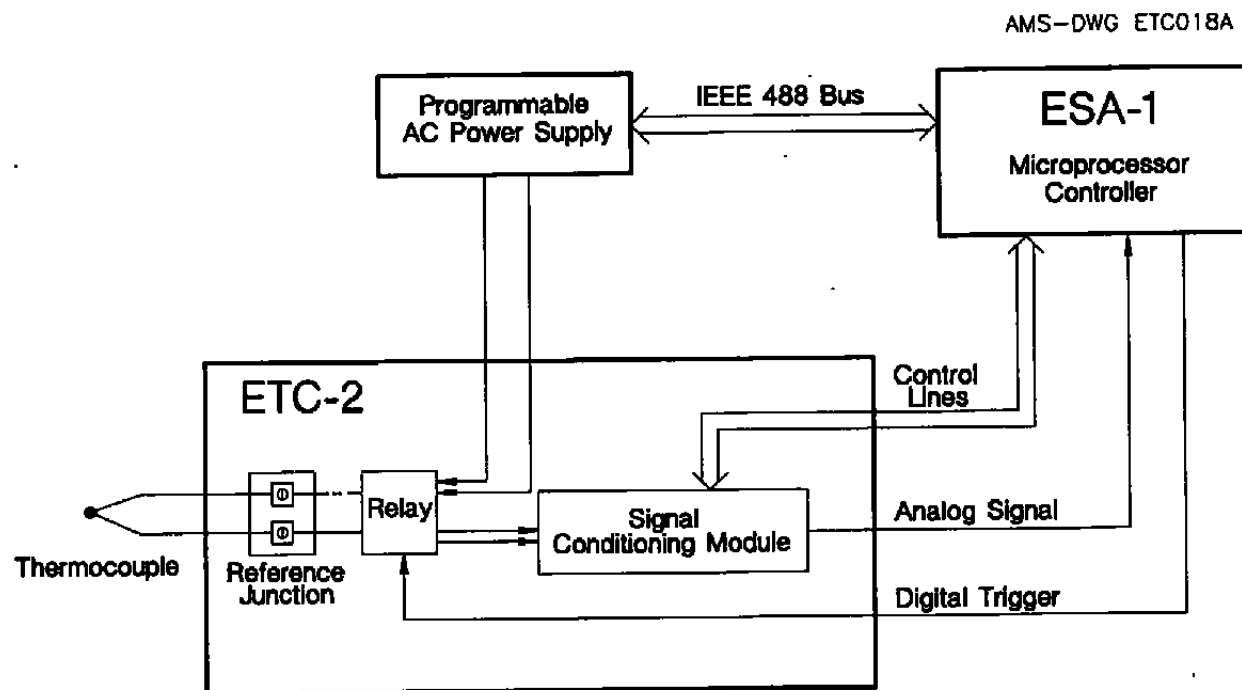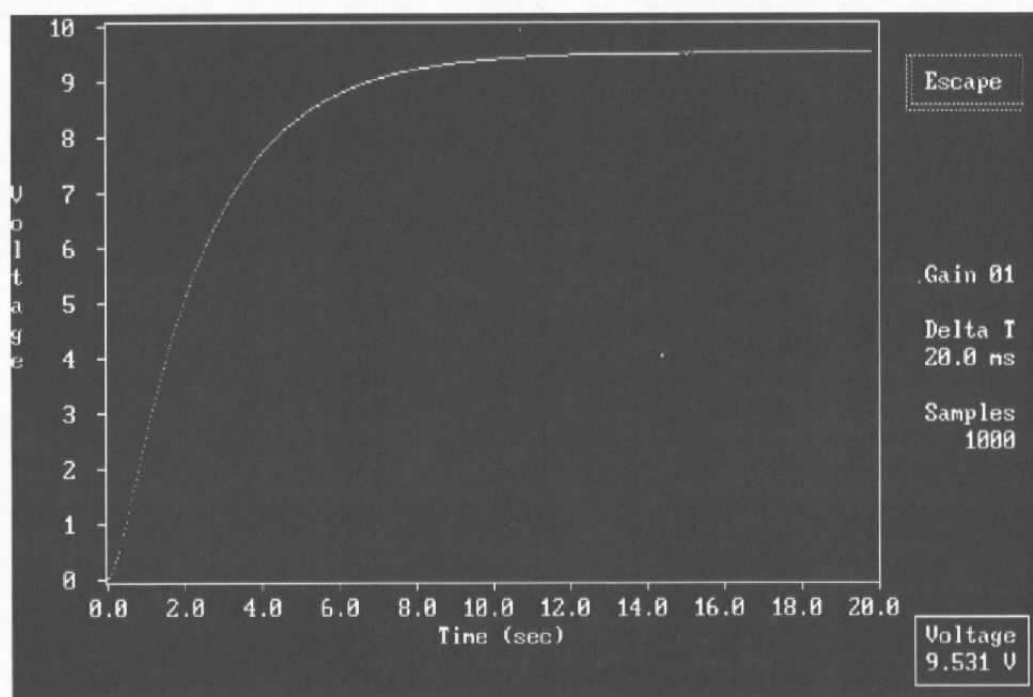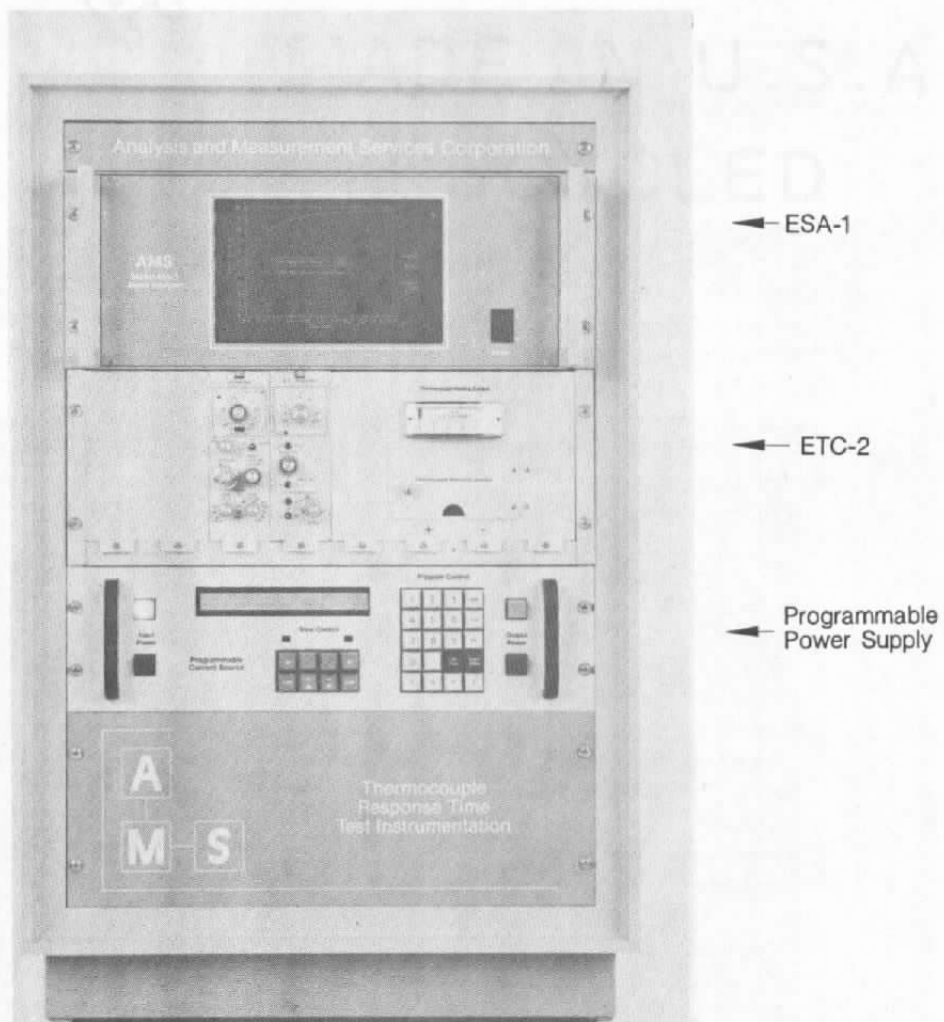
- **Power Supply**. The LCSR test can normally be performed using a 110 VAC power source from a regular wall socket. A Variac can be used to adjust the voltage as needed to test different sizes of thermocouples in different test conditions. This approach was used in development of the first LCSR test unit that was named ETC-1 and was used during the Phase I part of this project. In the Phase II project reported herein, we used a programmable AC power supply. The new unit has been named ETC-2. In addition to a programmable power supply, the ETC-2 contains two instrumentation amplifier and filter units and a faster relay than what was used in its predecessor, the ETC-1.

  The programmable AC power supply is capable of providing AC currents of up to 1000 Hz as opposed to 60 Hz that was produced by ETC-1. The advantage of this high frequency AC source is that it will help minimize or eliminate the Peltier effect far better than a 60 Hz power source. The power supply can also be programmed to minimize any magnetic effect. This is accomplished by programming the power supply to ramp the heating current down and then cut it off at the end of the LCSR heating cycle. This approach was not attempted in this project because: 1) the magnetic effect is limited to very fast Chromel/Alumel thermocouples which were not prevalent in this project, and 2) the magnetic effect is probably dominated by the inherent uncertainties of the LCSR test.

  The power requirement for LCSR testing of thermocouples depends on the type and size of the thermocouple and the conditions in which the thermocouple is tested. If the thermocouple is operating in a poor heat transfer medium, then a moderate amount of heating current will suffice, but if it is in a good heat transfer medium, it requires a high heating current. For the purpose of this discussion, a moderate heating current is defined as an AC current level in the neighborhood of about 0.5 amperes and a high heating current is defined as an AC current level of about 1.0 amperes or more.

  The resistance of the thermocouple and the associated extension wires can help determine the power requirements for a LCSR test. Generally, the resistance of a thermocouple loop including both the thermocouple and its extension wires has a range of about 3 to 30 ohms. Considering the LCSR electrical current requirements of 0.3 to 3 amperes, the maximum power requirement is about 300 watts. The power supply that we used in development of the ETC-2 delivers up to 1000 watts.

Relay. The relay in the LCSR test instrument must have three important characteristics. First, it must be a fast relay to avoid loosing any substantial portion of the LCSR transient when the relay switches the thermocouple from the power supply to the signal conditioning equipment. Secondly, the relay should not chatter and cause spikes at the beginning of the LCSR test transient. Figure 13.8 shows a LCSR transient that has spikes and chatters at its beginning.

The third requirement for the relay is its power rating. The relay must be rated to withstand up to 3 amperes or more of AC current that may be used in performing a LCSR test. The relay that has been used in ETC-2 has the required characteristics and is rated for several hundred thousand switching operations. No problems have been observed with spikes or relay chatters at the beginning of the LCSR transients that has been generated with the ETC-2 since it was assembled for this Phase II project.

- **Signal Conditioning Equipment.** The LCSR transient for typical thermocouples have amplitudes of less than one millivolt. Therefore, very high amplifier gains are often needed to increase the amplitude of the LCSR signals to a level within 1 to 10 volts which is usually needed to obtain accurate response time results. In the LCSR test equipment that was developed in this project, two stages of amplification had to be used. The details are given in Volume III. Typical amplifier gains that were required for laboratory testing of representative thermocouples ranged from 20,000 to 500,000 depending on the size of the thermocouple, the length of extension wires, and the test conditions. The consequence of using such high gains is high frequency noise that appears on the LCSR signal. To minimize the noise, Low-Pass filters must be used. In ETC-2, we have used combined amplifier/filter units instead of separate amplifiers and filters. This is advantageous in terms of cost, space, and weight reduction.

- **Analog to Digital Converter (A/D).** A twelve bit, 0 to 10 volts A/D is used in the ESA-1 to digitize (sample) the LCSR transient and bring them into the system for analysis. Only two channels of the A/D are used for the LCSR test even though the A/D has 16 input channels. One channel is used to send out a trigger signal to activate the relays in the ETC-2 and initiate the LCSR test, and the other channel is used to bring in the LCSR transient. In the tests that were performed during the development of the equipment, sampling times of 2 to 50 milliseconds were used and 1500 to 3000 data points were sampled depending on the time required for each LCSR transient to reach steady state.

The A/D inside the ESA-1 should be calibrated periodically as described in Volume III. This is the only component of the LCSR test instrument that requires periodic calibration. Although other components of the instrument such as the power supply can drift and would normally need calibration, this is not necessary for the LCSR application. The drift of the
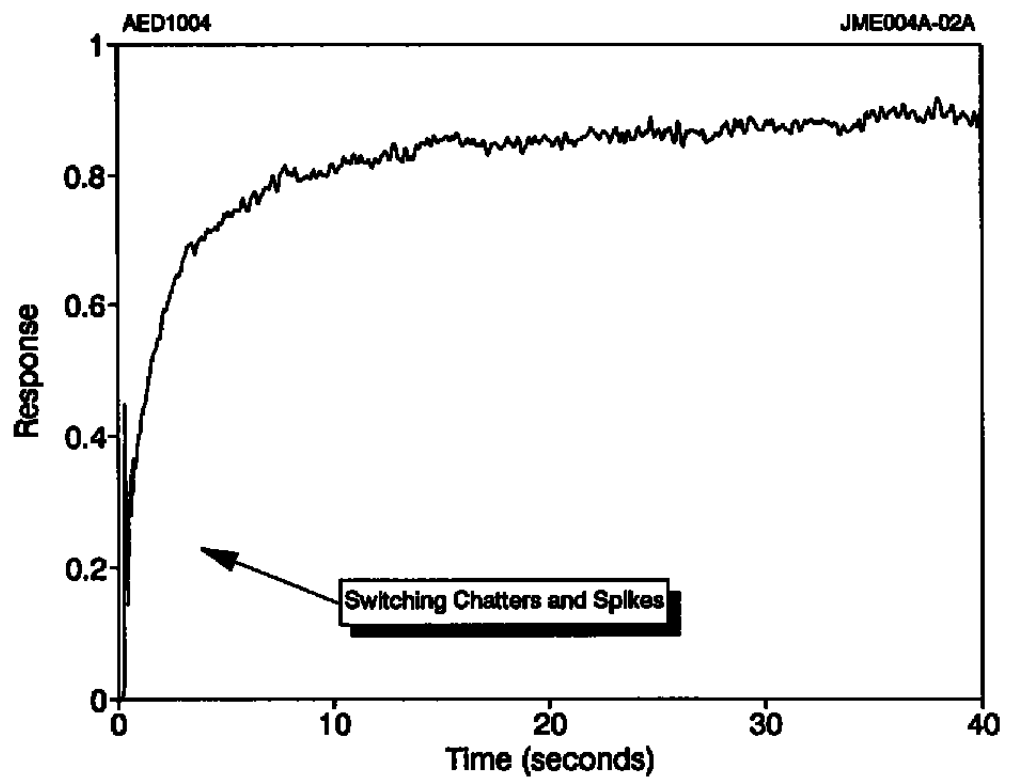
Figure 13.8. LCSR Transient with Switch Chatters and
Spikes at the Beginning.

power supply will not affect the accuracy of the LCSR test results. The filters and amplifiers in the ETC-2 may also drift. Again, the drift of these components can not have a significant effect on the accuracy of the LCSR results. What is often important is the dynamic linearity of the amplifiers and filters. These modules must be linear to provide accurate LCSR transients. If there is any doubt that the modules can become nonlinear, it is important to institute a procedure to check for linearity on a periodic basis.

- **Microprocessor**. All the software packages that have been installed in the LCSR test instrument developed were written and tested on IBM-PCs. Following the development of the software packages, a microprocessor system was developed based on the IBM-PC platform. The microprocessor was designed to automatically perform a LCSR test, analyze the data, and display the response time of the thermocouple tested. Instead of a keyboard, the ESA-1 is designed with a touch-screen by which the user can communicate with the system. The touch-screen provides versatility and allows modifications to be made with ease. There are no controls on the front panel of the ESA-1. All the controls have been built into the software and are available on the touch screen. Hard copies of the test data and the results can be obtained by connecting a printer to the system. The ESA-1 is also designed with a built-in modem to allow the user to communicate with a remote computer at AMS or another location for training, troubleshooting, or technical assistance. The remote computer can assume control of the ESA-1 via the modem. All software packages used in the ESA-1 are burned onto a computer cartridge that can be updated to reflect new additions to the software or the system. In addition to providing complete LCSR capability, the ESA-1 can be used as a general purpose data acquisition and data analysis system.

- **Software**. The ESA-1 contains the following software packages to perform the LCSR test, analyze the data, and display the results. These software packages were developed predominantly by AMS during this project. Some of the routines for these software packages were already available at AMS from developments for response time testing of RTDs.

    1. Software to interact with the ETC-2 and perform the LCSR test.

    2. LCSR sampling program that asks the user to specify the sampling time, total number of samples, and the number of LCSR repeats for averaging.

    3. LCSR averaging program to average the LCSR data as necessary to minimize the noise on the data and provide a smooth LCSR transient for optimum analysis.

    4. LCSR analysis software written to process the data and present the response time of the thermocouple tested. This software fits the

LCSR data to an appropriate mathematical function, identifies the modal time constants of the thermocouple, combines the modal time constants, applies the higher mode correction, and calculates the overall response time of the thermocouple under the conditions tested.

5.   Software to plot the LCSR data and display the results.

A listing of the major components of the LCSR test instrument is given in Table 13.1. This is followed by a listing of the default sampling and analysis parameters in the ESA-1 microprocessor (Table 13.2). The default parameters can readily be changed by the user as needed.

13.2   Instrument Qualification Testing

During the development of the ETC-2 and ESA-1, these units were tested at every step of the development to ensure that the final product will perform its function as intended. When the two units were completed and integrated into one package, a comprehensive set of tests were completed with the instrument to identify and resolve any problems and optimize the final product. Some of the test results are summarized here. The details are presented in Volume II and Volume III.

Table 13.3 shows equipment qualification test results in water and air using optimum LCSR parameters and stable thermocouples. These results are shown graphically in Figure 13.9. The results are from LCSR and plunge tests performed on each thermocouple under the same test conditions.

TABLE 13.1

Major Components of
LCSR Test Instrument

Item	Component	Make
1	Programmable Power Supply	Pacific Power Source
2	Amplifier/Filter Units	Gould
3	Analog-to-Digital Converter	Data Translation
4	Computer System	Various Suppliers
5	Software	AMS

TABLE 13.2

Default Values of LCSR Sampling and Analysis Parameters in ESA-1

LCSR Parameter	Default Setting
Delta T	.018
Number of Samples	1500
A/D Gain	1
Number of Data Sets	10
First Data File Name	c:tct0001.dat
Thermocouple Heating Time	10
Power Supply Voltage	6
Power Supply Frequency	1000
Current Limit	0.6
Input Gain	1
Output Gain	1
Cutoff Frequency	1
Initial Skip Factor	1
Vary Skip Factor	1
Maximum Skip Factor	1
Initial Number of Points Skipped	1
Maximum Number of Points Skipped	1
Set Initial Delta T Factor	1
Vary Delta T Factor	1
Maximum Delta T Factor	1
Second Mode Multiplier	1.5
A/D Channel	0
A/D Polarity	1
Zero Removal (On = 1, Off = 0)	1
Drift Removal (On = 1, Off = 0)	1
Spike Removal (On = 1, Off = 0)	1
Display Removal Switch (On = 1, Off = 0)	0

TABLE 13.3

Instrument Qualification Test Results

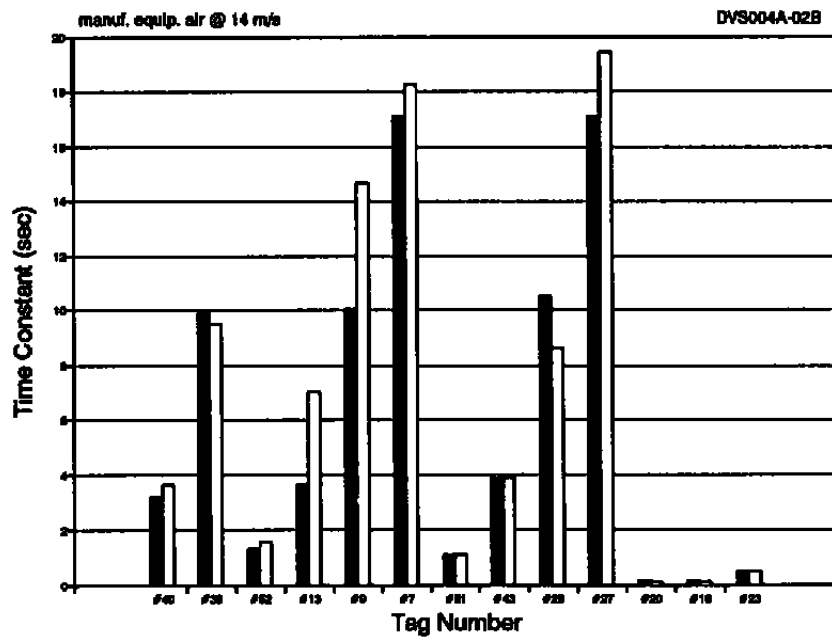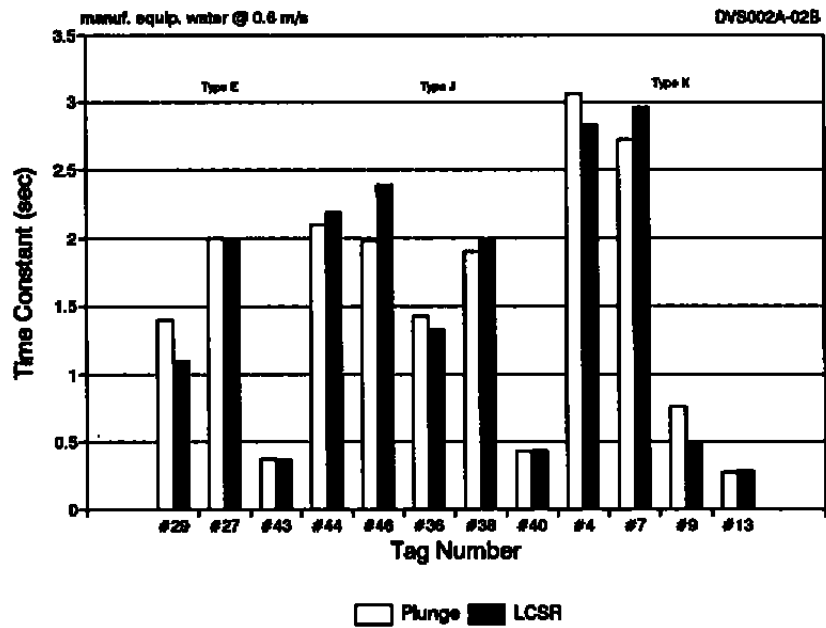| Tag Number	Response Time (sec)	
	Plunge	LCSR
water @ 0.6 m/s		
29	1.40	1.10
27	2.00	1.99
43	0.37	0.37
44	2.10	2.19
46	1.98	2.39
36	1.43	1.33
38	1.90	1.98
40	0.43	0.43
04	3.06	2.83
07	2.72	2.96
09	0.76	0.49
13	0.27	0.29
air @ 14 m/s		
40	3.20	3.63
38	9.90	9.48
52	1.28	1.54
13	3.66	7.03
09	10.03	14.68
07	17.13	18.27
51	1.12	1.10
43	3.88	3.90
29	10.55	8.61
27	17.10	19.45
20	0.16	0.10
18	0.14	0.12
23	0.50	0.56

Figure 13.9. Equipment Qualification Test Results.

The reasonable agreements between the plunge and the LCSR test results shown in Table 13.3 and Figure 13.9 indicate that the LCSR test instrument in its final configuration operates properly.

13.3 Repeatability of LCSR Test Results

The repeatability of the thermocouple response time test results obtained with the LCSR test instrument developed in this project has been determined by extensive laboratory testing. The details are given in Volume II. The key results are summarized here.

With all the parameters at their optimum values and maintained constant for each thermocouple, LCSR tests were performed three times on a group of thermocouples in air and another group in water. The results are listed in Table 13.4 and plotted in Figure 13.10. Note that the corresponding plunge test results are also shown to demonstrate not only the repeatability, but also the accuracy of the LCSR test instrument.

The results shown above are from consecutive tests performed by the same test engineer the same day. Additional repeatability tests were performed on a weekly basis to identify the one-week repeatability of the tests and the instrument. Furthermore, different test engineers were asked to perform the same tests on the same thermocouples to identify the person-to-person repeatability of the tests. The results of these tests have shown that the LCSR test instrument provides the expected repeatability and accuracy and is thus qualified for the intended laboratory and field measurements on typical thermocouples. The average repeatability and accuracy of the LCSR test results have been about 20 percent with the worst LCSR versus plunge test differences predominantly contained within a ± 50 percent band.

TABLE 13.4

Repeatability and Accuracy of the LCSR
Test Instrument

| Tag Number	Response Time (sec)			
	Plunge	LCSR 1	LCSR 2	LCSR 3
Water @ 0.6 m/s				
29	1.40	1.11	1.09	1.09
27	2.00	1.96	1.99	2.01
43	0.37	0.35	0.39	0.36
44	2.10	2.07	2.16	2.70
46	1.98	2.20	2.78	2.20
36	1.43	1.47	1.29	1.23
38	1.90	1.97	2.03	1.95
40	0.43	0.44	0.44	0.42
4	3.06	2.82	2.77	2.91
7	2.72	3.03	2.86	2.99
9	0.76	0.50	0.49	0.49
13	0.27	0.29	0.30	0.27
Air @ 14 m/s				
40	3.20	3.63	3.54	3.73
38	9.90	9.63	9.38	9.44
52	1.28	1.82	1.53	1.28
13	3.66	4.06	6.82	10.21
9	10.03	14.58	14.06	15.39
7	17.13	18.75	16.49	19.57
51	1.12	1.01	1.07	1.23
43	3.88	4.02	3.96	3.72
29	10.55	8.48	9.08	8.28
27	17.10	18.16	18.12	22.08
20	0.16	0.12	0.10	0.09
18	0.14	0.12	0.12	0.12
23	0.50	0.56	0.46	0.47
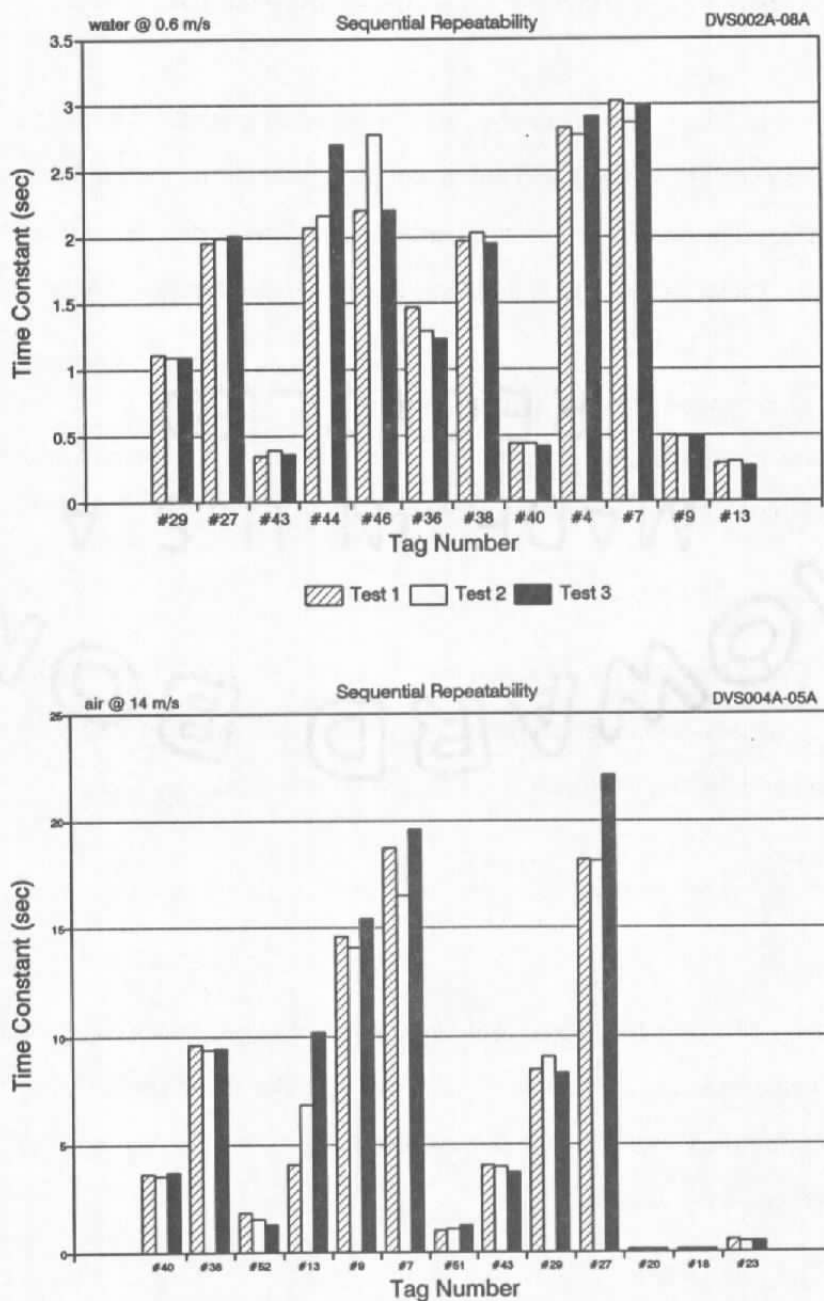
Figure 13.10. Results of Repeatability Testing of LCSR Test Instrument.

14. FACTORS AFFECTING RESPONSE TIME

A number of factors can affect the response time of a typical thermocouple. Among these are process condition effects and thermocouple size in terms of sheath outside diameter (for sheathed thermocouples) and wire size, junction style, and geometry (for exposed junction thermocouples). These factors and their effects are summarized in this chapter.

14.1 Effect of Process Flow and Temperature

We showed in Chapter 11 that the response time of a thermocouple may be approximated in terms of fluid flow rate as follows:

$$\tau = C_1 + C_3\, u^{-0.6} \tag{14.1}$$

where C_1 and C_3 are constants and u is the fluid flow rate. We also showed that, if the effect of temperature on internal component of response time is neglected, then the response time as a function of temperature at a reference flow rate can be written as:

$$\tau(T_2) = C_1 + C_3(T_1)\frac{h(T_1)}{h(T_2)}\, u^{-0.6} \tag{14.2}$$

Equations 14.1 and 14.2 were tested in a series of experiments conducted during this project. The results are discussed below. Note that in these discussions, the terms flow rate, flow, velocity, and flow velocity are used interchangeably to refer to the speed of fluid flow in terms of meters per second (m/s).

Figure 14.1 shows the response times of a group of thermocouples as a function of flow rate in water and in air, both at room temperature. Several points are clear from the data shown in Figure 14.1. These points are as follows (for a constant reference temperature):
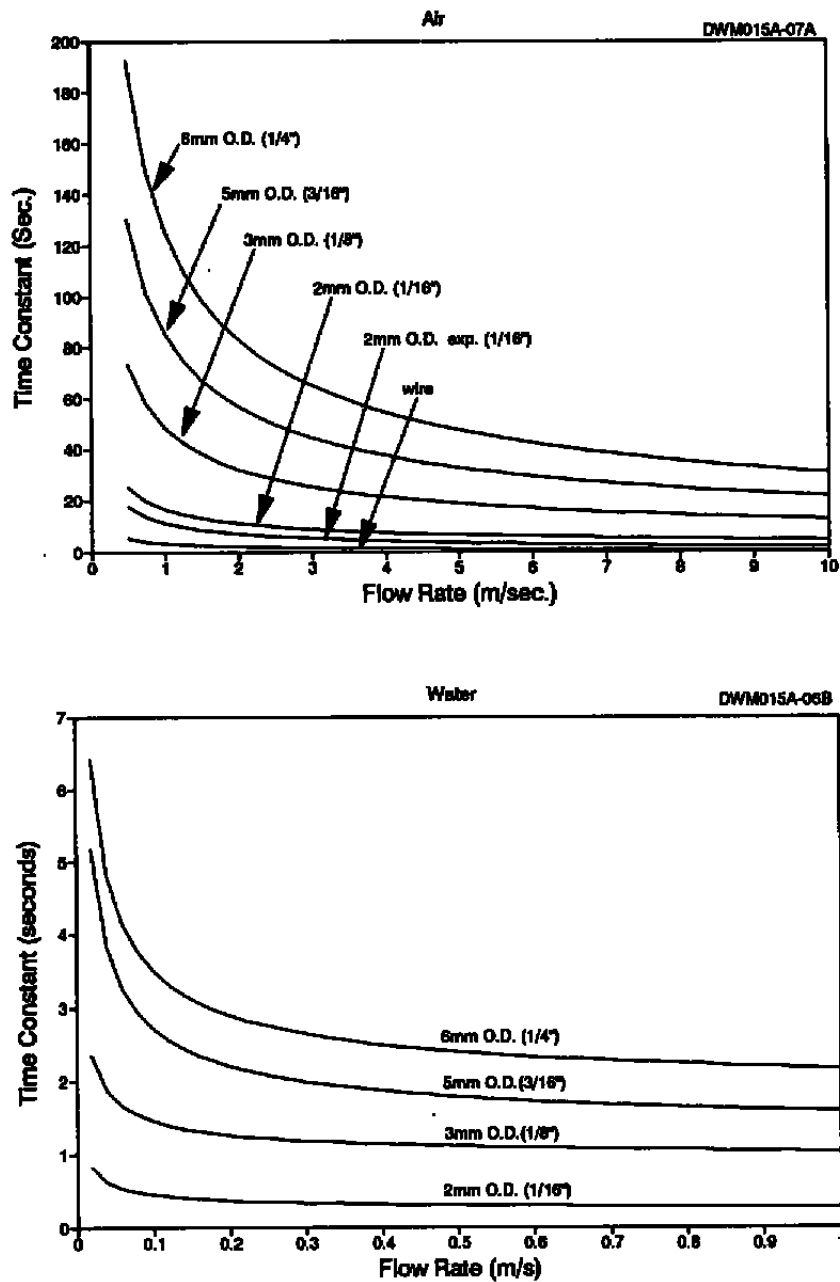
Figure 14.1. Response Versus Flow Data in Air and Water.

1. At moderate velocities, the response time of identical thermocouples are much slower in flowing air than flowing water.

2. Thermocouple response time improves (becomes smaller in value) as the flow rate is increased.

3. The correlation between response time and flow rate is generally very strong at low flow rates, and not so strong at high flow rates.

4. The response time of a thermocouple is a function of its outside diameter (O.D.) at the sensing tip, but at very high flow rates, the O.D. is not as important as it is at low flow rates.

The last point has an important bearing in industrial applications where both response time and ruggedness are important. Sometimes, small size thermocouples are selected to achieve a fast response time, and the selection process is often based on response time data from laboratory measurements at low flows. In these situations, it should be noted that at high flow rates or good heat transfer media, the thermocouple size has much less to do with response time than it does at laboratory conditions. Therefore, it is not always necessary to sacrifice ruggedness and durability for speed of response by selecting small diameter thermocouples.

Figure 14.2 presents the response time versus flow data plotted on a logarithmic scale for thermocouples in flowing air. Let us compare the response times of two of the sheathed thermocouples (3mm and 6mm). At 0.5 m/s, the response times of the two thermocouples are different by about 100 seconds, while the difference is only about 20 seconds at 5 m/s.

The procedure for developing the curves in Figure 14.1 was to make measurements using plunge tests in room temperature water and room temperature air. The plunge tests were performed on each thermocouple at three or more flow rates and the data were plotted in
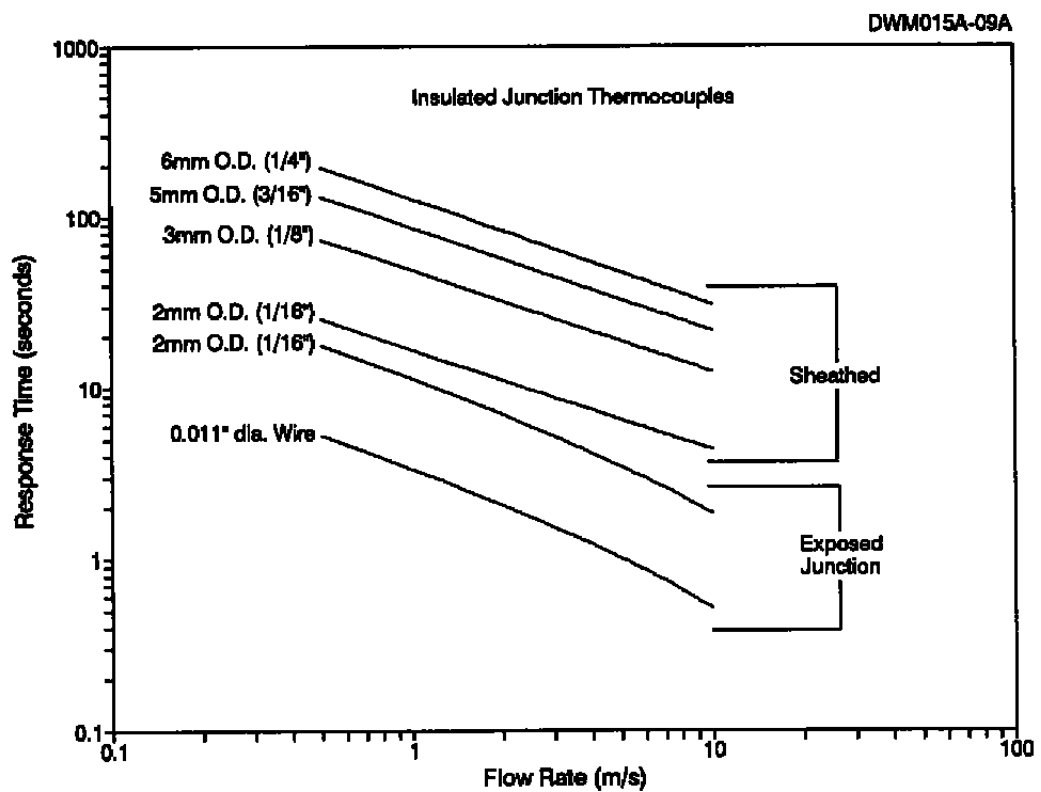
DWM015A-09A

Figure 14.2. Response Time Versus Flow Data
on Log-Log Scale.

terms of time constant versus flow rate raised to -0.6 power. Typical results are shown in Figure 14.3. The slope of each straight line in Figure 14.3 is equal to the constant C_3 in Equation 14.1, and the intercept is equal to the constant C_1. Once identified, these two constants can be substituted in Equation 14.1 and the response versus flow data plotted.

14.2   Response Time Versus Outside Diameter

The response time of thermocouples depends on the sheath or wire diameter at the tip of the thermocouple where the measuring junction is located. To improve the response time, thermocouples are made with reduced diameters at the sensing end as shown in Figure 14.4.

Response time versus diameter data are shown in Figure 14.5 for an insulated junction, a grounded junction, and a thermowell-mounted thermocouple[6]. These results correspond to 63.2 percent of step response from plunge tests in stirred water. As expected, for the same diameter, the grounded junction thermocouple is the fastest, and thermowell-mounted thermocouple is the slowest as apparent in the data in Figure 14.5. It should be pointed out that the thickness of the sheath or the thermowell does not play a major role on the resulting response time. What is important is any air gap within the thermocouple construction materials or, in the case of thermowell mounted sensors, in the interface between the outside wall of the sheath and the inside wall of the thermowell. It has been determined that a very small air gap (a fraction of a millimeter of radial distance) can increase the response time significantly. In some thermowell mounted sensors, the tip of the thermowell is filled with a thermal coupling compound to improve the response time. This approach is generally effective, but at high temperatures (above about 300°C), most thermal coupling compounds lose their heat transfer ability and cause the response time to increase.
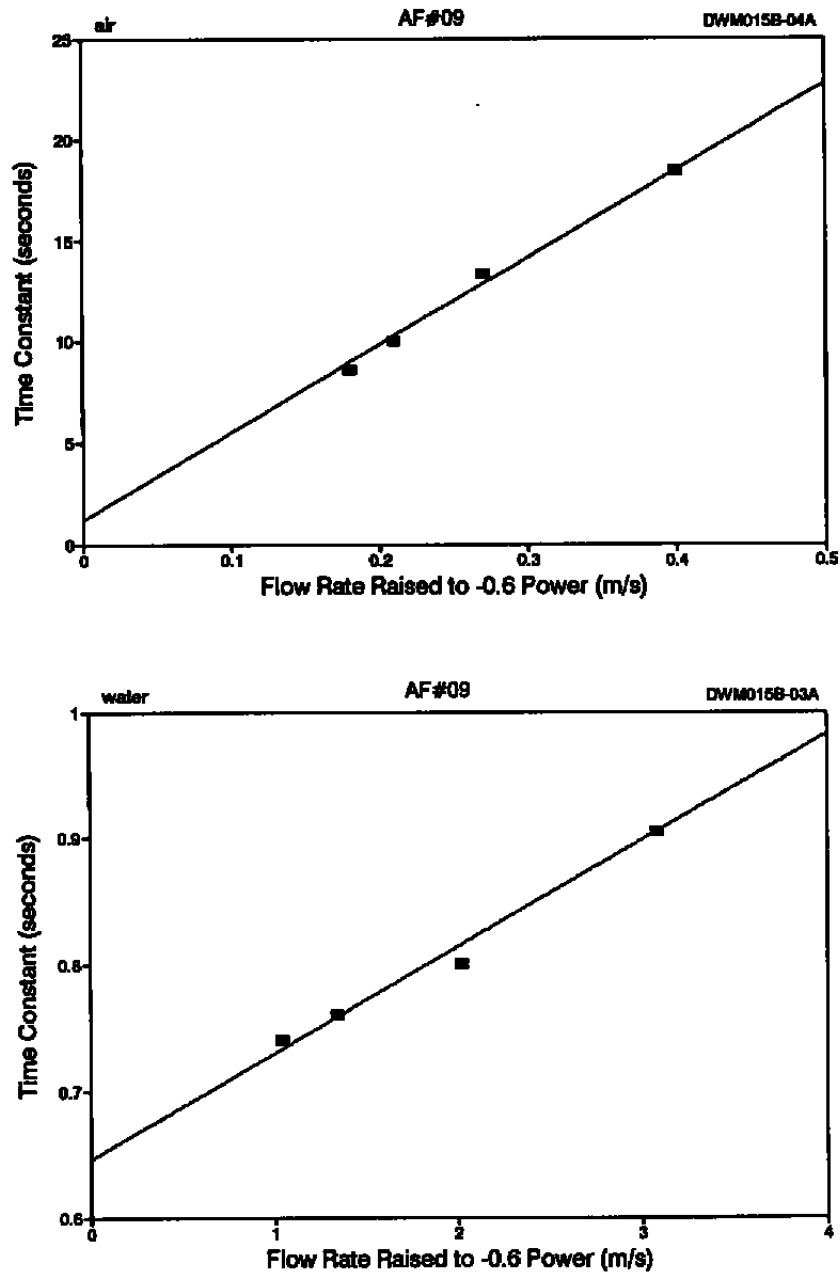
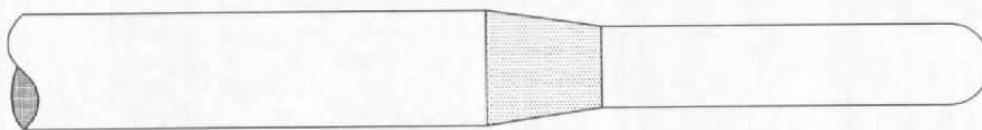Figure 14.3. Response Versus Flow Rate Raised to -0.6 Power.

189

AMS—DWG THC068A

Figure 14.4. Reduced Diameter Tip Design for Fast Response.
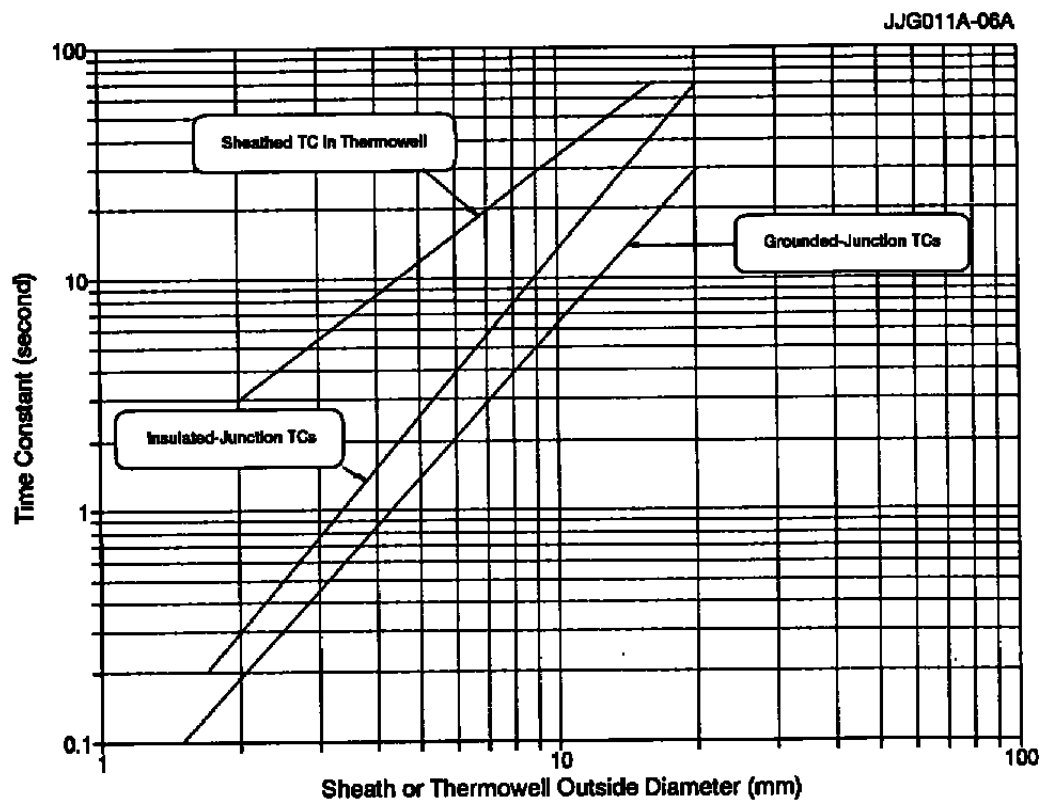
Figure 14.5. Response Time of Sheathed Thermocouples as a Function of Outside Diameter (From Plunge Test in Stirred Water).

191

General data showing the correlation between the response time and the size of thermocouples are shown in Figure 14.6. This information is based on data published in OMEGA Engineering Catalog[16], for the thermocouples shown in Figure 14.7. The OMEGA data were slightly altered to show the correlation in the form of a straight line.

The data in Figure 14.6 are the time constants of the thermocouples corresponding to 63.2 percent of step response in room temperature air at atmospheric pressure and a flow of approximately 20 m/s. The time constant results, shown in Figure 14.6, apply to bare wire (Butt Welded), and grounded junction thermocouples shown in Figure 14.7. For the beaded-type and the insulated junction thermocouples shown in Figure 14.7, the time constant data on the vertical axis of Figure 14.6 must be multiplied by 1.5. Same type of data for metal sheathed thermocouple sensors are shown in Figure 14.8 based on data in OMEGA Catalog.

14.3 Effect of Temperature on Response Time

Figure 14.9 shows response versus flow data for a thermocouple in water at both 20°C and 300°C. The curve for the 20°C was generated with the same procedure we described in Section 14.1. To generate the 300°C curve, the same room temperature response versus flow data were used with Equation 14.2 and the Rohsenow & Choi correlations given in Chapter 11.
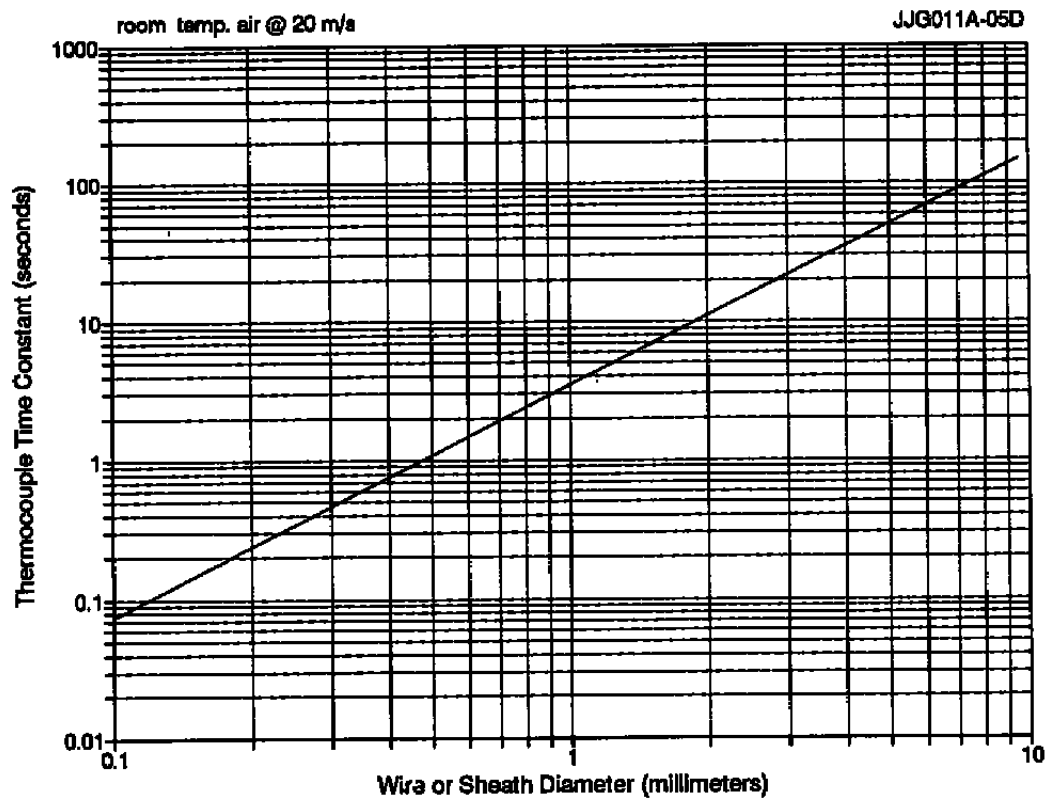
Figure 14.6. Correlation Between Response Time and Size
for Thermocouples Shown in Figure 14.7.

AMS—DWG THC069D

Bare Wire

Grounded Junction

Beaded - Type

Insulated Junction
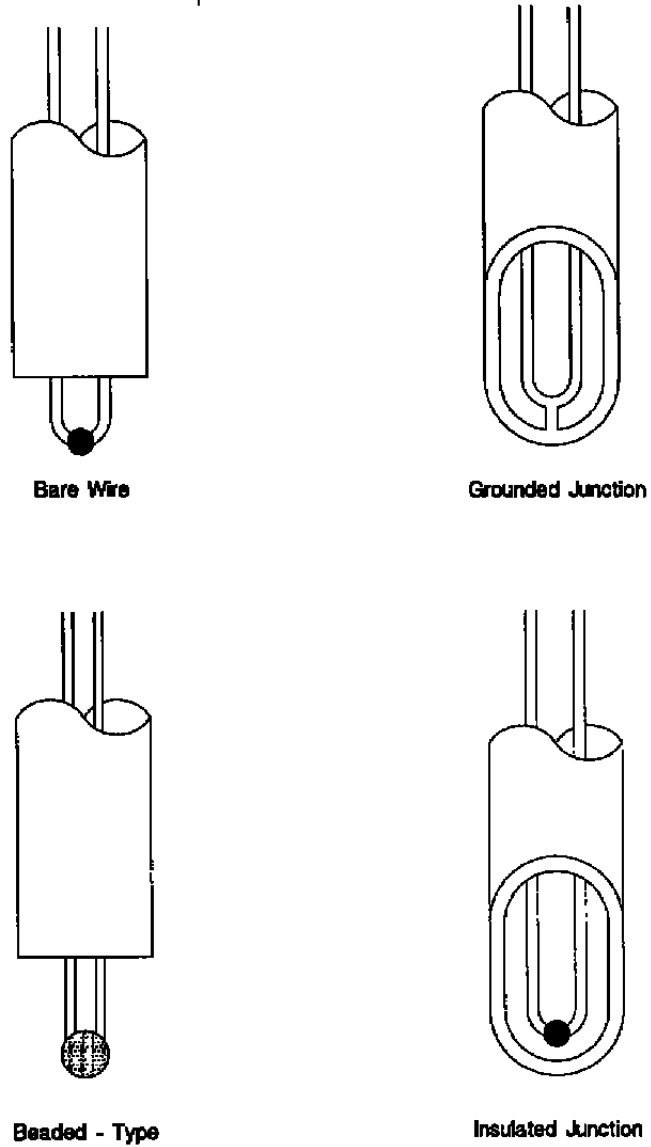
Figure 14.7. Thermocouples for the Data of Figure 14.6.

JJG011A-02A

Figure 14.8. Response Time Versus Diameter for Metal Sheathed Thermocouples.

Figure 14.9. Response Versus Flow Data at Two Temperatures
for a Thermocouple Tested in Water.

15. THERMOCOUPLE CALIBRATION

Although research on steady state performance of thermocouples was beyond the scope of this project, a limited amount of work was performed at the end of the project in this area. The results are summarized in this chapter.

15.1 Thermocouple Inhomogeneity Test

Unlike RTDs, thermocouples are not generally calibrated after use. This is because of the inhomogeneity problem inherent i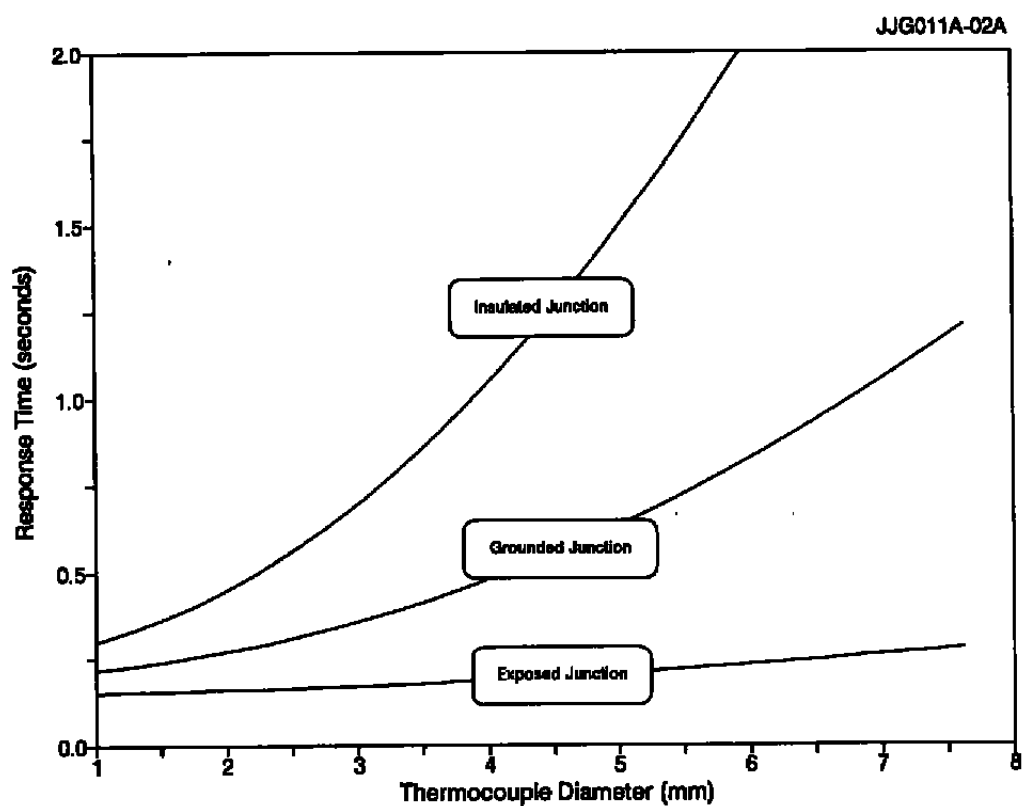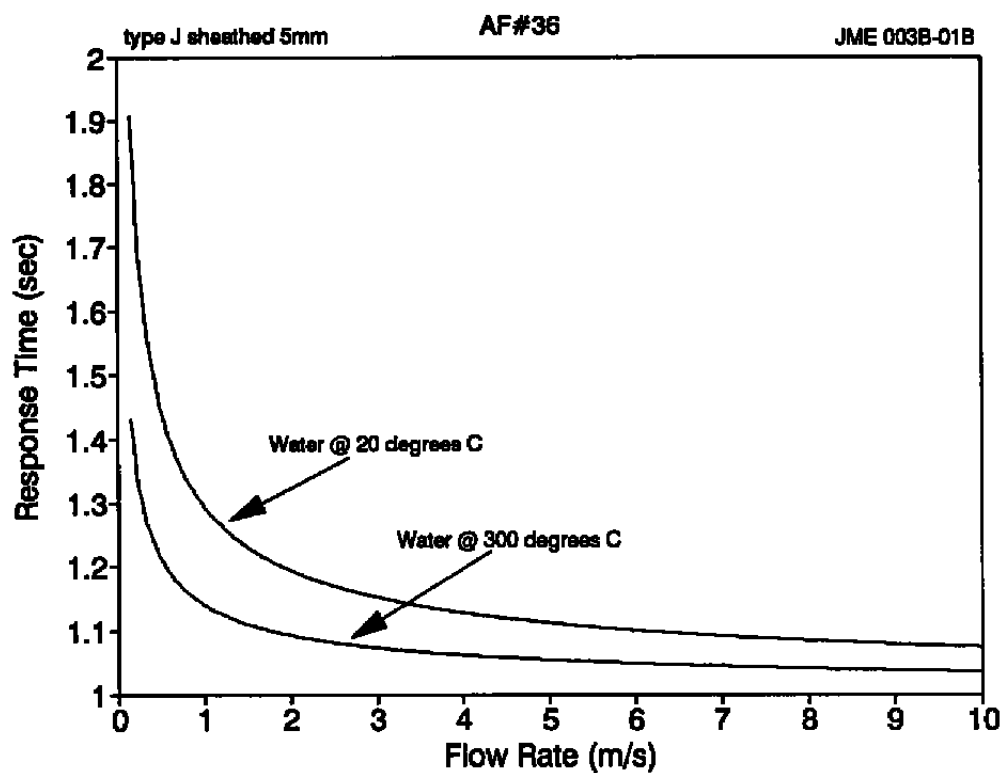n thermocouples. However, in some cases, it may be important to determine the reliability of past temperature measurements with the thermocouple. In this case, an inhomogeneity check of the thermocouple must be performed to determine if the thermocouple is suitable for a post-use calibration. To test for inhomogeneity, one needs a steep temperature gradient through which the thermocouple should be passed while its output is monitored for any significant change. A simple method for a gross inhomogeneity test is to run a heat gun along the thermocouple while monitoring its amplified output on a strip chart recorder, oscilloscope, or a voltmeter. Figure 15.1 shows a strip chart recording of the output of a thermocouple that had an inhomogeneous section. In this experiment, an otherwise normal thermocouple was bent and squeezed in an attempt to produce an inhomogeneous region in the thermocouple wire (Figure 15.2). The thermocouple was then tested in a simple apparatus that was developed in the project to provide a steep temperature gradient for inhomogeneity testing of thermocouples. It is apparent from the results in Figure 15.1 that the demonstration effort that was carried out was successful in showing the inhomogeneity problem.
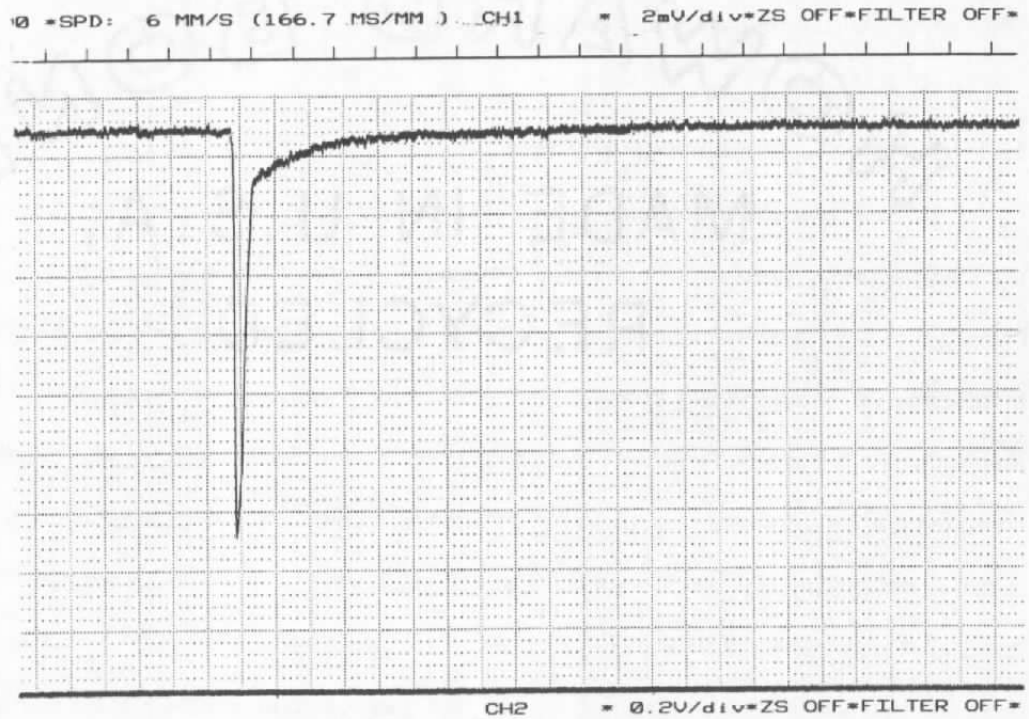
Figure 15.1. Thermocouple Inhomogeneity Test Results.

AMS—DWG THC014B

Inhomogeneity ——————▶

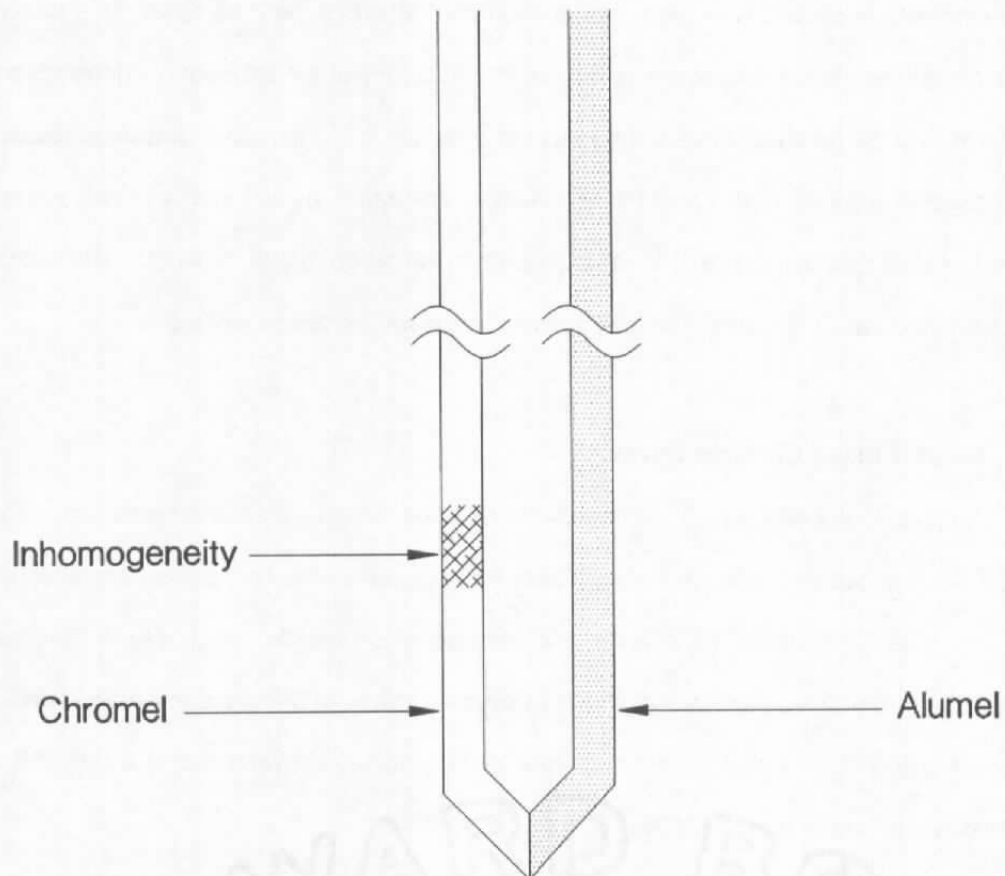Chromel ——————▶   ◀—————— Alumel

Figure 15.2. Illustration of Thermocouple With Inhomogeneity.

An inhomogeneity test is also important before calibration of new thermocouples and thermocouple wires if a high accuracy is desired.

Although an inhomogeneity test is important as a first step in calibration of thermocouples, it should be noted that a thermocouple that has successfully passed an inhomogeneity test is not necessarily accurate. The accuracy of a thermocouple depends on its calibration and the ability of the thermocouple to maintain the calibration. For example, some thermocouples (such as type K and E) can lose their calibration by as much as 1 percent within one minute after they are exposed to temperatures in the range of 320 to 540°C. This is due to a phenomenon called *"ordering"* or *"short-ranged ordering"* as described below[14].

15.2   Short-Ranged Ordering Phenomenon

According to Kollie, et.al.[7], at temperatures above 200°C, the Chromel element of type K and E thermocouples undergoes a solid state transformation that can cause calibration shifts of as much as 1.3 percent.   The error is eliminated when the thermocouple is reannealed because the order-disorder transformation is reversible. More specifically, short-ranged ordering of the Nickel and Chromium atoms of the Chromel alloy occurs between 200°C and 600°C, and the disordering occurs above 600°C.

Because of the ordering phenomenon, individual calibrations are not very useful for type K or E thermocouples. Rather, it is best to calibrate a representative thermocouple and apply the calibration to the remaining thermocouples from the same lot.

If a type K or E thermocouple is calibrated in temperatures where the ordering can occur, then the portion of the thermocouple that was in the calibration medium will suffer from the ordering phenomenon while the rest of the thermocouple will be normal. This leaves the thermocouple with a transition region (inhomogeneity). If the thermocouple is then used in a situation where the transition region can fall in a temperature gradient, measurement errors will be encountered. Although this error is usually small (less than 0.5 percent according to ASTM Standard E 839), the possibility that it can occur suggests that individual calibration of type K and E thermocouples may not always result in better accuracy or provide the intended benefit. In fact, the calibration can degrade the accuracy of the thermocouple.

Figure 15.3 shows laboratory calibration results for four thermocouples. These were calibrated by the comparison method using a type S thermocouple as reference. The calibrations were performed with the thermocouples installed in an Aluminum block in a furnace along with the type S reference. The results are given in terms of the differences between the temperatures indicated by the thermocouples and the corresponding temperatures measured with the type S thermocouple.

The ordering phenomenon is observable in the results shown in Figure 15.3. It is apparent that the deviations of the type K and E thermocouples increase above 300°C, including that of the type K special grade. In contrast, the type J thermocouple does not seem to have a different behavior above 300°C.

Type K
AFC #03 Indicated - Measured Difference   WLM005A-01A

Type E
AFC #07 Indicated - Measured Difference   WLM005A-09A

Type J
AFC #11 Indicated - Measured Difference   WLM005A-03A

Type K - Special Grade
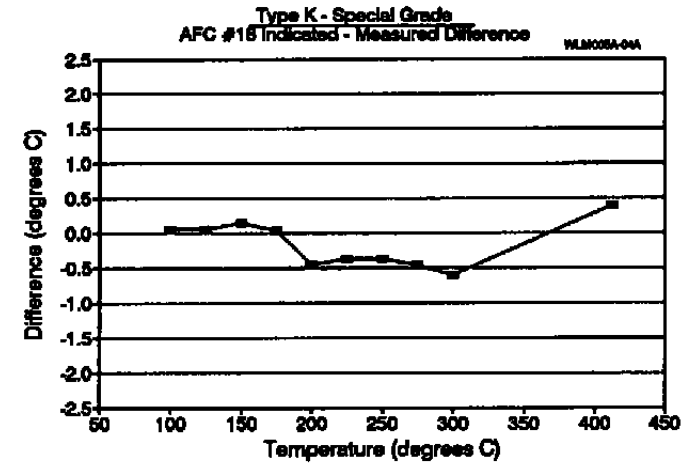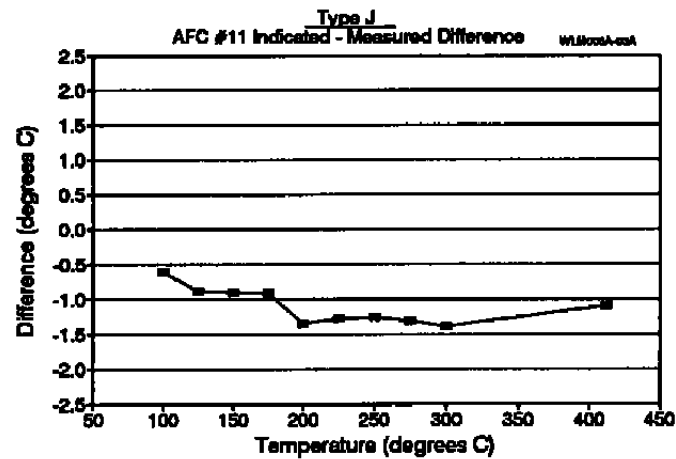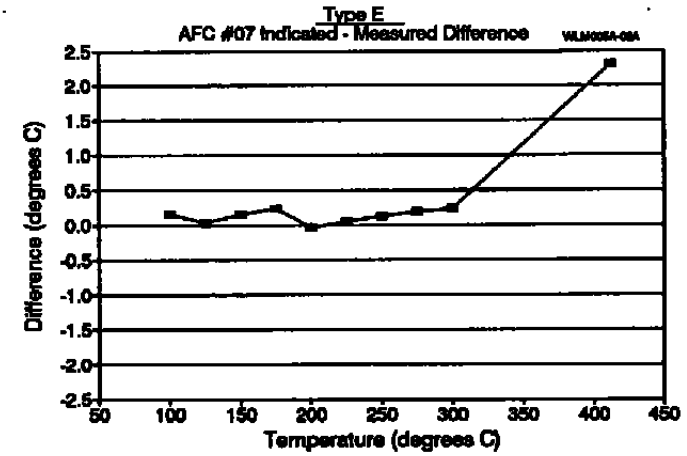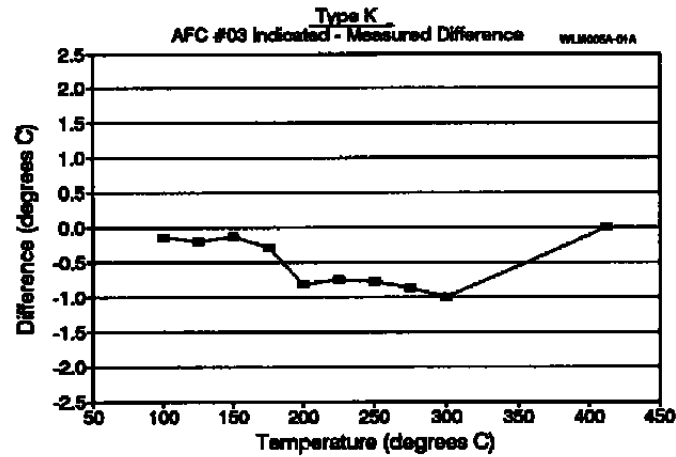AFC #18 Indicated - Measured Difference   WLM005A-04A

Figure 15.3. Thermocouple Calibration Results for Demonstration of Short-Range Ordering.

15.3 Effect of LCSR on Calibration of Thermocouples

In LCSR testing of RTDs and thermocouples, a question is often asked as to whether or not the LCSR test can affect the calibration of the sensor. In order to demonstrate the effect of the LCSR test, a number of thermocouples including a few special grade thermocouples were calibrated before and after a series of normal LCSR tests. These thermocouples were calibrated in an ice bath and an oil bath up to 300°C. A listing of the thermocouples used in this and other calibration experiments reported herein are given in Table 15.1. The list includes both special grade and standard grade thermocouples. The tolerances of the special grade thermocouples are generally twice as good as standard grade. We have used the terms standard grade and regular grade interchangeably in this report.

The calibrations were performed using the comparison method similar to the Method B described in ASTM Standard E 220 entitled, "Calibration of Thermocouples by Comparison Techniques"[18]. The thermocouples were calibrated against a Standard Platinum Resistance Thermometer (SPRT). The results are shown in Figure 15.4 in terms of the differences between the thermocouples and the SPRT. Four calibrations were performed as follows: three calibrations before LCSR testing, and one calibration after LCSR testing. The LCSR tests were performed with normal heating currents and heating times. The results of the pre and post LCSR calibrations are shown in Figure 15.4. These results are all for type K thermocouples, including a special grade assembly. Other thermocouple types were also tested for the effect of LCSR. The results for the other types are given in Volume II. The following has been concluded from the results in Figure 15.4 for the type K thermocouples tested:

1. The average accuracy of these thermocouples is about 0.5°C at 100°C and about 1°C at 300°C.

2. The special grade thermocouples are about twice as accurate as the regular grade thermocouples as expected.

TABLE 15.1

| Calibration Thermocouple Descriptions	
Tag Number	Description
AFC #01	Type K, 6 mm diameter, SS sheath
AFC #02	Type K, 5 mm diameter, SS sheath
AFC #03	Type K, 3 mm diameter, SS sheath
AFC #04	Type K, 2 mm diameter, SS sheath
AFC #05	Type E, 6 mm diameter, SS sheath
AFC #06	Type E, 5 mm diameter, SS sheath
AFC #07	Type E, 3 mm diameter, SS sheath
AFC #08	Type E, 2 mm diameter, SS sheath
AFC #09	Type J, 6 mm diameter, SS sheath
AFC #10	Type J, 5 mm diameter, SS sheath
AFC #11	Type J, 3 mm diameter, SS sheath
AFC #12	Type J, 2 mm diameter, SS sheath
AFC #13	Type K, 3 mm diameter, SS sheath (shipped as special grade)
AFC #14	Type J, 3 mm diameter, SS sheath (shipped as special grade)
AFC #15	Type K, 3 mm diameter, SS sheath, special grade
AFC #16	Type E, 3 mm diameter, SS sheath, special grade
AFC #17	Type J, 3 mm diameter, SS sheath, special grade
AFC# 18	Type K, 3 mm diameter, SS sheath, special grade
AFC #19	Type E, 3 mm diameter, SS sheath, special grade
AFC #20	Type J, 3 mm diameter, SS sheath, special grade
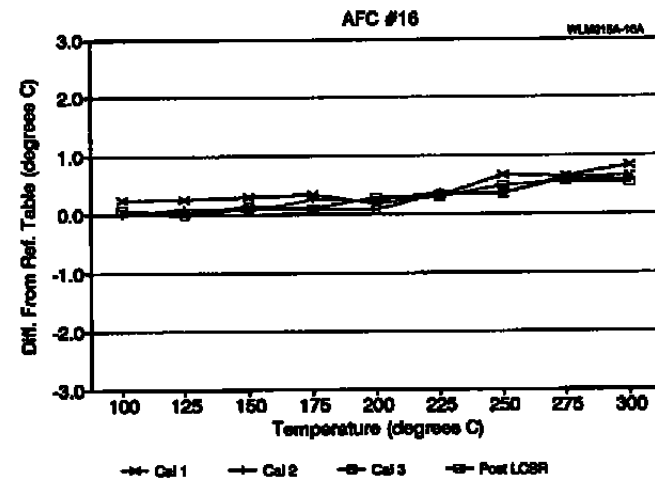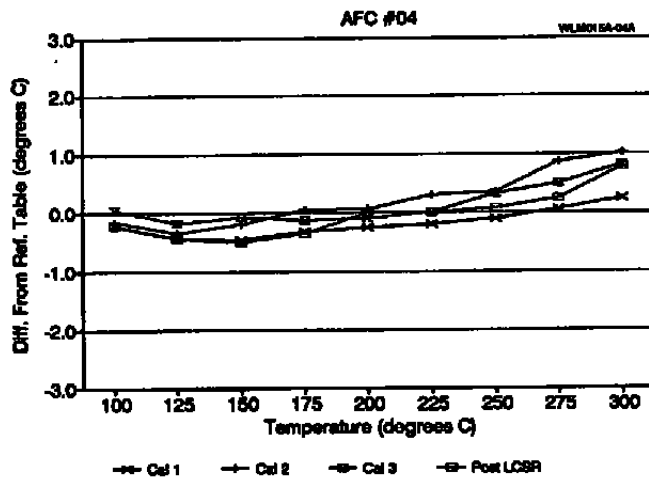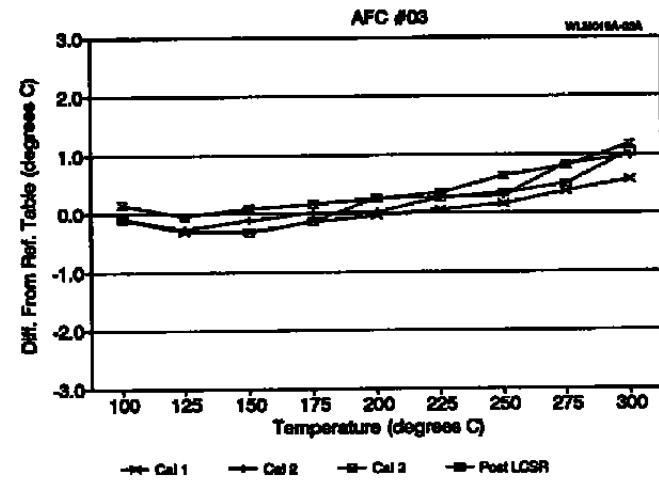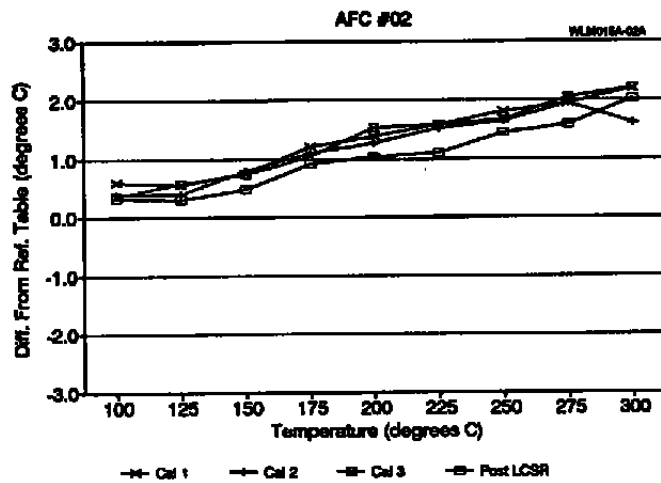
Figure 15.4. Calibration Results Before and After LCSR Testing for Type K Thermocouples.

3.   The average repeatability of our calibration process for these
      thermocouples is about ± 0.1°C.

4.   The average repeatability of the thermocouples in consecutive calibrations
      is ± 0.4°C. More data on thermocouple repeatability is shown in Section
      15.4 below.

5.   The calibration of these thermocouples are not affected by the LCSR
      method beyond their normal repeatability and the accuracy by which they
      were calibrated.

15.4 Stability of Thermocouples

The stability question has two components:

1.   Short term stability which can be characterized by consecutive laboratory
      calibrations performed over a short period of time such as a few days or
      a few weeks. Short term stability is also called repeatability.

2.   Long term stability which can be characterized by experimental aging
      studies such as those conducted by the author on RTDs as reported in
      reference 20. Long term stability is often expressed as drift rate or drift
      characteristics.

We performed a limited number of calibrations to address the short term stability of a few

typical thermocouples. This work involved several type K, J, and E thermocouples including six

special grade thermocouples of these three types. The results are summarized in Figure 15.5.

Each thermocouple was calibrated a number of times in a period of a few days. The calibration

data were then analyzed in terms of the deviations of each thermocouple at 300°C from that of

a SPRT that was included in the calibration. The deviations were categorized in terms of positive

and negative errors depending on whether the indications of thermocouples were larger or

smaller than that of the SPRT. The positive and negative deviations were then averaged and

plotted in a bar chart format for each of the three types of thermocouples as shown in

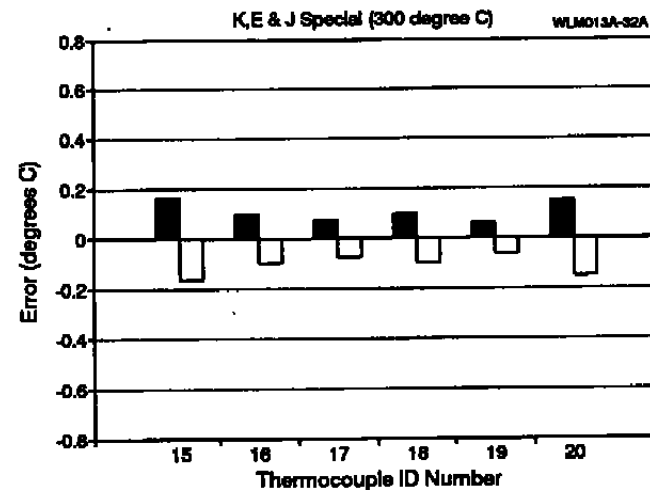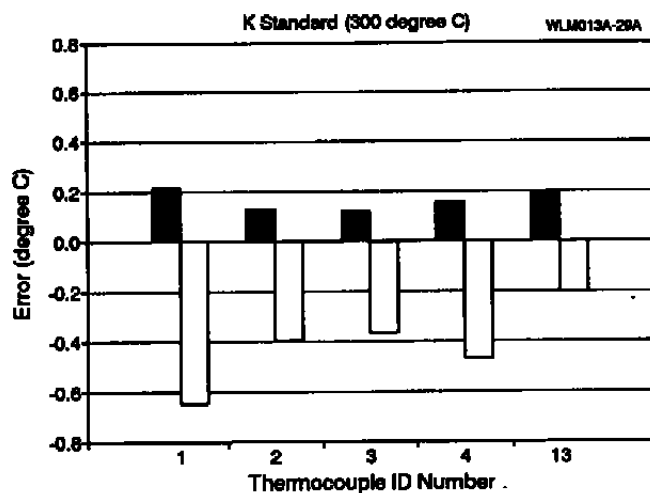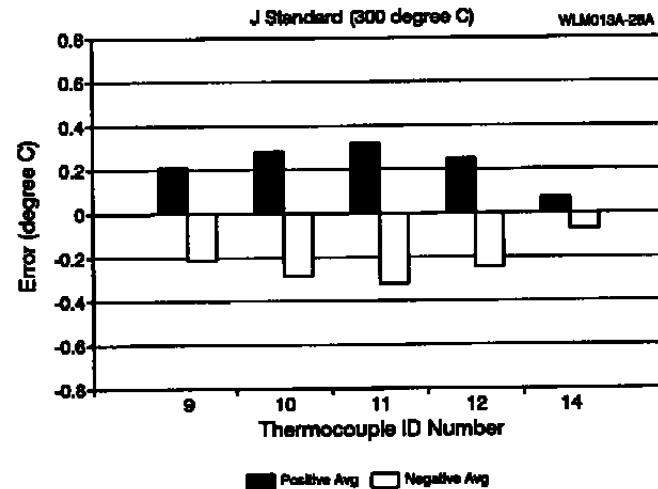Figure 15.5. The conclusions based on the data presented in Figure 15.5 are:
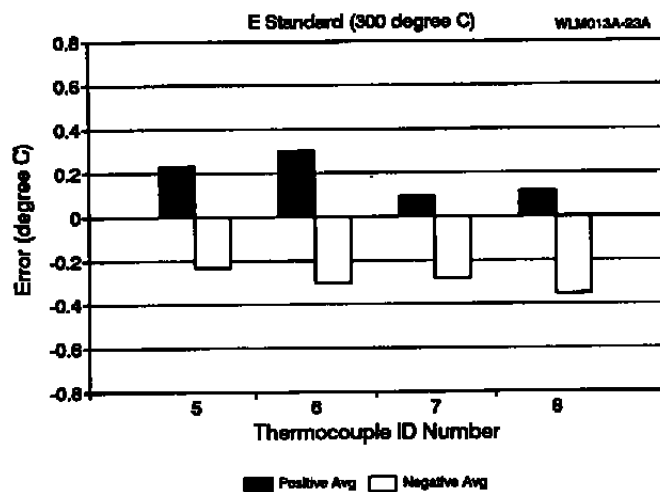
Figure 15.5. Repeatability of Typical Thermocouples.

1.   The short term stability (i.e., repeatability) of the regular grade thermocouples is ± 0.4°C as expected.

2.   The repeatability of the special grade thermocouples is ± 0.2°C as expected.

3.   The repeatability error of the type K thermocouples are larger than the type J and type E thermocouples.

Note that all these results are subject to a ± 0.1°C error of the calibration process.

15.5   Thermocouple Nonlinearities

As we discussed in Chapter 4, thermocouples are not generally as accurate as RTDs. One reason for this is the nonlinearity of thermocouples which present a challenge in processing of calibration data and in the design of signal conversion equipment. Some illustrations of thermocouple nonlinearities are presented in this section.

Figure 15.6 shows EMF versus temperature curves of the eight standardized thermocouples we described in Chapter 5. These curves are also referred to as thermocouple calibration curves. They show the maximum temperatures that can be measured with the thermocouples and demonstrate their relative nonlinearity characteristics. A more clear way of demonstrating thermocouple nonlinearities is to plot the difference between the thermocouple calibration curve and a straight line (Figure 15.7). Such differences are compared in Figure 15.8 for types J, K, and E thermocouples. The nonlinearity curves are shown up to 1000°C. This is not intended to imply that these thermocouples can all be used to 1000°C. For comparison purposes, the nonlinearity of a typical 100 ohm RTD is shown in Figure 15.9.
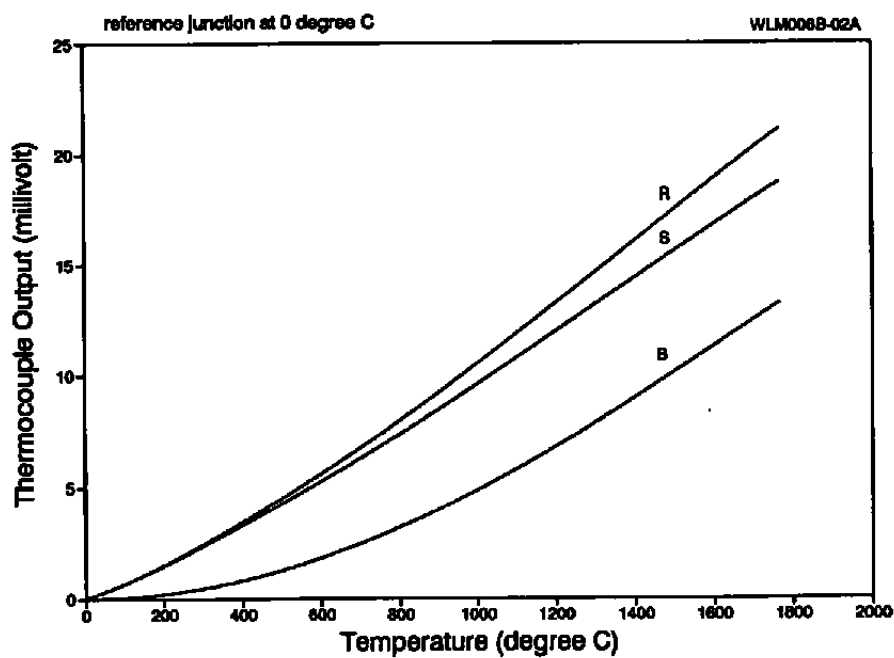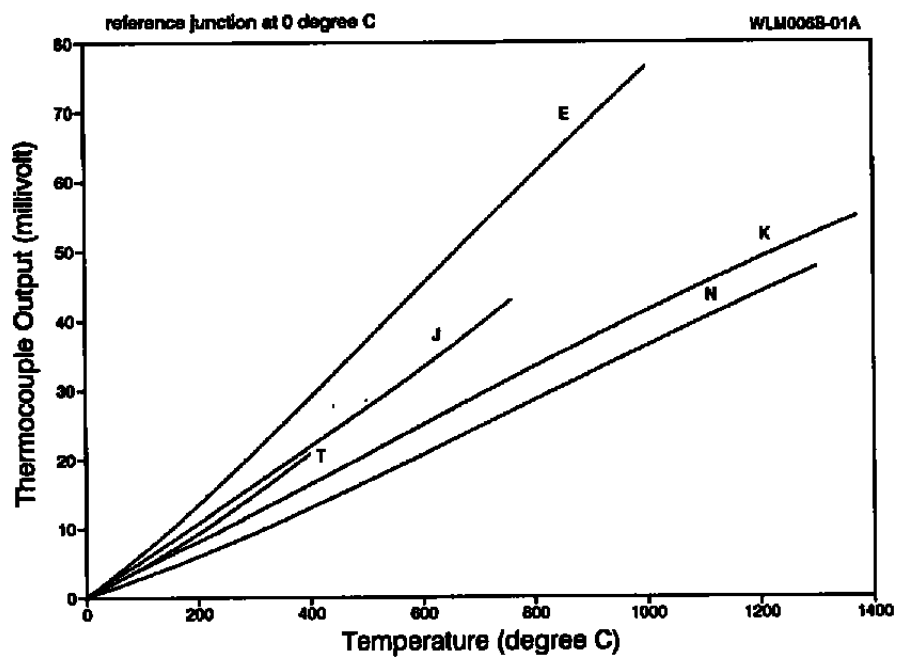
Figure 15.6. Thermocouple Calibration Curves.
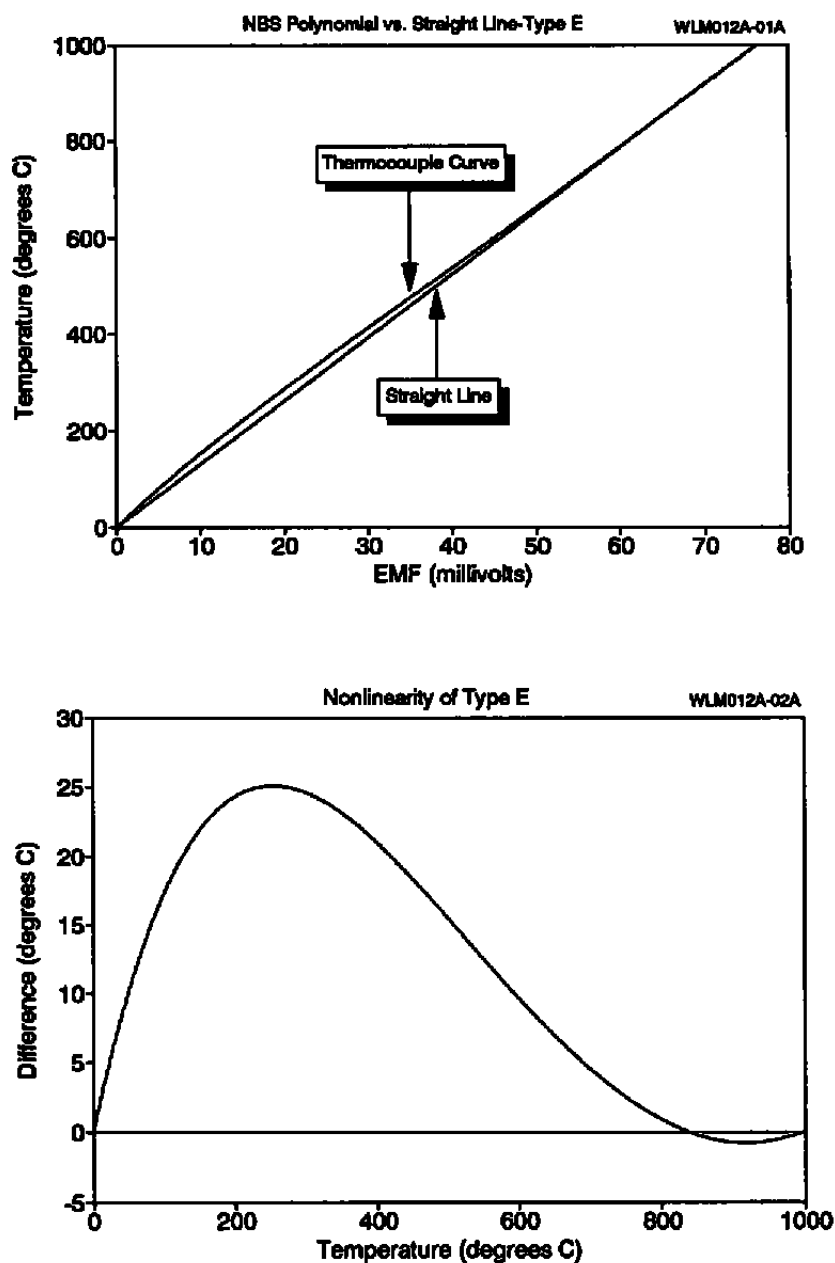
Figure 15.7. Difference Between Calibration Curve of a
Type E Thermocouple and a Straight Line.

Nonlinearity of Types J,K,E

WLM012A-07A

Type E

Type J

Type K

Difference (degree C)

Temperature (degree C)
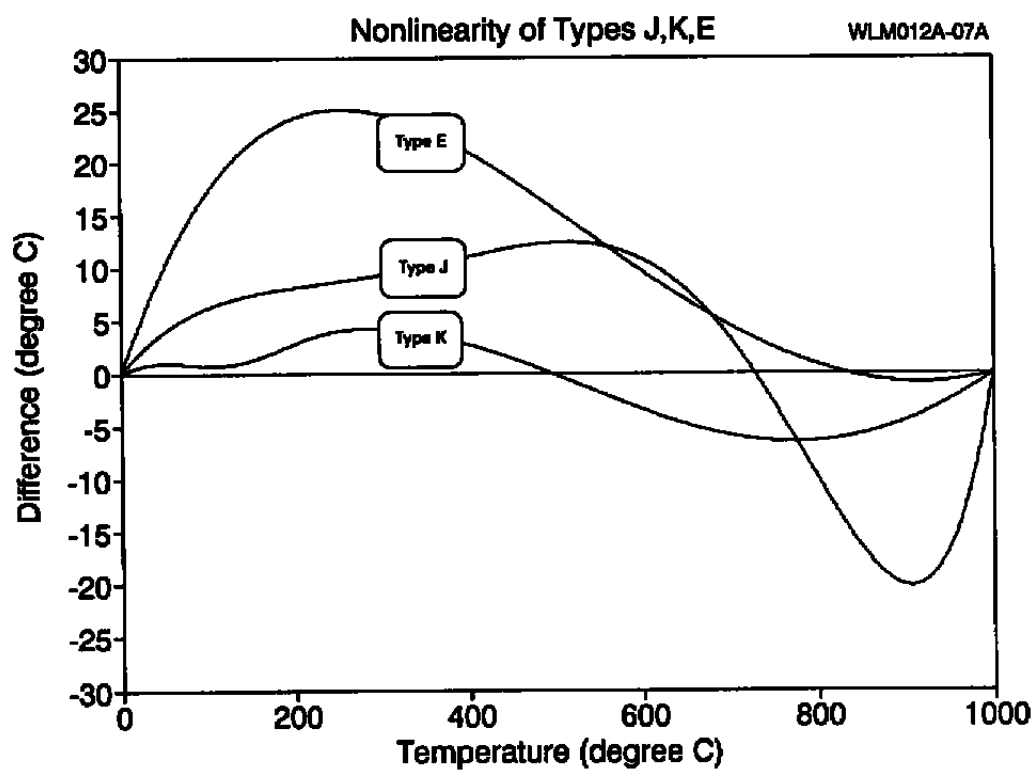
Figure 15.8. Thermocouple Nonlinearities.

KMP009A-03A

KMP009A-01D
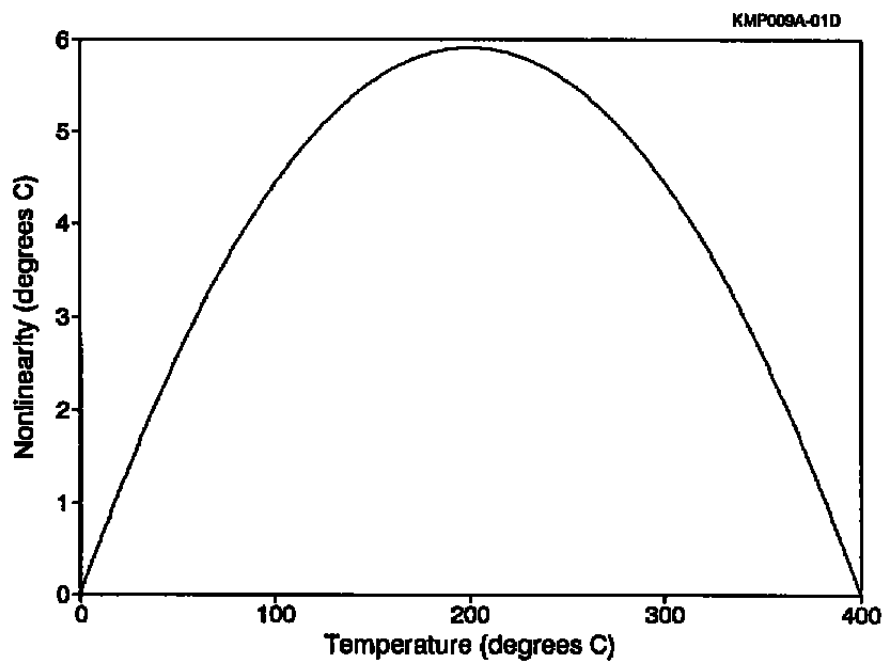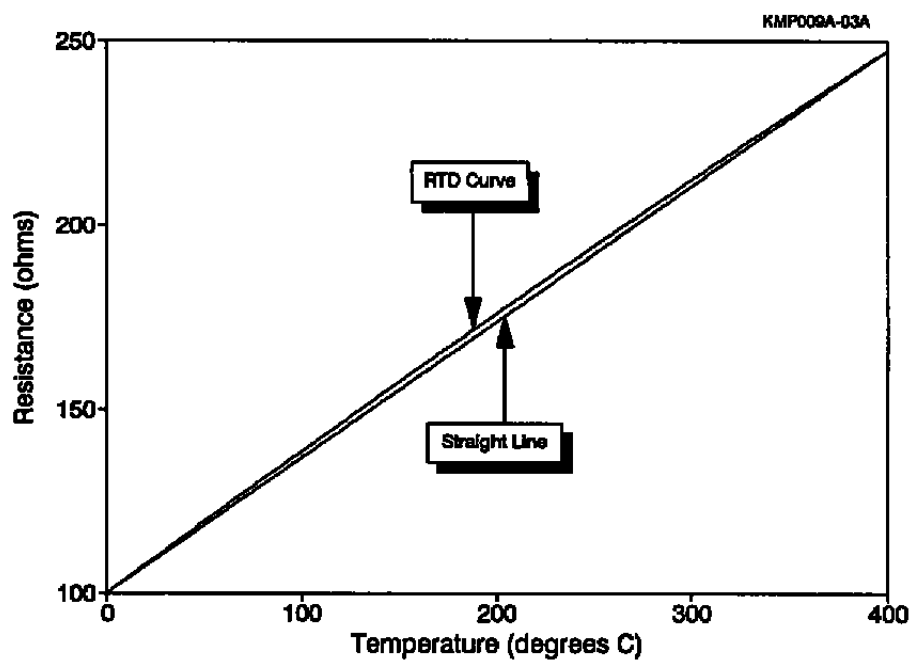
Figure 15.9. Nonlinearity of a Typical RTD.

16. RESPONSE TIME TESTING USING NOISE ANALYSIS

The noise analysis technique has been used successfully in the nuclear power industry for response time testing of pressure sensors, and to a lesser extent, temperature sensors such as RTDs and thermocouples. This method has been validated for nuclear plant pressure sensors, but not for temperature sensors. Although the noise method has not been validated for temperature sensors, it has been shown that it is useful in obtaining an estimate for the response time of RTDs and thermocouples and for monitoring for gross changes in response times.

The noise analysis technique is based on recording the random fluctuations that exist at the output of installed sensors while the process is operating. These fluctuations result from the inherent random temperature fluctuations which usually exist in most processes due to turbulence and other phenomena during operation. Assuming that the bandwidth of process fluctuations is significantly larger than the bandwidth of the sensor, one can usually analyze the sensor noise output to obtain its response time. The analysis can be performed in frequency domain or time domain. In frequency domain, the noise data is Fourier transformed and its power spectral density (PSD) is calculated. The PSD is then fitted to an appropriate model for the sensor from which the dynamic response is calculated.

In time domain, the data is analyzed using the Autoregressive (AR) model. The AR model uses the sensor noise data to identify the impulse response of the sensor, and then the step response. The step response is then used to obtain the sensor time constant.

213

Figure 16.1 shows the PSD of a thermocouple which was tested in the project with the noise method in the laboratory under two different test conditions; stirred water and stirred air. The details of how temperature noise was generated for this experiment are given in Volume II. The test results are summarized in Table 16.1. The results are compared with plunge test time constants to provide an estimate of the validity and accuracy of the noise method.

It should be pointed out that the noise tests discussed in this chapter were performed on a quick-look basis for demonstration purposes to indicate the potential of the noise analysis technique. Under more elaborate and careful test conditions, the agreement between the plunge and noise analysis results should be better than those shown in Table 16.1.

AF#20 Pipe Manifold Test

TST0003   JME005A-03A

AF#20 Heat-Gun Test

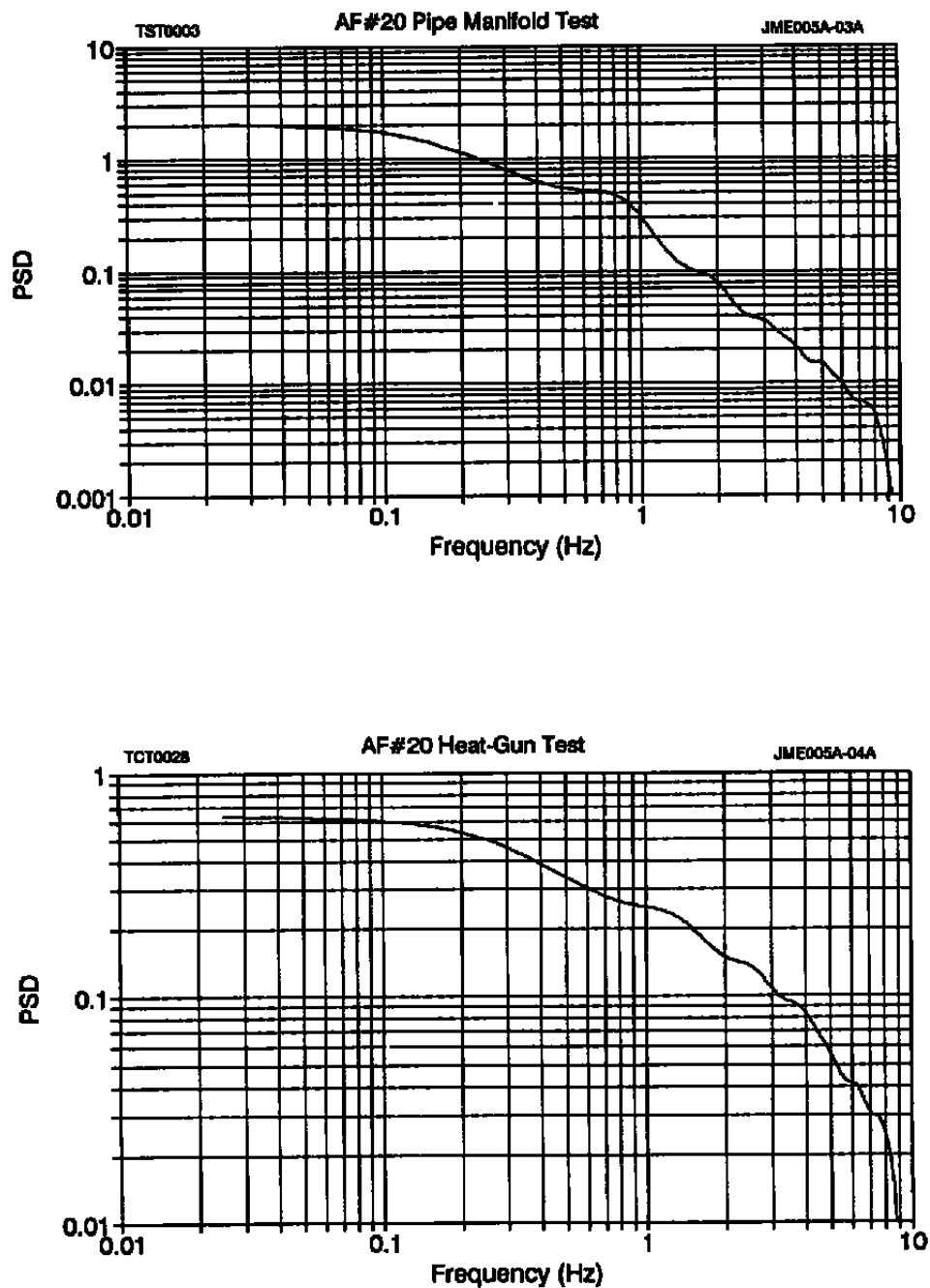TCT0028   JME005A-04A

Figure 16.1. Thermocouple PSDs from Laboratory Tests.

TABLE 16.1

Thermocople Noise Test Results

| Tag Number | Test Number | Response Time (sec) | |
		Plunge	Noise Analysis
Stirred air			
AF #20	1	0.16	0.12
AF #20	2	0.16	0.09
Stirred water			
AF #04	1	3.70	4.35
AF #20	2	0.05	0.50

17. TEST OF INSTALLATION INTEGRITY OF THERMOCOUPLES

In addition to providing quantitative response time results for thermocouples in liquids and gases, the LCSR method may be used as a qualitative means for checking the installation integrity of thermocouples embedded in solid materials or attached to solid surfaces.

Figure 17.1 shows two LCSR transients for a thermocouple embedded in a carbon-carbon structure of the type used in solid rocket motor nozzles. The thermocouple was secured in place with an adhesive cement, and the tests were performed once with the thermocouple fully inserted in a hole in the carbon-carbon material, and again with the thermocouple partially withdrawn from the hole, but still secured by the adhesive cement. It is apparent that the LCSR transients can clearly distinguish between the proper and improper installation. This work was done as an unfunded demonstration work in cooperation with the Lockheed Aeronautical System Company. As a part of NASA's solid propulsion integrity program, Lockheed was tasked with "Advanced Instrumentation" under the nozzle work package. In November 1989, in response to an interest expressed by Lockheed, AMS agreed to demonstrate the ability of the LCSR test for checking the installation integrity of thermocouples in solid material.

In addition to the laboratory tests mentioned above, field tests were carried out at Marshall Space Flight Center (MSFC) in Alabama, where thermostructural properties of composite material were being studied under firing conditions. In this facility, there was an interest in verifying that the thermocouples in the carbon-carbon material remain properly in place during the firing tests. Figure 17.2 shows test results for two thermocouples that were tested with the LCSR method before and after the firing tests . It is apparent that the response

LC #1 In Hole #2   KMP026A-02C
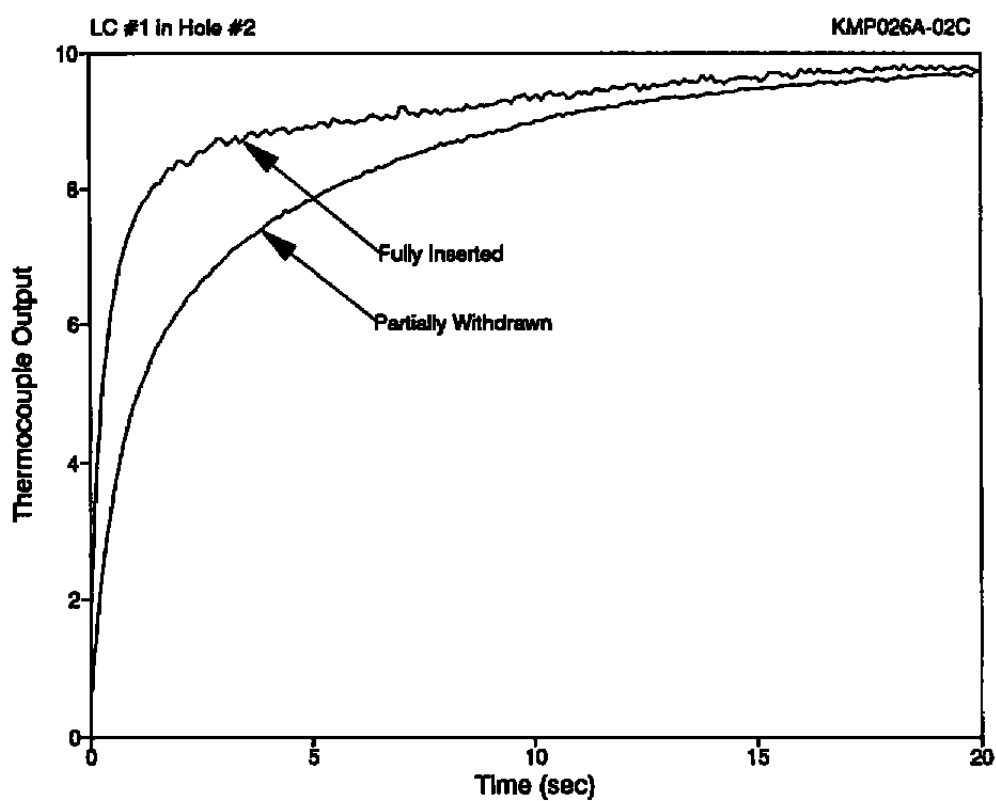
Figure 17.1. LCSR Transients from Testing the Installation Quality
of a Thermocouple in a Carbon-Carbon Structure.
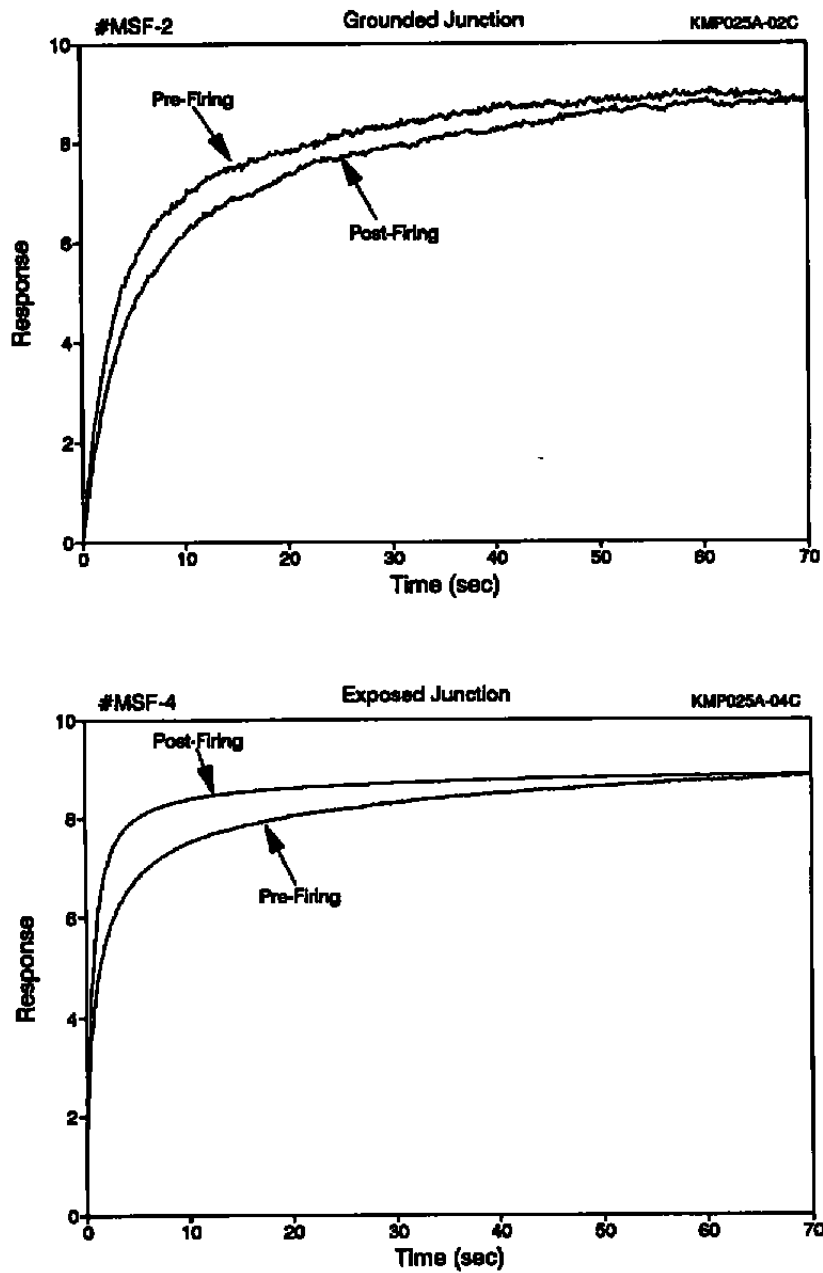
Figure 17.2. LCSR Transients for Two Thermocouples
Tested at MSFC.

time of one of the two thermocouples (MSF-2) degraded, and the response time of the other (MSF-4) improved during the firing tests. This can happen for either or both of the following reasons:

1. The thermocouples slightly moved during the firing tests. This can affect the quality of the thermal contact between the thermocouples and the host material resulting in a better or worse response time depending on how the contact quality was affected.

2. The response times of the thermocouples permanently changed due to the effect of high temperature on material properties inside the thermocouples. As we have discussed earlier in this report, high temperatures can cause the response time of a thermocouple to increase or decrease depending on how the properties and geometry of the material inside the thermocouple are altered by temperature.

The LCSR test transients in Figure 17.2 also show that thermocouple number MSF-4 is faster than MSF-2. This is expected because MSF-4 is an exposed junction thermocouple while MSF-2 is a sheathed thermocouple. That is, the LCSR test can easily be used to intercompare any two or more thermocouples in terms of their response time and reveal the outliers.

.

.

18. SMART THERMOCOUPLE SYSTEM

In addition to LCSR testing, the instrument that was developed in this project can be supplemented with a few additional hardware and software to provide a means for testing the steady state health, reliability and accuracy of sheathed thermocouples as installed in operating processes. The sections that follow present the methods that can be used to accomplish this and proceed to introduce the conceptual design of a smart thermocouple system. For the purpose of this discussion, a smart thermocouple system is one that indicates temperature like a conventional thermocouple, and in addition, provides qualitative information about the reliability and accuracy of the indicated temperature and the static and dynamic condition of the thermocouple sensor itself and the associated lead wires, signal conditioning equipment, and other hardware in the temperature measurement channel. These capabilities are important in identifying those thermocouples that have drifted out of tolerance or have become so sluggish that they should be replaced.

18.1   Testing the Condition of Installed Thermocouples

To verify the steady state performance of installed thermocouples, the following simple measurements may be made on a continuous basis and analyzed for abnormalities such as sudden shifts, spikes, noise, drift, and other changes (Figure 18.1):

- Measurement of thermocouple loop resistance (electrical resistance between points 1 and 2).

- Measurement of thermocouple insulation resistance (electrical resistance between points 1 and/or 2 of the thermocouple and points 3 and/or 4 on the sheath).

- Measurement of capacitance to ground (electrical capacitance between points 1 and/or 2 of thermocouple and points 3 and/or 4 on the sheath).
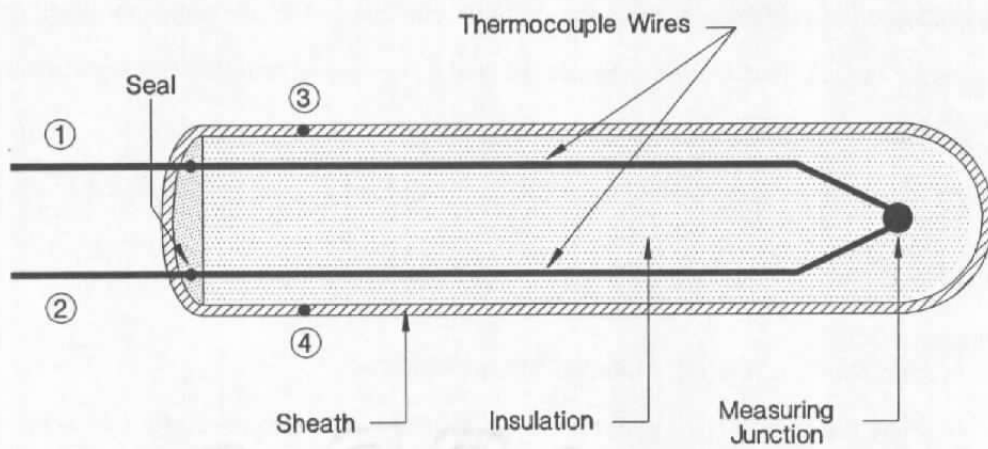
Figure 18.1. Measurement Points for Monitoring the Condition
of an Installed Thermocouple.

In addition, gross inhomogeneities or moisture in the thermocouple circuit may be detectable in-situ by applying a step electric current to the thermocouple (across points 1 and 2) and monitoring the thermocouple output when the current is cut off. This is the same procedure as in the LCSR test except that in this case, there is no need for analysis of the data except for an algorithm that can distinguish between normal and degraded LCSR transients.

The three simple measurements suggested above, as well as the application of current to the thermocouple circuit to check for moisture and inhomogeneity, have the potential to provide diagnostics not only about the health of the thermocouple, but also about the connectors, cables, and other components of the thermocouple circuit. However, experimental research is needed to prove these capabilities.

Another diagnostic tool that may be useful in checking thermocouple circuits is the "time domain reflectrometry" (TDR). Commercial TDR instruments are available that can be used for this purpose without a need for much further development.

18.2   Thermocouple Cross Calibration

In applications where redundant thermocouples are used for measuring the same or related temperatures, an intercomparison scheme can be implemented to identify the outliers. This method has been used very successfully in the nuclear power industry for checking the calibration of RTDs as installed in an operating plant at isothermal test conditions. The method is referred to as cross calibration, and is adaptable to redundant thermocouples. Table 18.1 shows a typical computer printout providing cross calibration results for 12 thermocouples tested in our laboratory. With the thermocouples installed in an oil bath at 200°C, four sets of

TABLE 19.1

Thermocouple Cross Calibration Results

Tag No.	Type	EMF (mv)				Avg	Temp. (°C)	ΔT (°C)
		Pass 1	Pass 2	Pass 3	Pass 4			
1	K	8.103	8.103	8.103	8.103	8.103	199.16	-1.17
2	K	8.116	8.115	8.115	8.115	8.115	199.46	-0.87
3	K	8.201	8.201	8.201	8.201	8.201	201.61	1.28
4	K	8.123	8.124	8.130	8.125	8.126	199.74	-0.59
5	E	13.471	13.471	13.471	13.470	13.471	200.71	0.38
6	E	13.500	13.500	13.499	13.499	13.500	201.10	0.77
7	E	13.513	13.514	13.510	13.512	13.512	201.26	0.93
8	E	13.433	13.442	13.430	13.420	13.431	200.17	-0.16
9	J	10.755	10.758	10.757	10.757	10.758	199.67	-0.66
10	J	10.831	10.834	10.834	10.833	10.834	201.04	0.71
11	J	10.725	10.725	10.725	10.725	10.725	199.07	-1.26
12	J	10.830	10.829	10.830	10.829	10.830	200.96	0.63
SPRT	Ω	45.334	45.334	45.334	45.334	45.334	200.38	0.05

200.33°C = Average Temperature

sequential measurements of the steady state output of the thermocouples were made as shown in Table 18.1. These measurements were then averaged and converted from EMF (volts) to equivalent temperatures. The resulting 12 temperatures were subsequently averaged and the difference between the average temperature and the temperature indicated by each thermocouple was calculated (ΔT).

In the cross calibration procedure, a criteria is usually specified, depending on the accuracy requirements, to reject a thermocouple from inclusion in the averaging process if its first pass deviation is beyond a pre-specified value. For example, in the results shown in Table 18.1, if a 1°C criteria was specified, thermocouple numbers 1, 3, and 11 would have not been used in calculating the average temperature.

A standard platinum resistance thermometer (SPRT) was also used in the cross calibration tests discussed above. As apparent in Table 18.1, the oil bath temperature that was measured with the SPRT was very close to the temperature indicated by the average of the twelve thermocouples. That is, the temperature as indicated by the average of the thermocouples corresponds closely to the true temperature of the oil bath as measured by the SPRT. Due to the random nature of the calibration differences between a large group of thermocouples or RTDs, it is often likely that the average temperature of the group would represent the true temperature of the process provided that a majority of the sensors have reasonable calibrations.

Another method called "signal validation" is available to improve the accuracy of the cross calibration results. This method is based on establishing an empirical correlation between a

number of "like" and "unlike" signals at a baseline process condition. For example, an empirical correlation can be established between any number of temperature, pressure, and flow signals in a closed system at a normal operating condition and used to identify the signals that may be drifting away from a normal or an average value. The signal validation techniques are undergoing extensive development and testing in the nuclear power industry for on-line detection of abnormal behavior of redundant sensors or systems.

18.3   A Smart Thermocouple System

The conceptual design of a smart thermocouple system is shown in Figure 18.2. The system as shown here consists of a number of conventional thermocouples that are installed in a process and connected to a microprocessor which performs measurements and diagnostics. The system is intended to indicate the temperature of the thermocouple, provide a confidence level in the indicated temperature, and identify the thermocouples that are sluggish, drifting, or failed based on pre-specified static and dynamic performance criteria. It is also intended to identify cable and connector problems.

The part of the system that measures the response time of a thermocouple was developed in this project based on the Loop Current Step Response (LCSR) method. Another module can readily be added to provide noise analysis capability. The noise analysis capability will be useful for providing real-time response time results and to cross check the LCSR results.
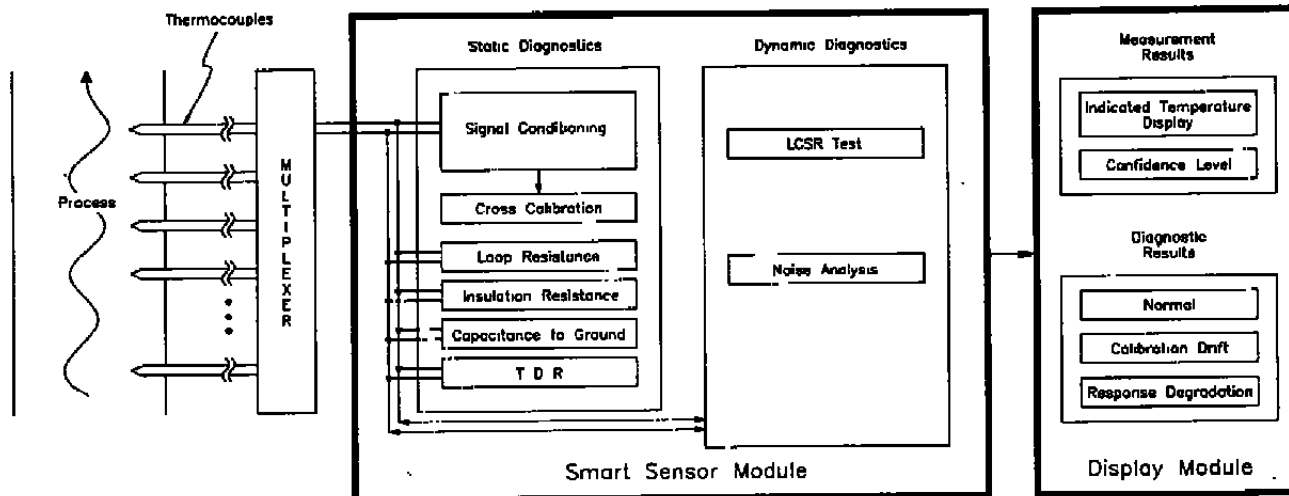
Figure 18.2. Smart Thermocouple System.

19. INDUSTRIAL APPLICATIONS OF LCSR TEST

19.1 General Applications

Not only in the aerospace industry, but also in the chemical, steel, and automotive industries and many manufacturing processes, there is a need to measure transient temperatures with thermocouples. In most of these applications, a knowledge of thermocouple response time under service conditions is crucial. The LCSR method can provide the response times and enable the user to correct the transient temperature data for the thermocouple lag or allow for it in the process control or data analysis procedures.

In some processes, small thermocouples are used at the cost of durability and ruggedness to achieve a fast dynamic response. With the capabilities that LCSR can provide, the size of thermocouples may not be a limitation. The response time can be measured and the temperature data corrected as if the thermocouple response was practically instantaneous.

19.2 Aerospace Applications

In the aerospace industries, the LCSR technique has many applications. Some examples are:

- Gas Temperature Measurements Inside Jet Engines During Transients. Such transients occur due to inlet distortion, starting, throttle transients, compressor instability, ignition testing, and combustion instability. These can be due to a single event, such as a weapon discharge or a periodic event such as an instability. Critical areas are turbine inlet gas temperature and the temperature of the air supplied to cool the turbine blades.

- **Gas Temperature Measurements During Testing with Intermittent Type Wind Tunnels.** Applications include hypervelocity ranges where projectiles are fired past measurement stations at hypersonic speeds and blowdown type wind tunnels.

- **Testing of Validity of Empirical Equations for Determining Time Constants.** Normally, the time constant of a thermocouple is determined by bench testing and extrapolation to operating conditions using an empirical scheme. The LCSR technique can test the validity of any extrapolation scheme or replace it by a more reliable interpolation scheme by performing measurements under both conditions.

- **Testing the Installation Integrity of Thermocouples.** It has been established that the LCSR technique can distinguish between installations where thermal contact is proper and installations having poor thermal contact. Additional research will be needed to establish baseline installation data and to quantify the degree of thermal contact based on LCSR data. Potential applications include measurements in the nozzle of solid rocket engines and wind tunnel heat transfer measurements using heated models which are injected into the air stream.

  The potential payback of testing the integrity of installed thermocouples is great due to the large number of thermocouples that are attached to a surface in order to monitor process temperatures. Surface mounted thermocouples are frequently attached with cement, which may float the thermocouple off the surface or produce varying degrees of contact at installation. In addition, multiple heating/cooling cycles may crack or otherwise deteriorate the bond, thus changing the response time of the thermocouple. Also, a thermocouple installed within a solid may become loose with time under the influence of thermal expansion.

20. CONCLUSIONS

A comprehensive research and development project was completed over a three-year period to develop full capability for measurement of response time of thermocouples as installed in operating processes. The project involved laboratory research with typical thermocouples of the types and sizes of interest to the aerospace community. The laboratory tests provided the data and the experience to develop automatic test equipment for general use.

The research and development carried out in this project was based on the Loop Current Step Response (LCSR) method. This method is now fully developed for remote measurement of "in-service" response times of thermocouples as installed in liquid and gaseous process media. The LCSR method is based on sending an electric current to the thermocouple junction through the normal thermocouple leads. This current heats the junction several degrees above the temperature of the thermocouple environment. The current is then cut off and the thermocouple output is recorded as it returns to the surrounding temperature. This output is an exponential transient which decays at a rate that corresponds to the response time of the thermocouple under the conditions tested. Therefore, the exponential transient can be analyzed to provide the response time of the thermocouple.

The response time of a thermocouple as obtained by the LCSR method is the same as the response time that would have been obtained for the thermocouple if the temperature of the process experienced a step change. The response time results in this report correspond to the time that is required for the thermocouple to reach 63.2 percent of its final steady state amplitude after a step change in the temperature of the thermocouple environment. Although this definition corresponds to the time constant of a first order system, its use is not intended to imply that thermocouples are necessarily represented by first order dynamics.

REFERENCES

1. Warshawsky, I., "Heat Conduction Errors and Time Lag in Cryogenic Thermometer Installation," Transaction of Instrument Society of America, #13 (4), 1974.

2. Carroll, R.M., Shepard, R.L., "Measurement of Transient Response of Thermocouples and Resistance Thermometers Using an In-Situ Method," Oak Ridge National Laboratory, Report Number ORNL/TM-4573, Oak Ridge, Tennessee, June 1977.

3. Kerlin, T.W., Miller, L.F., Hashemian, H.M., Poore, W.P., Shorska, M., Upadhyaya, B.R., Cormult, P., Jacquot, J.P., "Temperature Sensor Response Characterization", Electric Power Research Institute EPRI Report Number NP-1486, (August 1980).

4. "Safety Evaluation Report," U. S. Nuclear Regulatory Commission, Report Number NUREG/CR-0809, Washington, D.C., August 1981.

5. Magison, E.C., "Temperature Measurement in Industry," Instrument Society of America, Research Triangle Park, North Carolina, 1990.

6. Shepard, R.L., Carroll, R.M., "Thermocouple Response Time Measurement and Improvement," Notes on short course entitled "Sensor Response Time Testing in Nuclear Power Plants," College of Engineering, The University of Tennessee, Knoxville, Tennessee, Unit 3, June 1977.

7. Kollie, T.G., et al., "Large Thermocouple Thermometer Errors Caused by Magnetic Fields," Review of Scientific Instruments, Vol. 48, No. 5, American Institute of Physics, New York, N.Y., May 1977.

8. Kerlin, T.W., "Analytical Methods for Interpreting In-Situ Measurements of Response Times in Thermocouples and Resistance Thermometers," Oak Ridge National laboratory, Report Number ORNL/TM-4912, Oak Ridge, Tennessee, March 1976.

9. Kerlin, T.W., Hashemian, H.M., Petersen, K.M., "Time Response of Temperature Sensors," Paper C.I. 80-674, Instrument Society of America, International Conference and Exhibit, Houston, Texas, (October 1980).

10. Rohsenow, W.M., Choi, H.Y., "Heat, Mass and Momentum Transfer," Prentice-Hall, Englewood Cliffs, NJ (1961).

11. Perkins, H.C., Leppert, G., "Forced Convection Heat Transfer from a Uniformly Heating Cylinder," Journal of Heat Transfer, No. 84, pp. 257-263 (1962).

12. Shepard, R.L., "Private Discussions between H.M. Hashemian and R.L. Shepard," Oak Ridge National Laboratory, Oak Ridge, Tennessee, July 1991.

REFERENCES
(continued)

13. Hashemian, H.M., et al., "New Methods for Response Time Testing of Industrial Temperature and Pressure Sensors," Proc. of Annual Meeting of American Society of Mechanical Engineers (ASME), pp. 79-85, Anaheim, California, (December 1986).

14. ASTM Standard E839-89, "Standard Test Methods for Sheathed Thermocouples and Sheathed Thermocouple Material," American Society for Testing and Materials, Annual Book of ASTM Standards, Section 14, Vol. 14.03, pp. 321-334 (1990).

15. ASTM Standard E644-86, "Standard Methods for Testing Industrial Resistance Thermometers," American Society for Testing and Materials, Annual Book of ASTM Standards, Section 14, Vol. 14.03, pp. 285-301 (1990).

16. ISA Standard S67.06, "Response Time Testing of Nuclear Safety-Related Instrument Channels in Nuclear Power Plants," Instrument Society of America, 1984.

17. Hashemian, H.M., "Determination of Installed Thermocouple Response", U.S. Air Force, Arnold Engineering Development Center, Report Number AEDC-86-46, (December 1986).

18. Omega, "The Temperature Handbook," Omega Engineering, Inc., Stamford, Connecticut, 1990/91 Temperature Catalog.

19. ASTM Standard E220-86, "Calibration of Thermocouples By Comparison Techniques," American Society for Testing and Materials, Annual Book of ASTM Standards, Section 14, Vol. 14.03, pp. 90-100. (1990)

20. Hashemian, H.M., et al., "Aging of Nuclear Plant Resistance Temperature Detectors", U.S. Nuclear Regulatory Commission, Report Number NUREG/CR-5560, (June 1990).